PHYSIOLOGICALLY-BASED PHARMACOKINETIC MODELING OF DRUGS WITH TRANSPORTER-MEDIATED DISPOSITION: PREDICTION OF VINCRISTINE AND AMOXICILLIN DISPOSITION IN CHILDREN

Christine M. Lee

A dissertation submitted to the faculty at the University of North Carolina at Chapel Hill in partial fulfillment of the requirements for the degree of Doctor of Philosophy in the UNC Eshelman School of Pharmacy

Chapel Hill
2019

Approved by:

Dhiren R. Thakker

Kim L. R. Brouwer

William C. Zamboni

Matthew M. Laughon

Daniel Gonzalez

William R. Proctor

ABSTRACT

Christine M. Lee: Physiologically-based Pharmacokinetic Modeling to Predict the Disposition of Vincristine and Amoxicillin in Pediatric and Infant Populations
(Under the direction of Dhiren R. Thakker, Ph.D.)

The use of physiologically-based pharmacokinetic (PBPK) models to predict pediatric pharmacokinetics (PK) and select optimal doses is increasingly common. However, its application to pediatric drugs with transporter-mediated disposition has been limited by challenges in modeling drugs with a complicated interplay between metabolism and transport and a need for transporter ontogeny data.

The goal of this dissertation was to develop bottom-up PBPK models to predict the PK of two drugs with transporter-mediated disposition in pediatric populations: (1) vincristine, an intravenously administered anti-cancer agent that is cleared hepatically by the drug metabolizing enzymes cytochrome P450 (CYP) 3A4/5 and the efflux transporter P-glycoprotein (P-gp), and (2) amoxicillin, an orally administered antibiotic that requires the intestinal apical (AP) uptake transporter peptide transporter 1 (PEPT1) for absorption.

PBPK modeling of vincristine in adults that incorporated hepatic CYP3A4/5-mediated metabolism and P-gp-mediated efflux initially underestimated the extent of distribution of vincristine. Model predictions were improved by incorporating binding of vincristine to the microtubule protein β-tubulin. When the adult PBPK model was adapted to the pediatric population, simulating a 4.9-fold higher hypothetical expression level of β-tubulin in children as compared to adults improved predictions of the pediatric PBPK model. Despite its implied role

in vincristine clearance, P-gp-mediated efflux was not a key parameter in the model, leading to the conclusion that vincristine uptake into hepatocytes is the rate-limiting step in its clearance, rather than its efflux.

Amoxicillin demonstrates dose-dependent oral bioavailability despite its hydrophilicity and charge at physiological pH, properties that are consistent with a contribution of transporters and paracellular transport to its absorption. Studies performed in Caco-2 cell monolayers and adult human intestinal epithelia suggested that PEPT1 and an organic anion-transporting polypeptide (OATP) are involved in the AP uptake of amoxicillin. Efficient basolateral (BL) egress of amoxicillin implicates a BL transporter, likely the bidirectional peptide transporter. A relatively large (~20%) contribution of paracellular transport to the overall absorption of amoxicillin was observed. Lastly, PBPK models of oral amoxicillin predicted PK in adults, and in young children (≤ 5 years of age) after incorporating pediatric GI physiology and amoxicillin renal clearance.

ACKNOWLEDGMENTS

I will always be grateful to my advisor, Dr. Dhiren R. Thakker, for his support, guidance, and kindness. He has seen me through personal and professional challenges with incredible patience and generosity. I could not have asked for a better mentor on a scientific and personal level, and I would not be where I am today without him. Dhiren once said to me that his patience is not infinite; although I must have sorely tested its limits many times, he always had an answer for me when I needed one, and another way to push me to keep going and growing. I can only hope that I will be able to pay it forward and help others as he has helped me, and that his retirement from academia will be all the sweeter for having finally, successfully, graduated his last student.

I am deeply indebted to my committee members, Drs. William C. Zamboni, Daniel Gonzalez, Matthew M. Laughon, William R. Proctor, and especially to my committee chair, Dr. Kim L. R. Brouwer. They generously made their time, input, and resources available to me, and challenged me to be a better scientist. I am grateful to have had the opportunity to learn from all of them and for their suggestions, insights, support, and patience.

I would like to thank all the members of the Thakker laboratory, past and present, for their friendship, guidance, support, and scientific discussions, especially Drs. Ruth Everett, Nicole R. Zane, Hao Cai, Lawrence Ku, and Arul Muralidharan. In particular, Dr. Ruth Everett was instrumental in helping to keep me on track and was always ready to assist me in times of need, and it was a delight to work with her. In addition, I appreciated the positive energy and

assistance from our undergraduate student researchers, Benjamin Clements and Jacob Stroud, and I look forward to seeing them start their own careers as well.

I would also like to acknowledge my friends and colleagues in School of Pharmacy for their friendship, moral support, and assistance over the years: Izna Ali, Jacqueline Benzaçon, Phyllis Lee, Melina Malinen, Gloria Nyankima, Sara Salerno, Chitra Saran, and Jason Slizgi. They have made my time at UNC enjoyable and memorable, and I look forward to seeing what they do next. In the last two years of my research, Izna was also an unfailingly upbeat cheerleader and a great person to discuss scientific and professional issues with - I am excited for us to both embark on our new careers in Chicago.

Finally, I would like to thank my family for their love and support. My parents gave me a great foundation, as well as the freedom and security to pursue my interests. My sister Tiffany is always ready to step in and help others without being asked, and her support and sense of humor has been invaluable throughout my life. I am also grateful for the love, understanding, and support of my significant other, Omeed Ilchi. After so many years of seeing our friendship and relationship through the struggles of our respective doctoral programs, I look forward to us starting a new life together.

TABLE OF CONTENTS

LIST OF FIGURES

LIST OF TABLES

LIST OF ABBREVIATIONS

AAD	Antibiotic-associated diarrhea
AAG	α-acid glycoprotein
ALL	Acute lymphocytic leukemia
AOM	Acute otitis media
AP	Apical
ATP	Adenosine triphosphate
AUC	Area under the curve
b.i.d.	Twice daily dose
BCA	Bicinchoninic acid assay
BCS	Biopharmaceutics Classification System
BCRP	Breast cancer resistance protein
BL	Basolateral
BPCA	Best Pharmaceuticals for Children Act
BSEP	Bile salt export pump transporter
CHT	Choline high affinity transporter
CL	Clearance
DME	Drug-metabolizing enzyme
E3S	Estrone-3-sulfate
FBS	Fetal bovine serum
f_u	Fraction unbound
GFR	Glomerular filtration rate

GI	Gastrointestinal
glysar	Glycylsarcosine
GW918	[N-(4-[2-(1,2,3,4-tetrahydro-6,7-dimethoxy-2-isoquinolinyl)ethyl]-phenyl)-9,10-dihydro-5-methoxy-9-oxo-4-acridine carboxamide]
HBSS	Hank's balanced salt solution
IV	Intravenous
J	Flux
K_m	Michaelis-Menten constant
KRB	Krebs-Ringer buffer
LSC	Liquid scintillation counting
MCT	Monocarboxylic acid transporter
MEF	Middle ear fluid
MIC	Minimum inhibitory concentration
NCA	Noncompartmental analysis
NDA	New Drug Application
NEAA	Nonessential amino acids
OAT	Organic anion transporter
OATP	Organic anion transporting polypeptide
OCT	Organic cation transporter
P_{app}	Apparent permeability
PAT1	Proton-coupled amino acid transporter
PEPT1, PEPT2	Human peptide transporter 1 and 2
P-gp	P-glycoprotein

PK	Pharmacokinetics
PPAR α	Peroxisome proliferator-activated receptor α
PREA	Pediatric Research Equity Act
SERT	Serotonin reuptake transporter
t.i.d.	Thrice daily dose
TEER	Transepithelial electrical resistance
V_{max}	Maximal reaction rate

CHAPTER 1 : INTRODUCTION

Background

During drug development, it is important to study the clinical pharmacokinetics (PK) and pharmacodynamics of a drug in order to understand the relationship between dose/plasma levels and safety/efficacy. Phase I studies, typically performed in healthy adult volunteers, play an important role in understanding drug PK, selecting safe and effective doses, and predicting potential drug-drug interactions. However, it is ethically challenging to enroll infants and children into clinical trials. As a result, pediatric doses have been determined primarily by extrapolating adult doses rather than obtaining this information from clinical studies in the pediatric population. This extrapolation is often performed by adjusting for body weight, surface area, or allometric scaling methods. However, allometric scaling does not address developmental changes in total body composition, gastrointestinal (GI) function, and organ sizes, nor does it account for the ontogeny of drug metabolizing enzymes (DMEs) or drug transporters. The utility of these simple scaling approaches or allometric formulas is most limited in young children and infants, who have notable physiological differences compared to adults and who demonstrate age-related differences in drug disposition that are not scalable with body size[1]. Allometric formulas often overestimate drug clearance in young children, and these estimations are most unreliable in infants[2,3].

As a result, some drugs are historically used off-label in the pediatric population with limited data from clinical studies. As of 2003, it was estimated that between 50-75% of drugs

used in pediatric therapy were being used off-label without adequate scientific data[4], and other drugs were used in children at inappropriate doses. For example, the antibiotic chloramphenicol can cause life-threatening Gray Baby syndrome in neonates due to reduced clearance and low hepatic DME activity (specifically, the UGT2B7 enzyme), requiring age-based dose adjustment or selection of a different antibiotic for the infant population[5]. Neonates in particular, represent a population with an important gap in pediatric clinical data. A 2018 review suggests that up to 99.5% of infants in neonatal intensive care units receive medications that are used off-label with respect to the age group and dose[6]. In 20 general pediatric care wards over a 10-year period, between 18% and 70% of drugs were used off-label, most commonly antibiotics and bronchodilators[6]. In cases where pediatric clinical data are limited and pediatric PK studies cannot be conducted, it is particularly difficult to predict PK and select doses for drugs with age-dependent absorption or clearance processes. In 2002 and 2003, the Best Pharmaceuticals for Children Act (BPCA) and Pediatric Research Equity Act (PREA) were passed, respectively, to establish incentives and requirements for companies to study safety and efficacy of new drugs in pediatric patients[7]. Even so, the selection of appropriate doses and dosing regimens for pediatric clinical studies still presents a challenge, especially when allometric approaches are not appropriate.

Physiologically-based PK (PBPK) Modeling Approaches

Alternative modeling and simulation approaches have been used to select doses and predict pediatric and adult PK during drug development, and are especially useful for special populations (*e.g.*, hepatic impairment, pediatric populations). One such approach is simulation using PBPK models, which can estimate and simulate plasma/blood concentrations of a drug as a function of time by modeling drug disposition (absorption, distribution, metabolism, and

excretion) based on the cellular/molecular interactions of the drug *(e.g.*, cell permeability, affinity to and maximum rate of metabolism by specific enzymes), tissue/organ distribution and expression levels of metabolic enzymes and transporters, physicochemical properties of the drug, and other relevant parameters. Once a PBPK model has been developed for adults, its predictions can be refined and subsequently validated, by comparing the simulated/predicted PK parameters with clinically determined parameters. A validated adult PBPK model can be adjusted to account for the physiological differences between adult and pediatric populations, and thus applied to predict PK behavior of the drug in a pediatric population. There is increasing use of PBPK models in pediatric drug development to predict pediatric PK and support new drug applications (NDAs) to the Food and Drug Administration (FDA)[2]. In addition, the FDA has stated that allometric scaling is inappropriate for infant and neonatal populations, and recommends PBPK modeling as a possible alternative[2,8].

PBPK models use mass balance equations to describe the transfer of drugs between physiological "compartments" that are linked by blood flow (**Figure 1-1**). Age-relevant physiology can be incorporated by using appropriate volumes and flow rates, as well as age-relevant expression of DMEs and transporters[3]. "Top-down" PBPK approaches utilize clinical PK parameters of the drug, such as *in vivo* clearance and volume of distribution. Bottom-up PBPK approaches utilize *in vitro* data or *in silico* predictions to extrapolate drug parameters instead. An advantage of bottom-up PBPK approaches is the flexibility to scale individual *in vitro* parameters in an age-appropriate manner, accounting for multiple disposition and clearance processes that, in children, may develop at different rates. The ability to incorporate and scale *in vitro* parameters with a bottom-up PBPK model is also an advantage where data have been obtained using age-specific tissues, such as metabolism kinetics with human liver microsomes

(HLMs) prepared from pediatric liver tissue or protein binding values derived using plasma obtained from newborn subjects[9–11]. Bottom-up PBPK models have previously been developed in our laboratory for metabolically-cleared drugs in pediatric (voriconazole) and premature neonate (sildenafil) populations[12,13].

Intestinal Absorption and Transport Mechanisms

For oral pediatric drugs that require drug transporters for intestinal absorption, predicting oral bioavailability and PK in children is further complicated due to the lack of information on the effect of age on intestinal permeability and other factors that can impact absorption[14]. Once in the intestinal lumen, an orally administered drug must cross the intestinal epithelium to reach the portal blood compartment, either by a transcellular pathway (across the cells) or a paracellular pathway (between the cells) (**Figure 1-2**). For the transcellular pathway of absorption, the drug must cross the apical (AP) membrane to enter the enterocyte, and leave the enterocyte by egressing across the basolateral (BL) membrane. The AP, lumen-facing enterocytic membrane has an increased surface area due to the presence of microvilli that facilitate absorption. Generally, paracellular transport is inefficient because of the small surface area available for molecules to enter the paracellular space. In addition, the paracellular space is further constricted by the presence of tight junctions[15,16], which are pore-like structures formed by proteins (*e.g.* occludin, claudins) protruding out of the adjoining cells across the lateral membrane. Thus, molecules with large hydrodynamic radii cannot get across the tight junctions very efficiently. The tight junction pores exhibit charge selectivity, so that cationic compounds traverse them more readily than neutral or anionic compounds[16]. Tight junctions are regulated by cell signaling pathways (*e.g.*, *via* hormones or cytokine effects) and removal or recycling of the tight junction proteins[15].

The transcellular pathway (**Figure 1-2**) comprises passive diffusion (driven by a concentration gradient), active transport by membrane transporter proteins (transporter-mediated, an active process requiring adenosine triphosphate (ATP) or other indirect source of energy), or a combination of these mechanisms (mixed transport). Lipophilic neutral molecules traverse the AP and BL membranes *via* passive diffusion. Paracellular transport contributes very little to their intestinal absorption because of a very large surface area of the AP membrane with microvilli that is available to them in comparison to a much smaller area of the paracellular pores. For charged molecules (anions, cations, and zwitterions), an uptake transporter is generally required to cross the AP membrane, and a BL efflux transporter is required to remove it from enterocytes into the serosal blood capillaries (**Figure 1-2**). Some examples of AP uptake transporters for (i) cationic compounds are: organic cation transporters (OCT) 1, 2, 3, organic cation transporter novel (OCTN) 1 and 2, choline high affinity transporter (CHT), and serotonin reuptake transporter (SERT); (ii) for anionic compounds: organic anion transporting polypeptide (OATP) 1A2, 2B1, monocarboxylic acid transporter (MCT); (iii) for zwitterionic compounds: OATP2B1, amino acid transporters, and peptide transporter (PEPT) 1. The efficiency of the AP uptake transporter(s) and the lipophilicity, size, and charge of the compounds determine the relative contributions of the transcellular *vs.* paracellular route in the absorptive transport of these compounds.

Hydrophilic molecules, either charged or neutral, cannot cross the cell membranes *via* passive diffusion. Charged hydrophilic compounds cross the intestinal epithelium *via* a combination of transporter-mediated transcellular transport and paracellular transport routes, whereas neutral hydrophilic compounds traverse the intestinal epithelium entirely *via* the paracellular pathway.

A group of AP efflux transporters actively prevent lipophilic ionic compounds from entering the cells across the AP membrane of intestinal epithelial cells or pump these compounds out of the epithelial cells across the AP membrane into the intestinal lumen[17] (**Figure 1-2**). These transporters traverse the AP membrane multiple times, and thus have extracellular, transmembrane, and intracellular domains, including an intracellular domain that catalyzes hydrolysis of ATP to generate energy needed to pump the compounds out across the AP membrane. Among these transporters, P-glycoprotein (P-gp) and breast cancer resistance protein (BCRP) transport cationic compounds, and multidrug resistance-associated proteins (MRP) and BCRP transport anionic and zwitterionic compounds. AP uptake and absorptive transport of compounds is attenuated if they are substrates of one or more AP efflux transporters. The presence of a subset of efflux transporters, *i.e.*, MRP1, 3, and 4 in the BL membrane of intestinal epithelial cells[18], assist the absorption of anionic and zwitterionic compounds by actively pumping them out of the cells into the portal blood compartment. Bidirectional transporters, such as OSTα/β[19], and a peptide transporter (as yet uncharacterized) [20–22] present in the BL membrane of intestinal epithelial cells also facilitate egress of anionic and zwitterionic compounds into the portal blood compartment, and thus assist in their absorption. An interesting hypothesis published by the Thakker Laboratory postulates that there are no cation-selective efflux transporters in the BL membrane of intestinal epithelial cells[23]. They propose that most of the cationic compounds to which the intestine is exposed are weak bases that have a significant percentage of molecules in a neutral state at pH >7 within the enterocytes. Since the neutral population of these compounds can diffuse out of the BL membrane to be absorbed, there must be a lack of evolutionary pressure to develop/express cation-selective efflux transporters in the BL membrane of enterocytes.

Insufficient knowledge about the age-related differences in those aspects of the GI physiology that are relevant to transporter-mediated absorption, especially in infants, is a significant barrier to developing pediatric PBPK models for such oral drugs. Gastric pH is near neutrality at birth and becomes more acidic until reaching adult levels around 2 years of age[24]. A comparison of pH along the intestinal tract and regional transit times were similar in a small cohort of children (8 to 14 years old)[25,26]. However, the effect of age on intestinal permeability[14,27] and impact on the absorption of drugs due to differential expression of the uptake and efflux transporters and the tight junction proteins, as well as due to changes in other anatomical and physiological features of the GI tract, especially for infants, is not well understood[28,29].

PBPK Modeling for Pediatric Drug Disposition and Current Limitations: Goals of the Proposed Research

Although PBPK modeling is now an important tool in the development of pediatric drugs, significant knowledge gaps remain that limit its use, particularly for drugs with transporter-mediated disposition. *In vitro* to *in vivo* extrapolation of transport kinetics is difficult for pediatric drugs with transporter-mediated disposition because of limited information on the ontogeny of transporter expression and activity[30]. Historically, only gene expression data or total protein expression data were available in early studies of transporter ontogeny. However, there is poor correlation between gene expression, protein expression, and transport activity. In addition, measuring total protein expression of transporters does not reflect the expression of transporters localized to the plasma membrane, where they function. For example, the P-gp transporter is present in endosomal compartments and the cellular plasma membrane, but it must go from the endosomal compartment to the plasma membrane to be effective in actively pumping substrates

out of the cell[31]. Recent advances in mass spectrometric quantification of transporter proteins in the plasma membrane are improving the quality of data on transporter ontogeny, and will improve *in vitro* to *in vivo* extrapolations of transporter kinetic data, although availability of pediatric tissue samples can still be a limiting factor[32,33]. Studying the effect of age on transporter activity is also difficult, as fresh pediatric tissue with intact transporter function is extremely difficult to obtain for *in vitro* studies. Two-dimensional and three-dimensional hepatic *in vitro* models developed using hepatocytes isolated from fresh liver tissue have been very useful in studying hepatic transport and metabolism of drugs[34,35]; however, the availability of hepatocytes from pediatric populations is very limited, making it difficult to generate *in vitro* transport data for children. Although cryopreserved hepatocytes make it easier to develop pediatric *in vitro* models for hepatic metabolism and transport processes, in the past, cryopreservation has been shown to significantly reduce protein expression of transporters compared to their expression in freshly isolated hepatocytes[36] and freshly frozen liver tissue[37]. In addition to reducing protein expression, cryopreservation also increases the internalization of drug transporters, and tissue damage from the isolation process appears to downregulate transporter protein expression as well[36,38]. In contrast, the activity and expression of Phase I and Phase II DMEs are similar between freshly isolated *vs* frozen hepatocytes[36]. The limited availability of pediatric transport data complicates the development and use of scaling factors for transporter-mediated processes in PBPK modeling[8].

Compared to transporter expression in the liver, the ontogeny of intestinal transporters is less well studied, with very little information on the effect of age on differences in their expression along the GI tract[30]. The FDA has noted that for Biopharmaceutics Classification System (BCS) I drugs (high solubility, high permeability), there is “high confidence” in the use

of PBPK models, but not for other drug types for which predicting the effect of solubility, dissolution, and precipitation is challenging[8].

Despite these challenges, and recognizing the limitations in the use of pediatric *in vitro* models for transport/metabolism in the intestine and liver, the proposed research was undertaken to develop pediatric PBPK models for drugs whose disposition is significantly affected by one or more transporters. The rationale was that developing, implementing, and testing these models against limited pediatric clinical data would reveal the impact of gaps in the available hepatic and intestinal transporter ontogeny data on the success of PBPK models that will be developed using commercially available modeling software, *e.g.*, PK-Sim®, in predicting clinical PK parameters. It is also reasonable to assume that even imperfect models will provide better guidance to select safe and effective doses of these drugs in children than arbitrary dose selection or the inappropriate use of allometric methods to extrapolate adult doses to doses in children.

The approach used in designing studies for developing pediatric PBPK models was similar to the one used previously by the Thakker Laboratory[12] for drugs that are cleared predominantly by metabolism. In this approach, adult PBPK models were developed for the selected drugs by first examining the clinical data and determining the major clearance mechanisms, *e.g.*, metabolism by specific enzymes, renal clearance, transporter-mediated clearance or absorption, and subsequently (i) implementing *in vitro* models derived from relevant adult tissues, (ii) incorporating *in vitro* data into a PBPK model, and (iii) iteratively refining the model by comparing the predicted values of PK parameters with the available clinical PK parameters. After successful development of an adult model, it was adapted to *in vitro* data produced from the corresponding pediatric tissues to build a model for the target pediatric population.

For this work, two drugs were selected: (1) vincristine, a drug for which the efflux transporter, P-gp, expressed in the canalicular membrane of hepatocytes, has been reported to play an important role in its clearance[39]; and (2) amoxicillin, a drug for which an AP uptake transporter, PEPT1, has been implicated in its intestinal absorption and possibly in its renal clearance[40–42]. These drugs are first-line treatments in pediatric populations for treatment of cancer and acute otitis media (AOM), respectively. An overview of the disposition of vincristine and amoxicillin, and the rationale and proposed research for the development of pediatric PBPK models for these two drugs are provided below.

Vincristine Disposition and Impact of Age

Vincristine Use and Mechanism of Action

Vincristine is a vinca alkaloid that has been used widely as an anticancer agent since the 1960s. It is one of the first-line treatments for pediatric and adult leukemias and solid tumors. Vincristine is a key anticancer therapy used in the treatment of pediatric acute lymphocytic leukemia (ALL), which is the most common pediatric cancer and accounts for 26% of cancers diagnosed in children up to 14 years of age[43,44]. Vincristine undergoes hepatic clearance *via* metabolism by CYP3A4/5[45–47] and efflux into bile by P-gp[39]. Both of these processes are expected to be age-dependent.

Vincristine is a natural compound present in the Madagascan periwinkle plant *Catharanthus roseus* and has been used since the late 1950s in cancer therapy[48]. Other naturally occurring vinca alkaloids from this plant have been used clinically as chemotherapy, including vinblastine. Synthetic vinca alkaloids, such as vinorelbine and vindesine, also have been developed as anticancer agents. As a class, the vinca alkaloids are structurally composed of two alkaloid structural units, a catharanthine and vindoline unit (**Figure 1-3**), and all have anti-

mitotic activity *via* binding to β-tubulin[49,50].Vincristine inhibits mitosis by binding to the β-tubulin subunits that comprise the mitotic spindle microtubules, which form the cytoskeleton. Microtubules play a key role in mitosis and are constantly dissembling and reassembling in a dynamic equilibrium with an intracellular pool of unbound α- and β-tubulin. When the microtubules are dissembled, vincristine binds to the β-tubulin subunits, thus disrupting microtubule formation and inhibiting cancer cell growth[51] (**Figure 1-4**). However, this mechanism of action also affects noncancerous cells and leads to adverse effects. Microtubules are also important in the function of vesicular transport in neuronal axons, and thus vincristine can also cause neuronal degeneration and induce neurotoxicity[51].

Vincristine-induced Neurotoxicity

Vincristine-induced peripheral neuropathy is a serious dose-limiting side effect that occurs in up to 35-45% of patients[51,52]. Peripheral neuropathy can be debilitating and extremely painful, ranging from paresthesia and numbness to sensory loss and severe pain[53]. Muscle cramps and weakness are commonly encountered, and other motor functions are also affected. Although the drug-induced neuropathy is generally reversible once vincristine treatment is halted, symptoms can continue to worsen after discontinuation in up to 30% of patients[52]. The development of vincristine-induced peripheral neuropathy is highly dose-dependent, and both the individual dose and the cumulative dose influence the severity of neuropathy[53]. Neuropathic side effects have been observed at doses between 2 and 6 mg/m^2, and vincristine doses in many treatment protocols are capped at 2 mg, regardless of body surface area, to reduce the risk of peripheral neuropathy[53]. There are no treatments for preventing or reducing vincristine-induced peripheral neuropathy, and only dose reduction or discontinuation are effective. Thus, vincristine has a narrow therapeutic window.

Understanding the relationship between vincristine PK and peripheral neuropathy has been complicated by highly variable PK observed in pediatric and adult patients. In some early vincristine clinical studies in adults, an 11-fold variation in AUC was observed[54]. Increased clearance of vincristine also has been observed in infants and children compared to adults[48,51,55].

Vincristine Disposition

Distribution

Following intravenous dosing, vincristine is distributed rapidly and extensively throughout the body, with a volume of distribution that exceeds the total volume of body water (57 to 420 L/m^2 in adults, and 125 to 360 L/m^2 in children)[48]. In the plasma, vincristine binds to α-acid glycoprotein (AAG), but is not extensively protein bound (51-59% unbound)[56,57]. In human tissues, it accumulates primarily in the spleen, liver, kidney, and intestinal mucosa[48]. Vincristine is lipophilic and enters cells through passive diffusion; in the hepatocyte, organic anion transporters (OATPs) may contribute to a minor extent (<10%)[58] to its cellular uptake. Efflux of vincristine into the bile is mediated by P-gp and possibly by multidrug resistance-associated transporter proteins (MRPs)[58]. In cancer cells, MRP1 and MRP2 are associated with resistance to vincristine treatment; inhibition of MRP1 and 2 reverse vincristine treatment resistance[59]. Expression of MRP1 and/or P-gp compared to knockout mouse models significantly reduces brain concentrations of vincristine[39]. Together, these observations suggest that vincristine is a substrate of both P-gp and MRP transporters. As MRPs are also involved in biliary excretion, it is likely that efflux of vincristine into the bile also involves MRPs.

Interestingly, vincristine accumulates in cells *in vitro*, and the extent of accumulation is highly correlated with the intracellular levels of β-tubulin[60]. This correlation is also present when P-gp activity is inhibited by verapamil, indicating that β-tubulin is important in the intracellular

accumulation of vincristine as well as its mechanism of action. A correlation between tubulin binding capacity, tissue concentrations of vincristine, and vincristine partition coefficients was also observed in the organs of mice, dogs, and monkeys administered vincristine[61].

Metabolism

Vincristine is extensively metabolized to its primary metabolite, M1, by CYP3A4/CYP3A5 *via* N-dealkylation (**Figure 1-5**)[45]. In a small sample of adult rhabdomyosarcoma patients (n=4), plasma concentrations of M1 over a 20-hour period ranged from 2% to 22% of vincristine concentrations[62]. Unusually for a CYP3A substrate, vincristine is preferentially metabolized by the genetically polymorphic enzyme CYP3A5. Vincristine is also a substrate of the fetal isoform CYP3A7, which is not expected to play a major role in vincristine metabolism compared to CYP3A4 and CYP3A5. In a comparison of vincristine *in vitro* metabolism by recombinant CYP3A4, CYP3A5, and CYP3A7, CYP3A7 reduced vincristine levels by <10% (*vs* >25% for CYP3A4 and >90% for CYP3A5)[45]. It is hypothesized that the genetic polymorphism of CYP3A5 contributes to variability in vincristine disposition and toxicity[63,64]. This is substantiated by evidence that clearly suggests that CYP3A5 plays a dominant role in metabolic clearance of vincristine. Intrinsic clearance of vincristine is 9 to 14-fold higher with recombinant human CYP3A5 enzymes compared to CYP3A4, and the estimated hepatic clearance of vincristine in HLMs is 5-fold higher in hepatic microsomes from CYP3A5 high expressers (*CYP3A5*1/*1*)[45,46]. Patients with low CYP3A5 expression (*CYP3A5*1*) have decreased vincristine clearance and an increased incidence in vincristine-induced neurotoxicity[65].

Elimination

Vincristine is eliminated primarily *via* the feces after an intravenous dose, while renal clearance plays a small role[66]. After an intravenous dose of radiolabeled vincristine, 70% of the

total radioactivity was recovered in the feces in adults, with 8 to 15% recovered from the urine over 72 hours[66], indicating that vincristine and its metabolites undergo biliary excretion following hepatic oxidative metabolism. Plasma concentrations of alkaline phosphatase have been reported to be inversely correlated with vincristine clearance in adult and pediatric patients[54,67], an observation attributed by the authors to reduced biliary clearance. The three key hepatic transporters involved in biliary excretion are P-gp, MRP2, and the bile salt export pump transporter (BSEP)[68]. Of these, P-gp and MRP2 likely play a key role in the biliary excretion of vincristine, which is a known substrate of both transporters[58,59]. Although the role of P-gp and MRP2 in vincristine's biliary excretion has not been investigated clinically, chemical inhibition of P-gp in rats significantly reduces the biliary excretion clearance of vincristine by 4-fold[69]. In a perfused rat liver model, where 70% of vincristine is excreted into the bile after single-pass perfusion, the biliary excretion rate is significantly reduced by the P-gp inhibitor verapamil[70]. Therefore, it is likely that P-gp and possibly MRP2 contribute to the biliary excretion of vincristine in humans.

Effect of Age on Vincristine Disposition

Clearance of vincristine in infants and children is higher than in adults[48,51,55]. However, the physiologic factors that are responsible for higher clearance of vincristine in infants and children compared to adults have not been elucidated.

The volume of distribution of vincristine is highly variable, but not dissimilar between children and adults (57 to 420 L/m^2 in adults, and 125 to 360 L/m^2 in children)[48]. Although vincristine binds to AAG, and AAG levels increase in a sigmoidal fashion with age, the ontogeny of AAG is unlikely to impact vincristine disposition because it is not extensively protein-bound[71]. The extent of vincristine intracellular accumulation and tissue concentrations

appears to be associated with β-tubulin expression and protein levels[60,61]. However, data are not available for β-tubulin expression in pediatric populations, and it is unclear whether β-tubulin could contribute to age-related differences in accumulation or distribution.

As described earlier, vincristine is a substrate of the drug transporters P-gp and MRP2 that likely play a major role in its biliary excretion. Recent data suggest that some hepatic drug transporters are expressed at lower levels in infants or children compared to adults, including P-gp and OATP1B3[72]. In the liver, P-gp protein expression is age-dependent and significantly different among neonates, infants, children, and adults. In infants and children, the P-gp protein is expressed at ~60% and 80% of adult levels in infants and children, respectively, while hepatic MRP2 expression is not affected by age[72]. Hypothetically, reduced P-gp expression in children may lead to reduced biliary excretion of vincristine. However, one cannot exclude the possibility that uptake, rather than efflux, may be the rate-limiting step in vincristine biliary clearance[58,73]. Uptake of vincristine into the hepatocyte is thought to be a passive diffusion process with very little contribution (<10%) from OATP transporters despite the fact that vincristine is a substrate of OATP1B1, OATP1B3, and OATP2B1[58]. Thus, although both P-gp and OATP1B3 demonstrate age-dependent protein expression in the liver, the biliary excretion of vincristine may be dependent on rate-limiting passive uptake into hepatocytes which is not impacted by age.

Hepatic oxidative metabolism of vincristine may be reduced in infants but is unlikely to be impacted in pediatric patients over one year of age. In fetal hepatic tissue, CYP3A7 is the predominant isoform of CYP3A and CYP3A4 levels are low. During maturation, CYP3A7 levels decrease from fetal levels, while expression of CYP3A4 increases from near-undetectable levels to approximate adult levels around one year of age[74]. In contrast, CYP3A5 activity is dependent on genotype and does not change with age[74]. Vincristine is metabolized selectively by CYP3A5,

and less efficiently by CYP3A4, whereas CYP3A7 does not metabolize vincristine appreciably[45,46,73]. Thus, the increased clearance of vincristine in children (>1 year of age) compared to adults cannot be attributed to age-related differences in CYP3A expression. In infants, who express more CYP3A7 than CYP3A4, decreased metabolic clearance of vincristine would be expected, contrary to the increase in clearance reported[75,51,55], thus ruling out the role of developmental changes in CYP3A to higher clearance of vincristine in this age group.

Amoxicillin Disposition and Impact of Age

Amoxicillin Use and Mechanism of Action

Amoxicillin is a broad-spectrum β-lactam antibiotic, *i.e.*, effective against both gram-positive and gram-negative bacteria, and is one of the most frequently prescribed drugs in infants and children[76,77]. β-lactam antibiotics act by interfering with the synthesis of peptidoglycan, a major component of the bacterial cell wall[78]. Penicillin G and penicillin V were the first β-lactam antibiotics to be discovered. These were later modified to develop amoxicillin and several other penicillin β-lactam antibiotics (*e.g.*, ampicillin, flucloxacillin, mezlocillin, ticarcillin) in the 1960s and 1970s[79]. Unlike the sulfonamide and tetracycline antibiotics, the newer penicillins were better tolerated, with less renal toxicity, rashes, and ototoxicity. Tetracycline also concentrates in developing bones, and was not appropriate for pediatric use[79]. The penicillin β-lactam antibiotics are made up of a four-membered β-lactam ring attached to a five-membered thiazolidine ring (**Figure 1-7**). In general, they are small (<400 MW), hydrophilic, and charged at physiological pH. Both amoxicillin and ampicillin are zwitterions with low passive permeability, but amoxicillin has significantly higher oral bioavailability, likely due to its uptake by intestinal transporters[80]. The β-lactam structure resembles naturally occurring dipeptides and tripeptides, and thus many penicillin and cephalosporin β-lactam antibiotics are substrates for the

intestinal uptake transporter PEPT1 as well as the renal peptide transporter PEPT2, which is involved in reabsorption[81]. The penicillins are renally cleared[82], with net renal secretion greater than GFR, indicating a role of active transporters in renal clearance that exceeds the reuptake by PEPT2.

Amoxicillin is a first-line treatment for AOM, a common childhood disease that affects over 80% of children under 5 years of age[83], and is highly effective against the two most common AOM isolates, *Streptococcus pneumoniae* and *Haemophilus influenza*[84]. Recurrent AOM, defined by more than three episodes within six months, can cause long term damage to the middle ear and hearing loss[85]. Amoxicillin given in combination with the β-lactamase inhibitor clavulanate is also the first-line treatment for AOM to children after failure of initial antibiotic treatment. Children under two years of age are disproportionately affected and comprise 48% of the children diagnosed with AOM[83].

Due to the spread of β-lactam-resistant bacteria, daily doses of amoxicillin recommended by the American Academy of Pediatrics (2013; reaffirmed in 2019) have increased from 40 mg/kg to 60 mg/kg/day for infants and 80-90 mg/kg/day (divided twice daily) in children[77,86]. Higher doses of amoxicillin were also thought to achieve higher levels of middle ear fluid (MEF) that would exceed the minimum inhibitory concentrations (MIC) for *S. pneumoniae*, the most common middle ear pathogen (intermediately resistant, 0.12-1.0 μg/mL; highly resistant, ≥2 μg/mL)[77]. However, doses above 70 mg/kg/day do not appear to reduce rates of AOM treatment failure or relapse in children, suggesting that higher doses may not improve MEF penetration or efficacy[87,88]. In addition, infants have higher odds of AOM treatment failure and relapse compared to older children, and poorer amoxicillin penetration into the MEF[88].

Therefore, there is a need to understand the mechanisms underlying amoxicillin disposition in infants.

Antibiotic-associated Diarrhea (AAD)

Diarrhea is one of the most frequent adverse effects of oral antibiotic treatment, with a rate of 8.1% in children who are treated with amoxicillin[89]. This increases to 19.8% if amoxicillin is given in combination with the β-lactamase inhibitor clavulanate. Based on studies in adults, the mechanism of AAD is hypothesized to involve disturbance to the normal intestinal flora and overgrowth of pathogenic microorganisms (such as *Clostridium difficile*) after the intestinal flora have been altered. Clavulanate also appears to stimulate increased intestinal motility, contributing to AAD[89].

Incidence of AAD with penicillins, including amoxicillin and amoxicillin/clavulanate, is significantly greater in children under two years of age compared to older children, indicating that age is a risk factor in AAD[89]. Inappropriate selection of antibiotics and doses can increase the risk of AAD and its severity, while also burdening parents and caretakers.

Intestinal Absorption of Amoxicillin

Amoxicillin, a renally cleared drug[82], is hydrophilic (logP 0.61, logD -2.21 at pH 7[78]), and is zwitterionic at physiological pH. Thus, it is expected to have poor membrane permeability. However, in adults, amoxicillin has high oral bioavailability[90]. This is dose-dependent and decreases with dose from 90% for a 50 mg dose and 22% at 10 g (**Figure 1-6**)[91]. Therefore, intestinal drug transporters are likely to be involved in amoxicillin absorptive transport.

Intestinal Transporters Implicated in Amoxicillin Absorption

Amoxicillin is a substrate for PEPT1, a likely contributor to its AP enterocytic uptake[92]. PEPT1 is a proton-coupled intestinal transporter that is important in the intestinal absorption of dietary dipeptides and tripeptides, as well as certain β-lactam antibiotics[93]. After ingestion, dietary proteins are hydrolyzed by proteases and peptidases to thousands of highly variable peptides and free amino acids[94]. Consistent with its key role in nutritional intake, PEPT1 is highly expressed in the human small intestine; for example, PEPT1 comprised 50% of total transporter protein expressed in six adult donors[95]. Diet also impacts the expression of PEPT1; under fasted conditions in rats, PEPT1 gene expression and activity (*i.e.*, uptake of glycylsarcosine (glysar)) was increased[96]. This induction of PEPT1 by fasting is mediated by the nuclear receptor peroxisome proliferator-activated receptor (PPAR) α[96].

Uptake by PEPT1 is proton-dependent and sodium-dependent, with maximal activity observed at an extracellular pH of 6.0, *i.e.*, conditions expected in the human jejunum[93]. Studies using *in situ* rat intestinal perfusion and *in vitro* everted rat intestinal jejunum first indicated that certain β-lactam antibiotics (*i.e.*, those with a similar structure to tripeptides) were transported by the same carrier-mediated mechanism as the transport of dietary peptides[97]. Furthermore, uptake of the dipeptide glycylglycine was competitively inhibited by several β-lactam antibiotics (ciclacillin, cefadroxil, cephalexin) and *vice versa*[97]. Amoxicillin was later confirmed to be a substrate of PEPT1, as well as the renal drug transporter peptide transporter 2 (PEPT2)[92]. Comparison of the uptake and flux of β-lactam antibiotics across Caco-2 cell monolayers indicated that most, including amoxicillin, had low affinity for PEPT1 (K_i > 7 mM) and that steric resemblance to a tripeptide backbone was essential for uptake by PEPT1[81,98].

After being taken up into the enterocyte, efflux transporters would also be required for amoxicillin to egress across the BL membrane into the blood due to its anticipated poor

membrane permeability. On the BL membrane of enterocytes, possible candidates for the efflux of amoxicillin include MRP3[99], MRP4[100], BL peptide transporters[20], and organic solute transporter α/β (OST α/β)[19]. Of these, BL peptide transporters or MRP transporters appear to be likely candidates since amoxicillin is a peptidomimetic compound and substrate of PEPT1, and MRP transporters typically transport anionic or zwitterionic compounds[101]. As other β-lactam antibiotics (*e.g.*, cefadroxil, cephalexin, and other cephalosporins[102,103]) are known MRP3 or MRP4 substrates, it is possible that these transporters may also be involved in the efflux of amoxicillin on the BL membrane. Among the β-lactam antibiotics, those with 6-membered ring structures (the cephalosporin antibiotics) are transported by MRP4 more efficiently compared to those with 5-membered ring structures, such as amoxicillin[103].

Peptide transporters have also been tentatively identified on the BL membrane that may be responsible for both the BL uptake and BL efflux of peptide-like drugs, although to date, only BL uptake by these transporters has been characterized functionally. Evidence for BL efflux mediated by these transporters has not been provided as yet[20–22]. Like the AP uptake transporter PEPT1, the BL peptide uptake transporter is pH-dependent with broad substrate specificity for dipeptides and tripeptides[21]. Given the more acidic pH expected intracellularly as compared to the blood, and the unknown relevance of removing dietary peptides from the blood and transferring to enterocytes, the physiological role of this uptake transporter is unknown[21]. However, a BL efflux transporter for peptides is physiologically relevant for the absorption of dietary peptides that are taken up by AP PEPT1 but are not hydrolyzed intracellularly to a form that can easily cross the BL membrane[22]. Unlike PEPT1 and the BL peptide uptake transporter, the BL peptide efflux transport is a facilitative transport system, is bidirectional, and does not appear to be pH-dependent[20,104].

The contribution of these mechanisms to the oral absorption of amoxicillin has not been elucidated, although age-dependent differences in the contribution of these transport mechanisms and infant physiology may explain the high variability in amoxicillin PK and treatment failures observed in children[105].

Amoxicillin Distribution

Amoxicillin is not extensively protein bound (<20% bound to plasma proteins) with a volume of distribution of 0.26 to 0.41 L/kg[78]. The target for AOM, the middle ear, is not highly perfused. The kinetics of amoxicillin influx across the human middle ear mucosal membrane have not been studied; however, studies in an established chinchilla model of inner and middle ear diseases suggested that amoxicillin may require active transport across the middle ear mucosal epithelium[106]. Amoxicillin concentrations in the middle ear are highly variable, even between the left and right ears of the same patient. Concentrations between 4 and 8 µg/mL in the middle ear have been reported 3 hours after a 45 mg/kg oral dose in children, which would exceed the MIC for the majority of subjects, but were undetectable in 15% to 35% of subjects[107].

Amoxicillin Elimination

Amoxicillin has a short terminal half-life of approximately 1 to 1.5 hrs in adults, and renal clearance accounts for up to 80% of amoxicillin elimination[78]. It can be hydrolyzed in the gut to an inactive penicilloic acid by bacteria that produce β-lactamase[108]. Up to 25% of an amoxicillin oral dose is recovered in urine as the penicilloic acid[108], which may contribute to some variability in amoxicillin absorption. Amoxicillin undergoes active renal secretion that exceeds the glomerular filtration rate (GFR), with some reabsorption due to PEPT2 as well as PEPT1 to a lesser extent[92]. While specific transporters have not been identified in the renal secretion of amoxicillin, organic anion transporter 1 (OAT1) has been ruled out as an uptake

transporter for amoxicillin[92]. However, the renal clearance of amoxicillin is significantly reduced by the OAT inhibitor, probenecid[109], suggesting that another OAT transporter may be involved in its uptake and secretion.

Effect of Age on Amoxicillin Disposition

Gastric emptying and transit time do not appear to be significantly different in neonates or children compared to adults[110,111]. However, the composition of infant meals is higher in fat (breast milk is 50% fat) compared to a typical adult meal, and neonates eat more frequently (up to 10 times daily), making it difficult to extrapolate food effects to infants[112]. PK studies suggest that absorption (C_{max} and AUC) of another β-lactam, penicillin V, is significantly reduced in infants and children when given with food or with milk, but only slightly reduced in adults[112].

Sugar absorption tests (performed with mannitol) suggest that intestinal permeability is highest within the first two days of life and rapidly declines over the first month of life[113,114]. Sugar absorption studies conducted in premature infants also suggest that overall intestinal permeability is higher than in adults[14]. Transepithelial electrical resistance (TEER), indicative of the barrier property of the intercellular tight junctions, is significantly lower in neonatal intestinal tissue compared to adolescents and adults[27]. Therefore, if paracellular transport plays a significant role in amoxicillin intestinal absorption, it is possible that the difference in intestinal permeability in infants might play an important role in differential amoxicillin oral bioavailability in children compared to adults.

GFR reaches adult values after the first year of life, but continues to increase above the adult values, and peaks between two and five years of age before decreasing to typical adult levels[115]. During postnatal development, the proximal tubules have low passive paracellular permeability compared to the adult proximal tubules, and express different levels of the tight

junction proteins claudin-2 and occludin[116]. In contrast, tubular secretion reaches adult levels after the first year of life and remains steady to adulthood. Therefore, drugs that are primarily renally cleared and have net tubular secretion[117], such as amoxicillin, may have greater contribution of GFR in children between 2 and 5 years of age compared to adults (on a per kg basis)[115].

The expression and function of intestinal transporters implicated in the absorption of amoxicillin are likely to be affected by age. Gene expression (mRNA) of PEPT1 has been reported to be lower (0.8-fold) in the small intestine of 26 neonates and infants compared to older children and adolescents, with similar tissue distribution of the corresponding protein as determined by immunohistochemical staining[118]. Comparative studies of protein expression of PEPT1 in infants or children compared to adults have not been published. Studies in other species indicate that PEPT1 expression and activity are highest immediately after birth and during weaning, suggesting that the uptake of amoxicillin in infants may differ from that of adults[119,120].

Rationale for the Proposed Research

As outlined in the introductory paragraphs, the proposed research was undertaken to develop pediatric PBPK models for drugs with transporter-mediated disposition. Previously, the Thakker Laboratory has developed bottom-up PBPK models for drugs that are cleared by oxidative metabolism in pediatric (voriconazole) and premature neonate (sildenafil) populations[12,13]. The impact of age on drugs that undergo CYP-mediated hepatic metabolism is well studied compared to the impact of age on drugs that are absorbed and/or cleared *via* transporter-mediated processes. In part, this is due to sparse data on transporter ontogeny in the intestine, liver, and kidney, as well as technical difficulties in obtaining pediatric tissue and in

extrapolating *in vitro* transporter kinetic data to their role *in vivo* in the disposition of drugs[32,33]. Furthermore, although pediatric and adult physiological data are available for the purposes of PBPK modeling, gaps still remain in the understanding of some age-related differences that limit the application of PBPK models for pediatric predictions. Specifically, major gaps remain in incorporating pediatric GI physiology - the impact of age on food effects, bile secretion, differences in paracellular permeability, intestinal fluid composition and pH, and gastric fluid volume – into PBPK models to simulate and predict drug absorption in children[112].

The use of pediatric PBPK models is growing to estimate age-related PK changes and to select appropriate pediatric doses, potentially replacing expensive pediatric clinical PK trials[2,8], Thus, there is a need for better understanding of how pediatric physiology affects drug disposition, improved *in vitro* to *in vivo* extrapolation of transporter-mediated processes, as well as PBPK modeling of pediatric drugs for which transporters play a major role in disposition. The difficulties apparent in this approach are not dissimilar to those encountered elsewhere in pediatric research, namely limited pediatric PK data, pediatric physiology data, and pediatric tissue available for study. For PBPK model building and validation, observed concentration data points and PK parameters are more readily available for adults than for children and infants. Even where published pediatric concentration data and PK parameters are available in the literature, these data are often derived from a small number of patients, covering a broad range of ages and development (sometimes including adolescents). The pooling of data across multiple age groups, or data on only a few subjects representing age groups, make it difficult identify age-related effects. Despite these difficulties, the efforts to build pediatric PBPK models should continue so that the gaps in knowledge and their impact on our ability to predict safe and effective pediatric doses are uncovered and addressed.

For this research, two pediatric drugs whose disposition is likely affected by transporters were selected for the development of PBPK models using the following criteria: 1) drugs that are important in pediatric therapy; 2) drugs for which pediatric doses are extrapolated from adult data and, therefore, may be sub-optimal with respect to their efficacy or safety; and 3) drugs for which adult and pediatric concentration data and PK parameters are available in the literature for model validation.

As previously indicated, the first drug selected, vincristine, is used to treat a variety of pediatric cancers such as ALL as well as acute myeloid leukemia, non-Hodgkin's lymphoma, and Wilms tumor. As noted in this chapter, vincristine has a narrow therapeutic range due to its dose-limiting adverse effects of peripheral neuropathy. Understanding the relationship between vincristine PK and peripheral neuropathy is difficult because of the sparse clinical PK data in adults and children, despite a long history of use as an anti-cancer treatment. Furthermore, vincristine PK is highly variable and its clearance (per kg) has been reported in infants and children to be higher than in adults[51,55]. Because vincristine is cytotoxic, it is not feasible to administer the drug to healthy volunteers for extensive PK and drug-drug interaction studies. Therefore, applying a bottom-up PBPK model to predict disposition of vincristine in adults and children could assist in understanding the basis of age-related PK differences in distribution and clearance, and in elucidating safe and effective pediatric doses.

Amoxicillin was chosen as the second drug because it is one of the most commonly prescribed drugs for treatment of AOM in infants and children, and transporters are implicated in its oral absorption and renal clearance. As previously noted in this chapter, amoxicillin has low passive permeability, but high oral bioavailability, presumably due to significant contribution of intestinal drug transporters. Minimal clearance by metabolism was also a factor in selecting

amoxicillin, because it would simplify the development of an oral pediatric PBPK model of a drug for which transporters are important in absorption.

While PEPT1 is implicated in its uptake into enterocytes, the contribution of active AP uptake, paracellular transport, and BL efflux to the overall intestinal absorption of amoxicillin has not been elucidated prior to this research. Infants have higher intestinal permeability compared to adults, specifically higher paracellular permeability as determined by sugar absorption tests and TEER measurements[113,114]. Therefore, paracellular transport may play a larger role in infant intestinal absorption of amoxicillin, and the importance of transporters such as PEPT1 may differ by age group depending on the relative contribution of the paracellular *vs* transcellular pathways. As a key pediatric drug, amoxicillin is also a good candidate for pediatric PBPK modeling due to its widespread use and unanswered questions regarding its efficacy at higher doses. Recommended pediatric doses for AOM have increased in order to address the increase in antibiotic resistance, although higher doses may not improve MEF penetration or efficacy due to the dose-dependent absorption of amoxicillin[87,88]. Although amoxicillin is widely used, it is difficult logistically and ethically to perform clinical PK studies in children, especially in infants. Therefore, it is important to 1) understand the mechanisms of amoxicillin absorptive transport and dose-dependency, and 2) develop a pediatric PBPK model of amoxicillin that can be used to predict oral amoxicillin PK and understand its relation to the MIC of AOM microorganisms.

Hypotheses

The hypotheses tested in the research described in this dissertation are that: **i)** age-dependent changes in CYP3A expression/activity and P-gp expression/activity contribute to differences in the clearance and exposure of vincristine in infant and pediatric populations

compared to adults; and **ii)** amoxicillin intestinal absorption in adults and infants is influenced by age-dependent differences in PEPT1 expression and overall intestinal permeability, specifically paracellular permeability.

Specific Aims

A bottom-up PBPK model of vincristine requires incorporation of its physicochemical properties, as well as important parameters in its disposition, *i.e.*, metabolism by CYP3A4/5, efflux by P-gp, and intracellular binding to β-tubulin. *In vitro* metabolism parameters were obtained from the literature, as extensive kinetic studies had been performed in cryopreserved human hepatocytes (obtained from both low- and high-CYP3A5 expressors), human liver microsomes, and recombinant CYP3A4 and CYP3A5 enzymes. In contrast, although vincristine was well known as a substrate of P-gp, its kinetic parameters had not been previously determined. This was evaluated in Specific **Aim 1**, in which the *in vitro* kinetic parameters for P-gp efflux were obtained, the adult PBPK model of vincristine was developed and validated, and the adult PBPK model was adapted to a pediatric PBPK model of vincristine and validated:

Specific Aim 1: Develop PBPK models of IV vincristine in adult and pediatric (≤10 years) populations.

- 1a. Determine the kinetics of vincristine efflux (K_m and J_{max}) by P-gp in MDCKII-MDR1 cells.
- 1b. Develop a bottom-up PBPK model describing vincristine disposition in adults following IV administration and validate the model using existing adult clinical PK data
- 1c. Adapt the adult PBPK model to develop a pediatric PBPK model to describe vincristine disposition in children and validate the model using existing pediatric PK data.

Specific **Aims 2 and 3** were formulated to extend this modeling approach to a second drug with transporter-mediated intestinal absorption (*i.e*., amoxicillin) and develop a PBPK model of oral amoxicillin in adults and infants. Important factors to be evaluated in the model included key parameters in amoxicillin intestinal absorption and PK, *i.e.* intestinal permeability, relative contribution of paracellular *vs* transporter-mediated transcellular transport, and renal clearance. Sugar absorption studies in infants indicate that infants have higher intestinal permeability and paracellular permeability compared to adults in the first few months of life[113,114]. Although amoxicillin is a known substrate of PEPT1, and based on its properties (*i.e.*, small size and hydrophilic) is likely to have some paracellular component to its transport, the relative contributions of these mechanisms to amoxicillin absorptive transport have not been elucidated to date. Thus, Specific **Aims 2 and 3** were formulated to (1) understand the mechanisms of amoxicillin intestinal absorption, including understanding the relative contributions of paracellular *vs* transcellular transport (including PEPT1-mediated AP uptake), and (2) develop and validate PBPK models of oral amoxicillin in adults and infants that could predict amoxicillin PK and its relation to anticipated MIC of AOM microorganisms. In **Aim 2**, a three-compartmental modeling approach was utilized to determine the relative contribution of the paracellular *vs* transcellular pathways to the absorption of amoxicillin. An indirect modeling approach was needed because paracellular transport cannot be determined in isolation experimentally. A similar approach was previously used for the cationic and hydrophilic drugs metformin and ranitidine. The study demonstrated that the absorptive transport of ranitidine is approximately 45-60% paracellular[121] and involves AP uptake by anion transporters and BL efflux by multidrug resistance-associated proteins (MRP) 3, and that the transport is attenuated by AP efflux *via* P-gp and MRP2[122]. The role of PEPT1 in the AP uptake and intestinal

absorption of amoxicillin was determined *in vitro* using Caco-2 cell monolayers and adult intestinal epithelia. In **Aim 3**, a PBPK model of oral amoxicillin in adults was developed by incorporating the kinetic parameters determined in **Aim 2**. The adult model was refined and validated against existing clinical data, and then adapted to a PBPK model for the infant population.

Specific Aim 2: Determine the contribution of PEPT1 to AP enterocytic uptake and permeation of amoxicillin across Caco-2 cell monolayers and adult intestinal epithelia.

- 2a. Determine *in vitro* absorptive transport, AP/BL uptake, and AP/BL efflux of amoxicillin in Caco-2 cell monolayers and adult intestinal epithelia. Transport studies will be conducted in Caco-2 cell monolayers and in Ussing-type diffusion chambers using fresh human intestinal epithelia.
- 2b. Apply data from Aim 2a to a three-compartment kinetic model and determine the relative contributions of paracellular and transcellular absorptive transport of amoxicillin in Caco-2 cell monolayers and adult intestinal epithelium.
- 2c. Determine the relative contribution of PEPT1 to the overall absorptive transport and permeation of amoxicillin across Caco-2 cell monolayers and adult intestinal epithelium.

Specific Aim 3: Develop PBPK models to describe the PK of amoxicillin in adult and infant (≤2 years) populations following oral administration.

- 3a. Quantify the gene and protein expression of PEPT1 in Caco-2 cells, adult intestinal tissue, and infant intestinal tissue using rt PCR and proteomic mass spectrometry methods.
- 3b. Develop a PBPK model to describe the oral bioavailability and PK of amoxicillin in adults. The model will incorporate the uptake kinetics by PEPT1, P_{app}, the contribution of

paracellular transport, and PEPT1 expression. Validate the model using existing adult clinical PK data.

- 3c. Develop a PBPK model of amoxicillin in infants following oral administration by adapting the adult PBPK model from Aim 3b. The infant PBPK model will account for kinetic parameters of amoxicillin transport and age-related differences, *i.e.*, PEPT1 expression, P_{app}, GI physiology, and renal clearance. Confirm model estimations of oral bioavailability using existing population PK parameters of amoxicillin in infants.

Figure 1-1 Whole-body PBPK model structure.

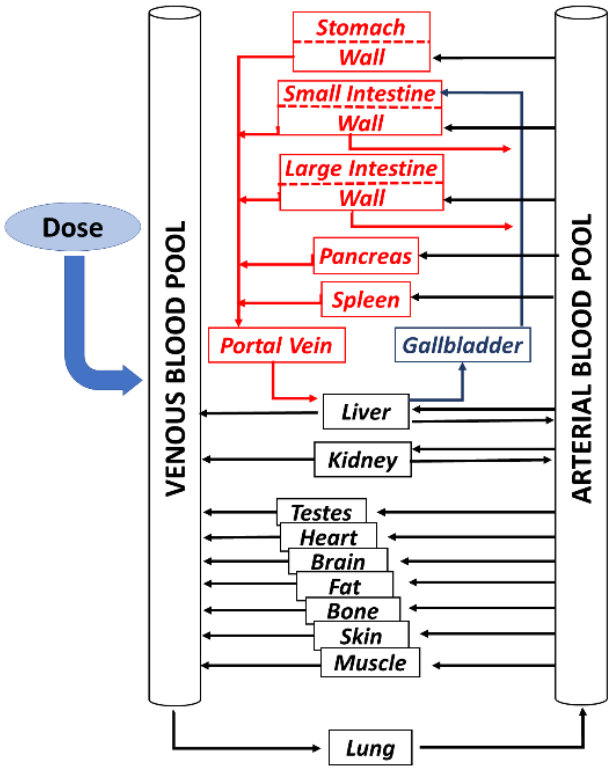

Simulated by PK-Sim® software package. Adapted from Willmann *et al*.[123]

Figure 1-2. Pathways of absorption across the intestinal epithelium and examples of AP and BL drug transporters.

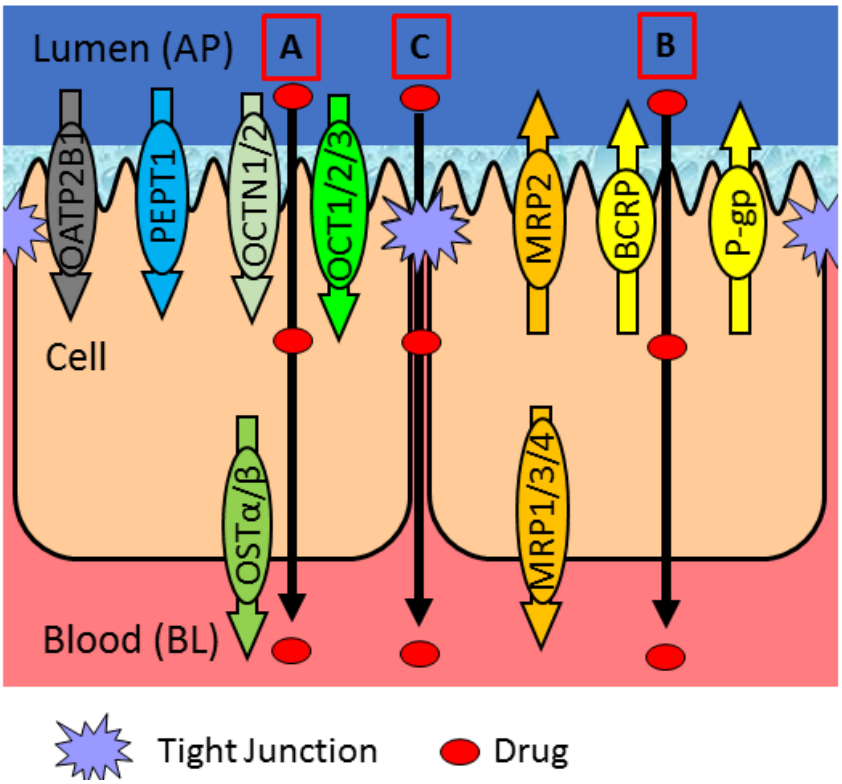

Adapted courtesy of Drs. William Proctor and Kevin Han. Compounds can be absorbed by two pathways across the intestinal epithelium: A) transcellular transport which can consist of both passive and B) active (transporter-mediated) processes, as well as C) paracellular transport *via* passive diffusion of drugs through the tight junctions. Examples of intestinal AP uptake (OATP2B1, PEPT1, OCTN1/2, OCT1/2/3), AP efflux (MRP2, BCRP, P-gp), and BL efflux (OSTα/β, MRP1/3/4) are also shown in the figure above.

Figure 1-3. Structure of vincristine (top) and its metabolite M1 (bottom).

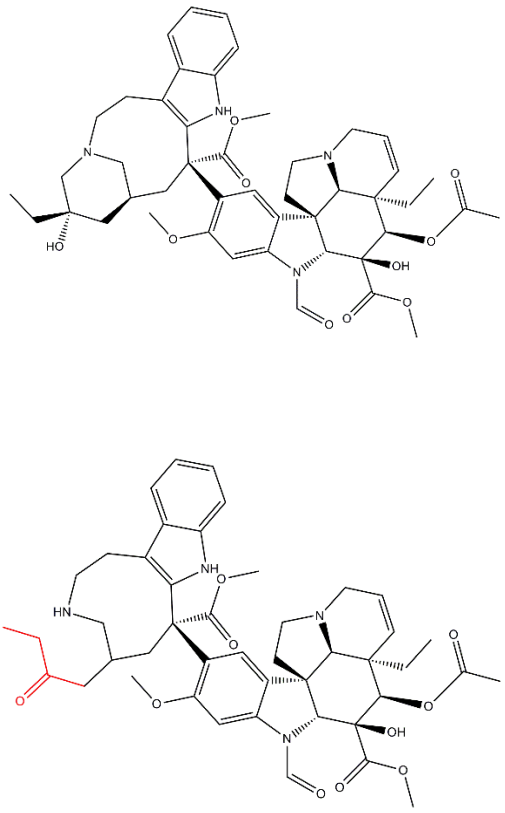

Figure 1-4. Vincristine binds to free β-tubulin subunits.

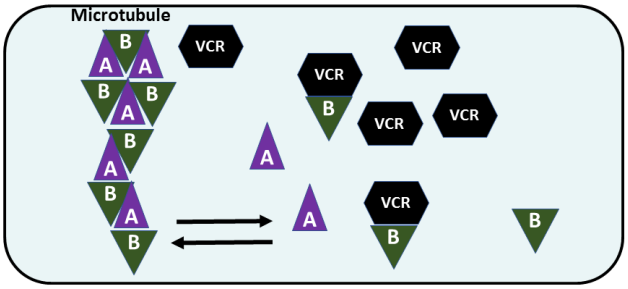

Microtubule structures are comprised of units of α-tubulin (represented by the triangles marked A) and β-tubulin subunits (represented by the triangles marked B). The microtubules are in equilibrium between an assembled and dissembled state within the cell and exchange subunits with an intracellular pool of unbound α- and β-tubulin when dissembling at the ends. Vincristine binds to the free intracellular β-tubulin, reducing the amount of unbound β-tubulin for microtubule reassembly[124].

Figure 1-5. Structure of catharanthine (top), vindoline (middle), and vindesine (bottom).

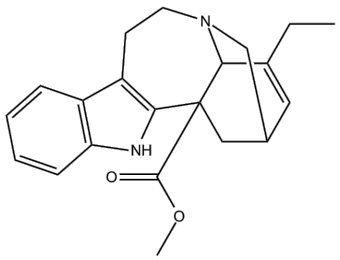

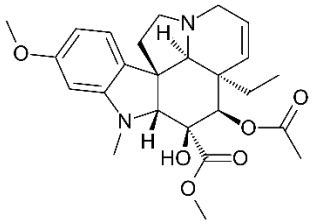

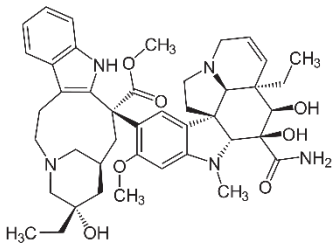

Figure 1-6. Increases in amoxicillin C_{max} and AUC are less than dose-proportional.

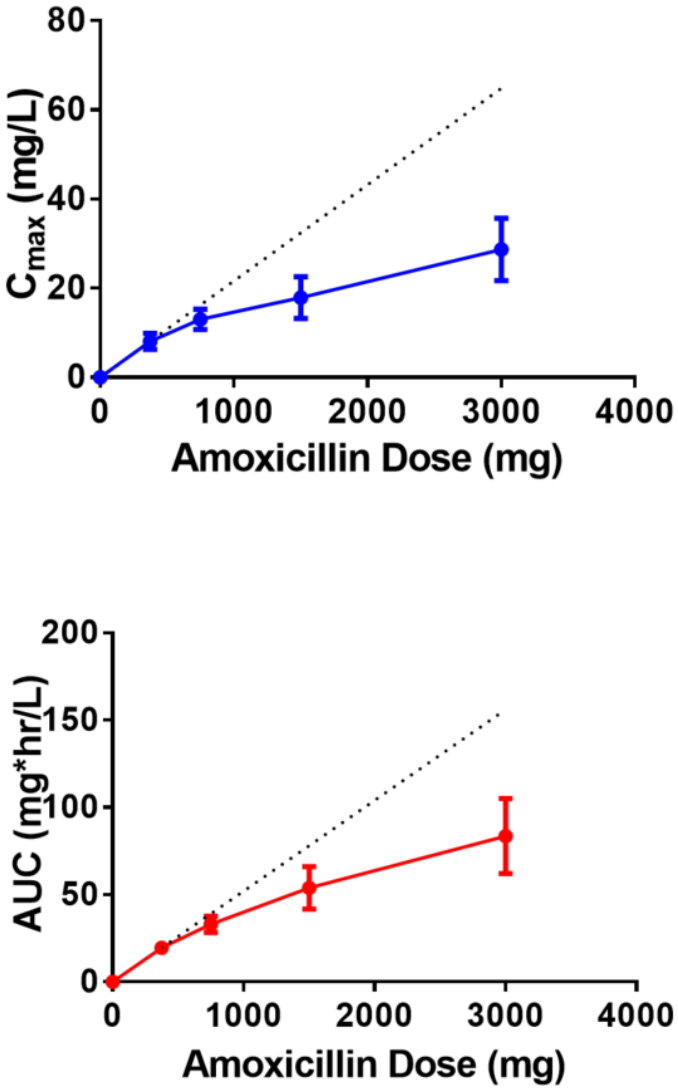

Oral doses of 375, 750, 1500, and 3000 mg amoxicillin tablets were administered to 12 healthy adult subjects in a fasting state. Solid lines represent mean ± SD. The dotted black line represents C_{max} or AUC values that would be expected if these parameters increased proportionally with the amoxicillin dose administered. Figures adapted from Sjovall *et al.*, 1985[91].

Figure 1-7. Basic structure of a penicillin β-lactam antibiotic.

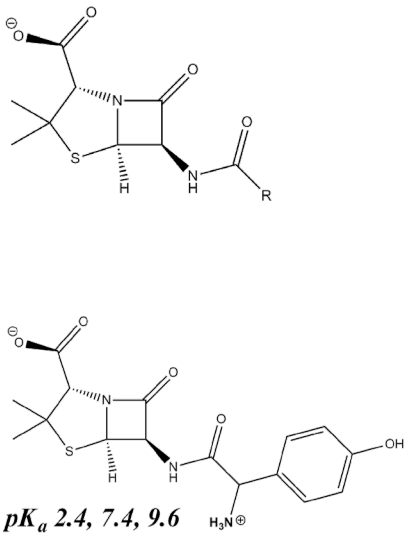

Basic structure of a penicillin, where R represents a side chain (top), and the structure of amoxicillin (bottom).

REFERENCES

1. Kearns GL, Abdel-Rahman SM, Alander SW, *et al.* Developmental Pharmacology--Drug Disposition, Action, and Therapy in Infants and Children. *N Engl J Med*. 2003;349(12):1157-67.

2. Leong R, Vieira MLT, Zhao P, *et al.* Regulatory Experience with Physiologically Based Pharmacokinetic Modeling for Pediatric Drug Trials. *Clin Pharmacol Ther*. 2012;91(5):926-31.

3. Maharaj A, Edginton A. Physiologically Based Pharmacokinetic Modeling and Simulation in Pediatric Drug Development. *CPT Pharmacometrics Syst Pharmacol*. 2014;3(11):e148.

4. Roberts R, Rodriguez W, Murphy D, *et al.* Pediatric Drug Labeling: Improving the Safety and Efficacy of Pediatric Therapies. *JAMA*. 2003;290(7):905-911.

5. Chen M, LeDuc B, Kerr S, *et al.* Identification of Human UGT2B7 as the Major Isoform Involved in the O-Glucuronidation of Chloramphenicol. *Drug Metab Dispos*. 2010;38(3):368-375.

6. Balan S, Azmi M, Hassali A, *et al.* Two Decades of Off‐label Prescribing in Children: A Literature Review. *World J Pediatr*. 2018;14(6):528-540.

7. Penkov D, Tomasi P, Eichler I, *et al.* Pediatric Medicine Development: An Overview and Comparison of Regulatory Processes in the European Union and United States. *Ther Innov Regul Sci*. 2017;51(3):360-371.

8. Wagner C, Zhao P, Pan Y, *et al.* Application of Physiologically Based Pharmacokinetic (PBPK) Modeling to Support Dose Selection : Report of an FDA Public Workshop on PBPK. *Clin Pharmacol Ther*. 2015;4(4):226-230.

9. Yanni SB, Augustijns PF, Benjamin DK, *et al.* In Vitro Investigation of the Hepatobiliary Disposition Mechanisms of the Antifungal Agent Micafungin in Humans and Rats. *Drug Metab Dispos*. 2010;38(10):1848-1856.

10. Yanni SB, Annaert PP, Augustijns P, *et al.* In Vitro Hepatic Metabolism Explains Higher Clearance of Voriconazole in Children versus Adults : Role of CYP2C19 and Flavin-Containing Monooxygenase 3. *Drug Metab Dispos*. 2010;38(1):25-31.

11. Yanni SB, Annaert PP, Augustijns P, *et al.* Role of Flavin-Containing Monooxygenase in

Oxidative Metabolism of Voriconazole by Human Liver Microsomes ABSTRACT : 2008;36(6):1119-1125.

12. Zane NR, Thakker DR. A Physiologically Based Pharmacokinetic Model for Voriconazole Disposition Predicts Intestinal First-Pass Metabolism in Children. *Clin Pharmacokinet*. 2014;53(12):1171-1182.

13. Zane NR. Predicting Pharmacokinetic Behavior and Dose of Sildenafil and Voriconazole in Neonatal and Pediatric Populations by in Vitro Metabolism and PBPK Modeling (Doctoral Dissertation). *Retrieved from Carolina Digit Repos*. 2015.

14. Rouwet E V, Heineman E, Buurman W a, *et al.* Intestinal Permeability and Carrier-Mediated Monosaccharide Absorption in Preterm Neonates during the Early Postnatal Period. *Pediatr Res*. 2002;51(1):64-70.

15. Itallie CM Van, Anderson JM. Claudins and Epithelial Paracellular Transport. *Annu Rev Physiol*. 2006;68:403-429.

16. Shen L, Weber CR, Raleigh DR, *et al.* Tight Junction Pore and Leak Pathways : A Dynamic Duo. *Annu Rev Physiol*. 2011;73:283-309.

17. Knight B, Troutman M, Thakker DR. Deconvoluting the Effects of P-Glycoprotein on Intestinal CYP3A : A Major Challenge. *Curr Opin Pharmacol*. 2006;6:528-532.

18. Toyoda Y, Hagiya Y, Adachi T, *et al.* MRP Class of Human ATP Binding Cassette (ABC) Transporters: Historical Background and New Research Directions. *Xenobiotica*. 2008;38(7-8):833-862.

19. Dawson PA, Hubbert M, Haywood J, *et al.* The Heteromeric Organic Solute Transporter α-β, Ostα-Ostβ, Is an Ileal Basolateral Bile Acid Transporter□. *J Biol Chem*. 2005;280(8):6960-6968.

20. Irie M, Terada T, Okuda M, *et al.* Efflux Properties of Basolateral Peptide Transporter in Human Intestinal Cell Line Caco-2. *Pflugers Arch Eur J Physiol*. 2004;449(2):186-194.

21. Berthelsen R, Nielsen CU, Brodin B. Basolateral Glycylsarcosine (Gly-Sar) Transport in Caco-2 Cell Monolayers Is PH Dependent. *J Pharm Pharmacol*. 2013;65(7):970-979.

22. Rohm F, Daniel H, Spanier B. Transport Versus Hydrolysis: Reassessing Intestinal Assimilation of Di- and Tripeptides by LC – MS / MS Analysis. *Mol Nutr Food Res*. 2019;1900263:1-10.

23. Proctor WR, Ming X, Bourdet D, *et al.* Why Does the Intestine Lack Basolateral Efflux Transporters for Cationic Compounds? A Provocative Hypothesis. *J Pharm Sci*. 2016;105(2):484-496.

24. Bartelink IH, Rademaker CMA, Schobben AFAM, *et al.* Guidelines on Paediatric Dosing on the Basis of Developmental Physiology and Pharmacokinetic Considerations. *Clin Pharmacokinet*. 2006;45(11):1077-1097.

25. Fallingborg J, Christensen LA, Ingeman-Nielsen M, *et al.* Measurement of Gastrointestinal PH and Regional Transit Times in Normal Children. *J Pediatr Gastroenterol Nutr*. 1990;11:211-214.

26. Batchelor HK, Kendall R, Desset-Brethes S, *et al.* Application of in Vitro Biopharmaceutical Methods in Development of Immediate Release Oral Dosage Forms Intended for Paediatric Patients. *Eur J Pharm Biopharm*. 2013;85(3 PART B):833-842.

27. Ralls MW, Miyasaka E a., Herman RS, *et al.* Enteral Deprivation Leads to a Loss of Intestinal Epithelial Barrier Function in Pediatric Patients. *J Am Coll Surg*. 2012;215(3):S75-S76.

28. Batchelor HK, Kendall R, Desset-brethes S, *et al.* Application of in Vitro Biopharmaceutical Methods in Development of Immediate Release Oral Dosage Forms Intended for Paediatric Patients. *Eur J Pharm Biopharm*. 2013;85(3):833-842.

29. Batchelor H. Paediatric Biopharmaceutics Classification System: Current Status and Future Decisions. *Int J Pharm*. 2014;469(2):251-253.

30. Abdel-Rahman SM, Amidon GL, Kaul A, *et al.* Summary of the National Institute of Child Health and Human Development-Best Pharmaceuticals for Children Act Pediatric Formulation Initiatives Workshop-Pediatric Biopharmaceutics Classification System Working Group. *Clin Ther*. 2012;34(11):S11-24.

31. Fu D, Arias IM. Intracellular Trafficking of P-Glycoprotein. *Int J Biochem Cell Biol*. 2012;44(3):461-464.

32. Prasad B, Unadkat JD. Optimized Approaches for Quantification of Drug Transporters in Tissues and Cells by MRM Proteomics. *AAPS J*. 2014;16(4):634-48.

33. Peng KW, Bacon J, Zheng M, *et al.* Ethnic Variability in the Expression of Hepatic Drug Transporters: Absolute Quantification by an Optimized Targeted Quantitative Proteomic Approach. *Drug Metab Dispos*. 2015;43(7):1045-1055.

34. Brouwer KL, Keppler D, Hoffmaster K a, *et al.* In Vitro Methods to Support Transporter Evaluation in Drug Discovery and Development. *Clin Pharmacol Ther*. 2013;94(1):95-112.

35. Yang K, Guo C, Woodhead JL, *et al.* Sandwich-Cultured Hepatocytes as a Tool to Study Drug Disposition and Drug-Induced Liver Injury. *J Pharm Sci*. 2016;105(2):443-459.

36. Lundquist P, Lööf J, Floby E, *et al.* The Impact of Solute Carrier (SLC) Drug Uptake Transporter Loss in Human and Rat Cryopreserved Hepatocytes on Clearance Predictions. *Drug Metab Dispo*. 2014;42:469-480.

37. Kimoto E, Yoshida K, Balogh LM, *et al.* Characterization of Organic Anion Transporting Polypeptide (OATP) Expression and Its Functional Contribution to the Uptake of Substrates in Human Hepatocytes. *Mol Pharm*. 2012:3535-3542.

38. Li Q, Yang H, Peng X, *et al.* Ischemia/Reperfusion- Inducible Protein Modulates the Function of Organic Cation Transporter 1 and Multidrug and Toxin Extrusion 1. *Mol Pharm*. 2013;10(7):2578-2587.

39. Wang F, Zhou F, Kruh GD, *et al.* Influence of Blood-Brain Barrier Efflux Pumps on the Distribution of Vincristine in Brain and Brain Tumors. *Neuro Oncol*. 2010;12(10):1043-1049.

40. Wang L, Wang C, Liu Q, *et al.* PEPT1- and OAT1/3-Mediated Drug-Drug Interactions between Bestatin and Cefixime in Vivo and in Vitro in Rats, and in Vitro in Human. *Eur J Pharm Sci*. 2014;63:77-86.

41. Luckner P, Brandsch M. Interaction of 31 Beta-Lactam Antibiotics with the H +/Peptide Symporter PEPT2: Analysis of Affinity Constants and Comparison with PEPT1. *Eur J Pharm Biopharm*. 2005;59(1):17-24.

42. De Cock PAJG, Standing JF, Barker CIS, *et al.* Augmented Renal Clearance Implies a Need for Increased Amoxicillin-Clavulanic Acid Dosing in Critically Ill Children. *Antimicrob Agents Chemother*. 2015;59(11):7027-7035.

43. Ward E, DeSantis C, Robbins A, *et al.* Childhood and Adolescent Cancer Statistics, 2014. *CA Cancer J Clin*. 2014;64(2):83-103.

44. Inaba H, Greaves M, Mullighan C. Acute Lymphoblastic Leukemia. *Lancet*. 2013;381(9881):1-27.

45. Dennison JB, Kulanthaivel P, Barbuch RJ, *et al.* Selective Metabolism of Vincristine in

Vitro by CYP3A5. *Drug Metab Dispos*. 2006;34(8):1317-1327.

46. Dennison JB, Jones DR, Renbarger JL, *et al.* Effect of CYP3A5 Expression on Vincristine Metabolism with Human Liver Microsomes. *J Pharmacol Exp Ther*. 2007;321(2):553-63.

47. Dennison JB, Mohutsky M a, Barbuch RJ, *et al.* Apparent High CYP3A5 Expression Is Required for Significant Metabolism of Vincristine by Human Cryopreserved Hepatocytes. *J Pharmacol Exp Ther*. 2008;327(1):248-257.

48. Gidding CEM, Kellie SJ, Kamps W a., *et al.* Vincristine Revisited. *Crit Rev Oncol Hematol*. 1999;29(3):267-287.

49. Keglevich P, Hazai L, Kalaus G, *et al.* Modifications on the Basic Skeletons of Vinblastine and Vincristine. *Molecules*. 2012;17(5):5893-5914.

50. Levêque D, Jehl F. Molecular Pharmacokinetics of Catharanthus (Vinca) Alkaloids. *J Clin Pharmacol*. 2007;47(5):579-588.

51. Gidding CE, Meeuwsen-de Boer GJ, Koopmans P, *et al.* Vincristine Pharmacokinetics after Repetitive Dosing in Children. *Cancer Chemother Pharmacol*. 1999;44(3):203-9.

52. Verstappen C, Koeppen S, Heimans J, *et al.* Induced Peripheral Neuropathy With Unexpected Off-Therapy Worsening. *Neurology*. 2005;64(6):1076.

53. Park SB, Goldstein D, Krishnan A V, *et al.* Chemotherapy-Induced Peripheral Neurotoxicity : A Critical Analysis. 2013;63(6):419-437.

54. Van den Berg HW, Desai ZR, Wilson R, *et al.* The Pharmacokinetics of Vincristine in Man: - Reduced Drug Clearance Associated with Raised Serum Alkaline Phosphatase and Dose-Limited Elimination. *Cancer Chemother Pharmacol*. 1982;8(2):215-219.

55. Crom WR, de Graaf SS, Synold T, *et al.* Pharmacokinetics of Vincristine in Children and Adolescents with Acute Lymphocytic Leukemia. *J Pediatr*. 1994;125(4):642-9.

56. Donigian DW, Owellen RJ. Interaction of Vinblastine, Vincristine, and Colchicine with Serum Proteins. *Biochem Pharmacol*. 1973;22:2113-2119.

57. Israels T, Damen CWN, Cole M, *et al.* Malnourished Malawian Patients Presenting with Large Wilms Tumours Have a Decreased Vincristine Clearance Rate. *Eur J Cancer*. 2010;46(10):1841-1847.

58. Nicolaï J, Thevelin L, Bing Q, *et al.* Role of the OATP Transporter Family and a Benzbromarone-SensitiveEfflux Transporter in the Hepatocellular Disposition of Vincristine. *Pharm Res*. 2017;34(11):2336-2348.

59. Van Zanden JJ, De Mul A, Wortelboer HM, *et al.* Reversal of in Vitro Cellular MRP1 and MRP2 Mediated Vincristine Resistance by the Flavonoid Myricetin. *Biochem Pharmacol*. 2005;69(11):1657-1665.

60. Reichle A, Diddens H, Altmayr F, *et al.* Beta-Tubulin and P-Glycoprotein: Major Determinants of Vincristine Accumulation in B-CLL Cells. *Leuk Res*. 1995;19(11):823-829.

61. Wierzba K, Sugiyama Y, Okudaira K, *et al.* Tubulin as a Major Determinant of Tissue Distribution of Vincristine. *J Pharm Sci*. 1987;76(12):872-875.

62. Dennison JB, Renbarger JL, Walterhouse DO, *et al.* Quantification of Vincristine and Its Major Metabolite in Human Plasma by High-Performance Liquid Chromatography/Tandem Mass Spectrometry. *Ther Drug Monit*. 2008;30(3):357-64.

63. Guilhaumou R, Simon N, Quaranta S, *et al.* Population Pharmacokinetics and Pharmacogenetics of Vincristine in Paediatric Patients Treated for Solid Tumour Diseases. *Cancer Chemother Pharmacol*. 2011;68:1191-1198.

64. Guilhaumou R, Solas C, Bourgarel-Rey V, *et al.* Impact of Plasma and Intracellular Exposure and CYP3A4, CYP3A5, and ABCB1 Genetic Polymorphisms on Vincristine-Induced Neurotoxicity. *Cancer Chemother Pharmacol*. 2011;68(6):1633-8.

65. Sims RP. The Effect of Race on the CYP3A-Mediated Metabolism of Vincristine in Pediatric Patients with Acute Lymphoblastic Leukemia. *J Oncol Pharm Pract*. 2014.

66. Sethi VS, Jackson D V, White DR, *et al.* Pharmacokinetics of Vincristine Sulfate in Adult Cancer Patients. *Cancer Res*. 1981;41(September):3551-3555.

67. Groninger E, Meeuwsen-de Boar T, Koopmans P, *et al.* Pharmacokinetics of Vincristine Monotherapy in Childhood Acute Lymphoblastic Leukemia. *Pediatr Res*. 2002;52(1):113-118.

68. Patel M, Taskar KS, Zamek-Gliszczynski MJ. Importance of Hepatic Transporters in Clinical Disposition of Drugs and Their Metabolites. *J Clin Pharmacol*. 2016;56(S7):S23-S39.

69. Song S, Suzuki H, Kawai R, *et al.* Vincristine and Digoxin in Rats. *Drug Metab Dispos*.

1999;27(6):689-694.

70. Watanabe T, Miyauchi S, Sawada Y, *et al.* Kinetic Analysis of Hepatobiliary Transport of Vincristine in Perfused Rat Liver. Possible Roles of P-Glycoprotein in Biliary Excretion of Vincristine. *J Hepatol*. 1992;16(1-2):77-88.

71. Maharaj AR, Gonzalez D, Cohen-Wolkowiez M, *et al.* Improving Pediatric Protein Binding Estimates: An Evaluation of A1-Acid Glycoprotein Maturation in Healthy and Infected Subjects. *Clin Pharmacokinet*. 2017:1-13.

72. Prasad B, Gaedigk A, Vrana M, *et al.* Ontogeny of Hepatic Drug Transporters as Quantified by LC-MS/MS Proteomics. *Clin Pharmacol Ther*. 2016;100(4):362-370.

73. Dennison JB, Mohutsky M a, Barbuch RJ, *et al.* Apparent High CYP3A5 Expression Is Required for Significant Metabolism of Vincristine by Human Cryopreserved Hepatocytes. *J Pharmacol Exp Ther*. 2008;327(1):248-57.

74. Zane NR, Chen Y, Wang MZ, *et al.* Cytochrome P450 and Flavin-Containing Monooxygenase Families: Age-Dependent Differences in Expression and Functional Activity. *Pediatr Res*. 2018;83(2):527-535.

75. Stevens JC, Hines RN, Gu C, *et al.* Developmental Expression of the Major Human Hepatic CYP3A Enzymes. *J Pharmacol Exp Ther*. 2003;307(2):573-582.

76. Chai G, Governale L, McMahon AW, *et al.* Trends of Outpatient Prescription Drug Utilization in US Children, 2002-2010. *Pediatrics*. 2012;130(1):23-31.

77. Lieberthal AS, Carroll AE, Chonmaitree T, *et al.* The Diagnosis and Management of Acute Otitis Media. *Pediatrics*. 2013;131(3):e964-99.

78. Thambavita D, Galappatthy P, Mannapperuma U, *et al.* Biowaiver Monograph for Immediate-Release Solid Oral Dosage Forms : Amoxicillin Trihydrate. *J Pharm Sci*. 2017;106(10):2930-2945.

79. Geddes AM, Klugman KP, Rolinson GN. Introduction: Historical Perspective and Development of Amoxicillin/Clavulanate. *Int J Antimicrob Agents*. 2007;30(SUPPL. 2):109-112.

80. Gordon RC, Regamey C, Kirby WMM. Comparative Clinical Pharmacology of Amoxicillin and Ampicillin Administered Orally. *Antimicro*. 1972;1(6):504-507.

81. Brandsch M, Knütter I, Leibach FH. The Intestinal H+/Peptide Symporter PEPT1: Structure-Affinity Relationships. *Eur J Pharm Sci*. 2004;21(1):53-60.

82. Sjovall J, Westerlund D, Alvan G. Renal Excretion of Intravenously Infused Amoxycillin and Ampicillin. *Br J Clin Pharmacol*. 1985;19(2):191-201.

83. Coco A, Vernacchio L, Horst MA, *et al.* Management of Acute Otitis Media after Publication of the 2004 AAP and AAFP Clinical Practice Guideline. *Pediatrics*. 2010;125(2):214-220.

84. Mather MW, Drinnan M, Perry JD, *et al.* A Systematic Review and Meta-Analysis of Antimicrobial Resistance in Paediatric Acute Otitis Media. *Int J Pediatr Otorhinolaryngol*. 2019;123(May):102-109.

85. Salah M, Abdel-Aziz M, Al-Farok A, *et al.* Recurrent Acute Otitis Media in Infants: Analysis of Risk Factors. *Int J Pediatr Otorhinolaryngol*. 2013;77(10):1665-1669.

86. Lister PD, Pong A, Chartrand SA, *et al.* Rationale behind High-Dose Amoxicillin Therapy for Acute Otitis Media Due to Penicillin-Nonsusceptible Pneumococci: Support from in Vitro Pharmacodynamic Studies. *Antimicrob Agents Chemother*. 1997;41(9):1926-1932.

87. Harrison CJ, Welch DF. Middle Ear Effusion Amoxicillin Concentrations in Acute Otitis Media. *Pediatr Infect Dis J*. 1988;17(7):657-658.

88. Sox CM, Finkelstein JA, Yin R, *et al.* Trends in Otitis Media Treatment Failure and Relapse. *Pediatrics*. 2008;121(4):674-679.

89. Kuehn J, Ismael Z, Long PF, *et al.* Reported Rates of Diarrhea Following Oral Penicillin Therapy in Pediatric Clinical Trials. *J Pediatr Pharmacol Ther*. 2015;20(2):90-104.

90. Paintaud G, Alván G, Dahl ML, *et al.* Nonlinearity of Amoxicillin Absorption Kinetics in Human. *Eur J Clin Pharmacol*. 1992;43(3):283-288.

91. Sjovall J, Alvan G, Westerlund D. Dose-Dependent Absorption of Amoxycillin and Bacampicillin. *Clin Pharmacol Ther*. 1985;38(3):241-250.

92. Li M, Anderson GD, Phillips BR, *et al.* Interactions of Amoxicillin and Cefaclor with Human Renal Organic Anion and Peptide Transporters. *Drug Metab Dispos*. 2006;34(4):547-555.

93. Mackenzie B, Loo DDF, Fei Y, *et al.* Mechanisms of the Human Intestinal H ⁺ -Coupled

Oligopeptide Transporter HPEPT1. *J Biol Chem*. 1996;271(10):5430-5437.

94. Daniel H. Molecular and Integrative Physiology of Intestinal Peptide Transport. *Annu Rev Physiol*. 2004;66:361-384.

95. Drozdzik M, Gro C, Penski J, *et al.* Protein Abundance of Clinically Relevant Multidrug Transporters along the Entire Length of the Human Intestine. *Mol Pharm*. 2014;11(10):3547-3555.

96. Shimakura J, Terada T, Saito H, *et al.* Induction of Intestinal Peptide Transporter 1 Expression during Fasting Is Mediated via Peroxisome Proliferator-Activated Receptor Alpha. *Am J Physiol Gastrointest Liver Physiol*. 2006;291(5):G851-6.

97. Nakashima E, Tsuji A, Mizuo H, *et al.* Kinetics and Mechanism of In Vitro Uptake of Amino-Beta-Lactam Antibiotics by Rat Samll Intestine and Relation to the Intact-Peptide Transport System. *Biochem Pharmacol*. 1984;33(21):3345-3352.

98. Brandsch M. Transport of Drugs by Proton-Coupled Peptide Transporters: Pearls and Pitfalls. *Expert Opin Drug Metab Toxicol*. 2009;5(8):887-905.

99. Rost D, Mahner S, Sugiyama Y, *et al.* Expression and Localization of the Multidrug Resistance- Associated Protein 3 in Rat Small and Large Intestine. *Am J Physiol Gastrointest Liver Physiol*. 2001;282:720-726.

100. Ming X, Thakker DR. Role of Basolateral Efflux Transporter MRP4 in the Intestinal Absorption of the Antiviral Drug Adefovir Dipivoxil. *Biochem Pharmacol*. 2010;79(3):455-462.

101. Hillgren KM, Keppler D, Zur a a, *et al.* Emerging Transporters of Clinical Importance: An Update from the International Transporter Consortium. *Clin Pharmacol Ther*. 2013;94(1):52-63.

102. De Waart DR, Van De Wetering K, Kunne C, *et al.* Oral Availability of Cefadroxil Depends on ABCC3 and ABCC4. *Drug Metab Dispos*. 2012;40(3):515-521.

103. Akanuma S, Uchida Y, Ohtsuki S, *et al.* Molecular-Weight-Dependent, Anionic-Substrate-Preferential Transport of β-Lactam Antibiotics via Multidrug Resistance-Associated Protein 4. *Drug Metab Pharmacokinet*. 2011;26(6):602-611.

104. Terada T, Sawada K, Saito H, *et al.* Functional Characteristics of Basolateral Peptide Transporter in the Human Intestinal Cell Line Caco-2. *Am J Physiol*. 1999;276(6 Pt 1):G1435-G1441.

105. Pichichero ME, Reed MD. Variations in Amoxicillin Pharmacokinetic/Pharmacodynamic Parameters May Explain Treatment Failures in Acute Otitis Media. *Pediatr Drugs*. 2009;11(4):243-249.

106. Huang Y, Yang Z, Cartier L, *et al.* Estimating Amoxicillin Influx/Efflux in Chinchilla Middle Ear Fluid and Simultaneous Measurement of Antibacterial Effect. *Antimicrob Agents Chemother*. 2007;51(12):4336-4341.

107. Seikel K, Shelton S, McCracken Jr. GH. Middle Ear Fluid Concentrations of Amoxicillin after Large Dosages in Children with Acute Otitis Media. *Pediatr Infect Dis J*. 1997;16(7):710-711.

108. Cole M, Kenig MD, Hewitt VA. Metabolism of Penicillins to Penicilloic Acids and 6-Aminopenicillanic Acid in Man and Its Significance in Assessing Penicillin Absorption. *Antimicrob Agents Chemother*. 1973;3(4):463-468.

109. Shanson DC, McNabb R, Hajipieris P. The Effect of Probenecid on Serum Amoxycillin Concentrations up to 18 Hours after a Single 3 g Oral Dose of Amoxycillin: Possible Implications for Preventing Endocarditis. *J Antimicrob Chemother*. 1984;13:629-632.

110. Bonner JJ, Vajjah P, Abduljalil K, *et al.* Does Age Affect Gastric Emptying Time? A Model-Based Meta-Analysis of Data from Premature Neonates through to Adults. *Biopharm Drug Dispos*. 2015;36(4):245-257.

111. Maharaj AR, Edginton AN. Examining Small Intestinal Transit Time as a Function of Age - Is There Evidence to Support Age-Dependent Differences Among Children? *Drug Metab Dispos*. 2016;(July):1080-1089.

112. Batchelor H. Influence of Food on Paediatric Gastrointestinal Drug Absorption Following Oral Administration: A Review. *Children*. 2015;2(2):244-271.

113. van Elburg RM, Fetter WPF, Bunkers CM, *et al.* Intestinal Permeability in Relation to Birth Weight and Gestational and Postnatal Age. *Arch Dis Child Fetal Neonatal Ed*. 2003;88(1):F52-F55.

114. Riezzo G, Indrio F, Raimondi F, *et al.* Maturation of Gastric Electrical Activity, Gastric Emptying and Intestinal Permeability in Preterm Newborns during the First Month of Life. *Ital J Pediatr*. 2009;35(1):6.

115. Chen N, Aleksa K, Woodland C, *et al.* Ontogeny of Drug Elimination by the Human Kidney. *Pediatr Nephrol*. 2006;21(2):160-8.

116. Haddad M, Lin F, Dwarakanath V, *et al.* Developmental Changes in Proximal Tubule Tight Junction Proteins. *Pediatr Res*. 2005;57(3):453-457.

117. Horber FF, Frey FJ, Descoeudres C, *et al.* Differential Effect of Impaired Renal Function on the Kinetics of Clavulanic Acid and Amoxicillin. *Antimicrob Agents Chemother*. 1986;29(4):614-619.

118. Mooij MG, de Koning BAE, Lindenbergh-Kortleve DJ, *et al.* Human Intestinal PEPT1 Transporter Expression and Localization in Preterm and Term Infants. *Drug Metab Dispos*. 2016;(July):1014-1019.

119. Shen H, Smith DE, Brosius FC. Developmental Expression of PEPT1 and PEPT2 in Rat Small Intestine, Colon, and Kidney. *Pediatr Res*. 2001;49(6):789-795.

120. Nosworthy MG, Bertolo RF, Brunton J a. Ontogeny of Dipeptide Uptake and Peptide Transporter 1 (PepT1) Expression along the Gastrointestinal Tract in the Neonatal Yucatan Miniature Pig. *Br J Nutr*. 2013;110(2):375-281.

121. Bourdet DL, Pollack GM, Thakker DR. Intestinal Absorptive Transport of the Hydrophilic Cation Ranitidine: A Kinetic Modeling Approach to Elucidate the Role of Uptake and Efflux Transporters and Paracellular vs. Transcellular Transport in Caco-2 Cells. *Pharm Res*. 2006;23(6):1178-1187.

122. Ming X, Knight BM, Thakker DR. Vectorial Transport of Fexofenadine across Caco-2 Cells: Involvement of Apical Uptake and Basolateral Efflux Transporters. *Mol Pharm*. 2011;8(5):1677-1686.

123. Willmann S, Lippert J, Sevestre M, *et al.* PK-Sim®: A Physiologically Based Pharmacokinetic 'Whole-Body' Model. *Biosilico*. 2003;1(4):121-124.

124. Wilson L, Jordan MA. New Microtubule / Tubulin-Targeted Anticancer Drugs and Novel Chemotherapeutic Strategies. *J Chemother*. 2014;16(sup4):83-85.

CHAPTER 2 : PHYSIOLOGICALLY-BASED PHARMACOKINETIC MODELS FOR ADULTS AND CHILDREN REVEAL A ROLE OF INTRACELLULAR TUBULIN BINDING IN VINCRISTINE DISPOSITION[1]

Introduction

The vinca alkaloid vincristine is a chemotherapeutic agent used as first-line therapy for pediatric acute lymphocytic leukemia (ALL) and acute myeloid leukemia. ALL is the most common pediatric cancer, accounting for 26% of cancer diagnosed in children up to 14 years of age. Younger children are disproportionately affected by ALL, with the highest incidence in children 2 to 5 years old[1,2]. Vincristine is also an important anti-cancer agent in other adult and pediatric cancers, including Wilms' tumor, Hodgkin's disease, and non-Hodgkin's lymphoma[3]. Vincristine disrupts mitosis by binding to the β-tubulin subunits of intracellular microtubule structures. This anti-mitotic effect is also responsible for its dose-limiting toxicity of peripheral neuropathy, often manifested by tingling, numbness, a burning sensation, and muscle weakness[4].

Understanding the relationship between vincristine drug pharmacokinetics (PK) and risk of peripheral neuropathy is limited by sparse availability of clinical PK data[3]. Increased risk of peripheral neuropathy has been reported in pediatric patients with reduced vincristine clearance, although systemic exposure to vincristine has not been correlated with vincristine neurotoxicity[5,6]. However, other studies indicate that clinical outcomes in children with ALL are

[1] [1] This chapter has been published in *CPT: Pharmacometrics & Systems Pharmacology (PSP)* and is presented in the style of that journal. The chapter contains some changes (underlined) with respect to the published paper. The original citation is as follows:
Lee CM, Zane NR, Veal G, Thakker DR. *CPT Pharmacometrics Syst Pharmacol.* 2019; Oct;8(10):759-768. Epub Aug 30, 2019.

related to the clearance and exposure of vincristine[7]. Significant neurotoxicity in pediatric patients has been observed when vincristine is co-administered with azole antifungals, which are potent CYP3A inhibitors (*e.g.*, itraconazole, voriconazole), thereby increasing vincristine exposure[8]. Nutritional status may also impact clinical outcomes and neurotoxicity risk by affecting clearance of the drug and hence exposure to it; in pediatric patients with Wilms' tumor and malnutrition, decreased vincristine clearance and a 2-fold increase in exposure (area under the curve, AUC) has been observed compared to pediatric patients without malnutrition[9].

Pediatric PK data for vincristine is limited despite a long history of use in pediatric cancer. As a cytotoxic agent, vincristine is unlikely to be administered to healthy volunteers for prediction of vincristine PK or drug-drug interactions. Therefore, understanding and predicting the potential age-related impact on vincristine disposition is essential for informing proper dosing and treating pediatric cancer patients.

The objective of the current study was to develop physiologically-based pharmacokinetic (PBPK) models to predict the disposition of vincristine following intravenous (IV) administration to adults and children. Previously, we have developed bottom-up PBPK models for pediatric disposition of voriconazole and sildenafil, which are both predominantly cleared *via* hepatic oxidative metabolism[10,11]. Like voriconazole and sildenafil, vincristine is metabolized by CYP3A4. Its clearance in infants and children, when normalized to body surface area or body weight, is higher than in adults, despite decreased CYP3A4 expression and activity in children[12,5,13]. In contrast to voriconazole and sildenafil, vincristine is preferentially metabolized by the genetically polymorphic enzyme CYP3A5, and it undergoes biliary excretion *via* P-glycoprotein (P-gp, also known as MDR1), a hepatic efflux transporter that is expressed at approximately 60% and 80% of adult levels in infants and children, respectively[14]. Pediatric

patients who are high expressers of CYP3A5 have higher metabolite plasma concentrations and lower incidence of peripheral neuropathy *vs.* low expressers[6]. A similar approach could be applied to vincristine to predict its disposition in adults and children, and thus assist in providing safe and effective dosing of this drug with narrow therapeutic window.

Materials and Methods

Materials

[^{3}H]-Vincristine was purchased from American Radiolabeled Chemicals, Inc (MO). GW918 was a gift from GlaxoSmithKline (NC). Madin-Darby canine kidney strain II cells, expressing human P-gp transporter after transfection with human MDR1 cDNA (MDCKII-MDR1), were obtained from the Netherlands Cancer Institute (Amsterdam, The Netherlands).

Cell culture

MDCKII-MDR1 cells were seeded at a density of 100,000 cells/cm^2 on 12-well Transwell^{TM} plates (Corning) and maintained in a CO_2 incubator at 37^{o}C. Cell monolayers were used for experiments 6 days post-seeding.

Transport studies

To obtain estimates of apparent Michaelis-Menten constant (K_m) and maximal flux (J_{max}) for P-gp-mediated AP efflux of vincristine, *in vitro* transport studies were conducted with MDCKII-MDR1 cell monolayers overexpressing P-gp as previously described[15]. Monolayers were incubated in transport buffer (pH 7.4) at 37^{o}C. Dose solutions were added to the AP compartment for absorptive transport and BL compartment for secretory transport. To determine the transport of vincristine in the absence of P-gp activity (*e.g.*, approximating conditions of

permeability due to passive diffusion)[16], the P-gp inhibitor GW918 (1 μM) was included, and transport determined. Samples were analyzed by liquid scintillation spectrometry. Calculation of apparent J_{max} and K_m parameters for P-gp-mediated efflux of vincristine were performed as previously described using nonlinear regression analyses (GraphPad Prism 7)[15].

Pharmacokinetic data

Individual adult vincristine concentration-time data were obtained by digitizing published PK profiles (GetData Graph Digitizer, v2.26)[17–19]. Pediatric vincristine concentration-time data were obtained from a PK study of 25 patients with localized Wilms tumors, with ages ranging from 5 months to 9 years. Samples were analyzed at Newcastle University (UK) using a validated liquid chromatography-mass spectrometry (LC-MS) assay as described previously[9]. A subset of these concentration-time data have previously been published[9]. Pediatric concentrations were dose-normalized to account for the range of doses given (0.3 to 1.8 mg). Noncompartmental analysis was performed on the digitized adult concentration data and the pediatric concentration data using Phoenix 8.0 (Certara).

PBPK model & simulation

A whole-body adult PBPK model was first developed using PK-Sim® software (Open Systems Pharmacology Suite, v7.1) that incorporated vincristine physicochemical parameters (**Table 2-1**). Population-based PK simulations were performed for virtual adult (18 – 65 years old) and pediatric (0 – 9 years old) populations of 100 subjects each, comprising an equal proportion of male and female subjects. Physiologic parameters for the virtual adult population were generated based on the physiology of an average white American as described in the 1997 National Health and Nutrition Examination Survey.

Age-relevant physiologic data from the International Commission on Radiological Protection were used to generate the virtual pediatric population[20]. Human β-tubulin isotype class I (TUBB) was selected to represent overall β-tubulin binding for this model as it is both highly expressed and present in most human tissues[21]. Gene expression levels of CYP3A4/5, P-gp, and TUBB were obtained from UNIGENE and E-GEOD databases using the PK-Sim® built-in database query. CYP3A4 expression was adjusted for age using the built-in PK-Sim® ontogeny function. The equation for CYP3A4 ontogeny in the liver used in PK-Sim® is:

$$A = PMA^n / (A_{0.5}^n + PMA)$$

Where PMA is the post-menstrual age in weeks; A is the activity at PMA; $A_{0.5}$ is the PMA at 50% activity compared to adult; n is the Hill coefficient. As described in the PK-Sim® Ontogeny Database (Version 7.3), an n of 3.331 and $A_{0.5}$ of 73.019 is used by the PK-Sim® software.

Rate constants for β-tubulin binding of vincristine have not been determined previously as, once bound to tubulin, the vincristine-tubulin dimers associate and form microstructures that interfere with light-scatter methods of determining binding and dissociation constants[22]. Therefore, published constants (k_{off}, K_D) for another vinca alkaloid of a similar chemical structure, vinblastine (**Figure 2-1**), were used and optimized by parameter estimation.

Parameter estimation was performed using the built-in PK-Sim® tool on the kinetic parameters for P-gp transport (k_m, J_{max}) and specific binding to β-tubulin (k_{off}, K_D, and relative expression of TUBB). A multiple optimization approach was used with randomized start values.

Model evaluation

Model performance was evaluated by comparing simulated plasma concentration-time profiles (population mean and 95% prediction interval) to observed concentration data. Models

were accepted if simulated concentration-time profiles fit the overall shape of observed profiles, the majority of observed concentration data fell within the 95% prediction interval for simulated data, and the simulated PK parameters were within 2-fold of the observed parameters.

Mean simulated adult PK parameters were also compared to published experimental PK parameters derived from clinical studies with cancer patients[17–19]. Mean simulated pediatric PK parameters were compared to the pediatric PK results from 25 children (0-12 years; Newcastle University)[23]. Model robustness was further evaluated by comparing model simulations to additional published PK studies in which PK parameters (but not concentration data) were available.

Sensitivity analyses

Sensitivity analyses were performed using the PK-Sim® tool to evaluate the effect of the metabolism (CYP3A4 and CYP3A5 K_m, V_{max}, and expression), P-gp efflux (K_m, J_{max}, and expression), and tubulin binding (k_{off}, K_D, TUBB expression) input parameters on performance of the adult PBPK model. These three parameters were selected for sensitivity analyses as potential significant contributors to vincristine distribution and clearance. Input values were evaluated with over a 100% variation range (*i.e.*, 2-fold) to determine the impact on the simulated PK parameters (AUC, CL, V_D).

Results

PBPK Model for Vincristine Disposition in Adults after IV Administration

The whole-body PBPK model structure is shown in **Figure 2-1a**. Tissue to plasma partition coefficients were determined in PK-Sim® using a method described by Schmitt *et al*[24].

In vitro kinetic constants (K_m and V_{max}) for the formation of the vincristine metabolite M1 by recombinant CYP3A4 and CYP3A5 were used[25]. Vincristine is metabolized by both CYP3A4 and CYP3A5, and the intrinsic clearance of vincristine by CYP3A5 is approximately 12-fold higher than by CYP3A4 despite similar affinity of both enzymes for vincristine[25]. Gene and protein expression of CYP3A4, but not CYP3A5, are age-dependent and follow a pattern of ontogeny[12]. CYP3A5 is not highly expressed except in those with a specific genetic polymorphism.

Kinetic constants for P-gp efflux of vincristine in MDCK1-MDR1 cells, determined experimentally in this study, were used for initial modeling. Although vincristine is well known as a substrate of P-gp, kinetic parameters of its efflux have not previously been reported. Kinetic studies of P-gp efflux are often performed *in vitro* using inside-out membrane vesicle systems overexpressing MDR1; however, it is difficult to achieve adequate intravesicular concentrations of lipophilic compounds such as vincristine for evaluation[26,27]. The permeability (P_{app}) of vincristine (10 μM) across MDCKII-MDR1 monolayers is 7-fold greater in the BL to AP direction (157 nm/s) than in the AP to BL direction (22 nm/s), consistent with AP efflux. Secretory transport of vincristine was significantly attenuated by GW918, an inhibitor of P-gp, decreasing the efflux ratio ($P_{app,\ BL\ to\ AP}$ /$P_{app,\ AP\ to\ BL}$) from 7.1 to 1.5, providing evidence that the AP efflux of vincristine is mediated by P-gp. An apparent J_{max} of 46.6 pmol/min and K_m of 17.1 μM was obtained for vincristine flux mediated by P-gp ($R^2 = 0.862$). Based on the surface growth area for each Transwell^{TM} (1.12cm^2) and average cell yield listed by the manufacturer (1.12×10^6 cells; Corning Guidelines for Use: Transwell^{TM} Permeable Supports), the J_{max}. was estimated to be 416 pmol/min/million cells.

The adult PBPK model for vincristine that incorporates CYP3A4/5 metabolism, P-gp efflux, and specific binding to β-tubulin adequately described the observed concentration data (**Table 2-1**,**Figure 2-2**). *In vitro* metabolism and transport kinetics are scaled to organs by the following equation by PK-Sim®:

$$V_{max,organ} = k_{cat} \cdot SF \cdot e_{rel,organ} = k_{cat,s} \cdot e_{rel,organ}$$

in which $V_{max,organ}$ is the tissue-specific maximum velocity, k_{cat} is the catalytic rate constant (1/min), SF is the organ-specific scaling factor (µmol/L), e_{rel} is relative expression of the enzyme or transporter protein, $e_{rel,s}$ is the apparent catalytic rate constant, and E_o is the enzyme or transporter concentration in the organ (µmol/L).

For initial model building and optimization, an IV infusion (15 minutes) of 2 mg vincristine was simulated to match the dosing regimen of the observed clinical study that provided concentration data[19]. A majority of these observed concentration data were within the 95% prediction interval of simulated vincristine plasma concentrations. To further evaluate the adult PBPK model, doses of 2 mg vincristine given by IV bolus and 60-minute infusion were also used in order to evaluate simulated PK parameters as compared to two other published studies[18,28]. Overall, the adult PBPK model predicted PK parameters (AUC, $t_{1/2}$, V_D, CL) well within a 2-fold margin of published parameters from all three PK studies (**Table 2-2**).

PBPK Model for Vincristine Disposition in Children after IV Administration

The adult PBPK model for vincristine disposition was initially adapted to develop a pediatric model by incorporating age-related physiological differences, including the ontogeny of CYP3A4 expression. Although vincristine is also metabolized by CYP3A7, this enzyme is a fetal isoform that is not present after 6 months postnatal age[12,25]. Therefore, kinetic parameters for

CYP3A4 and CYP3A5, but not CYP3A7, were included in the model. However, the simulation showed that vincristine distribution was not well described by the model (**Figure 2-3**). Despite incorporating the tubulin binding parameters (k_{off}, K_D) optimized in the adult PBPK model, the pediatric PBPK model over-predicted vincristine concentrations relative to observed concentrations. The over-prediction error was greatest with the concentrations in the first four hours post-dose, suggesting that the extent of distribution of vincristine was being under-predicted in the virtual pediatric population. Age-related differences in the expression of CYP3A4 and P-gp proteins do not explain the over-prediction of vincristine concentrations by the model, as these are expressed at lower levels in children compared to adults and would be expected to impact the clearance of vincristine[14].

Differences in specific binding to β-tubulin were considered as potential factors affecting the distribution of vincristine in children. Expression of TUBB was evaluated, since it is not known whether the expression of β-tubulin isotypes is different in children compared to adults. To evaluate the effect of relative expression of TUBB on the distribution of vincristine in the virtual pediatric population, the pediatric expression of TUBB was varied up to 150-fold of the adult reference concentration and the PK parameters were simulated. Linear regression analysis demonstrated that in the simulated pediatric population, the V_D of vincristine is significantly correlated with TUBB concentration ($p<0.0001$). Parameter estimation was also performed using adult relative expression of TUBB to optimize pediatric TUBB expression. Surprisingly, model optimization suggested that simulating a higher expression of TUBB in children (approximately 4.9-fold of adult expression) improved predictions. Specifically, predictions of vincristine concentrations in the distribution phase as well as prediction of pediatric V_D and $t_{1/2}$ improved significantly, although the AUC was underestimated to a greater extent (**Figure 2-3b, Table**

2-3). Following this adaptation, the pediatric model adequately described the observed pediatric concentration data for vincristine. PK parameters were also predicted within a 2-fold margin of published parameters (**Table 2-3**).

Sensitivity Analyses

Sensitivity analysis demonstrated that simulated adult vincristine $AUC_{0-\infty}$, $t_{1/2}$, and CL are sensitive to CYP3A4 V_{max} and CYP3A4 expression (**Table 2-4**). A 100% increase in CYP3A4 relative expression decreased AUC and $t_{1/2}$, and increased CL by greater than 25%, indicating that CYP3A4 expression was an important parameter in the model for predicting vincristine exposure and clearance. The PK parameters were not sensitive to CYP3A5 V_{max} and relative expression in the model.

Changes in K_m, V_{max}, and relative expression of P-gp did not impact PK parameters; PK parameters changed by less than 10% when these input parameters were increased by 100%.

The K_D of tubulin binding to vincristine, as well as relative expression of TUBB, had a substantial impact on $AUC_{0-\infty}$, $t_{1/2}$, and CL, as well as vincristine V_D. A 100% increase in K_D caused an increase in $AUC_{0-\infty}$ by 20% and a decrease in $t_{1/2}$, V_D, and CL by 13%, 34%, and 21%, respectively. Increasing the relative expression of TUBB by 100% had the opposite effect, decreasing $AUC_{0-\infty}$ by 20%, but increasing $t_{1/2}$, V_D, and CL by 30%, 50%, and 19%, respectively. In contrast, PK parameters were not sensitive to changes in the k_{off} value.

Discussion

Due to ethical considerations, development of pediatric drugs typically relies upon PK studies conducted in adults to arrive at safe and effective doses in children. Subsequent pediatric dose selection, PK predictions, and predictions of drug-drug interactions are thus extrapolated

from adult data, adjusted by allometric scaling. However, allometric scaling does not address developmental changes in hepatic function, renal function, organ sizes, or total body composition, nor does it account for the ontogeny of drug metabolizing enzymes or drug transporters. For example, the expression of CYP3A4 and the hepatic efflux transporter P-gp demonstrates patterns of ontogeny that could impact the disposition of substrate drugs in infants and younger children[12,14]. Bottom-up PBPK modeling provides a more rigorous approach to predict pediatric PK parameters. In this approach, an adult PBPK model is first developed and validated using available clinical PK data, then adapted to a pediatric PBPK model by incorporating *in vitro* metabolism/transport data, generated using relevant pediatric tissues, age-related changes in physiological parameters and the expression of drug metabolizing enzymes and transporters. For drugs such as voriconazole and sildenafil that are cleared predominantly by oxidative metabolism, we previously demonstrated that mechanistic PBPK modeling approaches can be used to predict PK in children and premature neonates, respectively[10,11].

In the present study, the objective was to apply this PBPK modeling approach to vincristine, which is cleared *via* P-gp-mediated hepatic efflux and CYP3A-mediated hepatic oxidative metabolism. Vincristine is used as a first-line therapy in common pediatric leukemias such as ALL, and in pediatric solid tumor cancer treatment. Vincristine exhibits high inter-patient variability, and there is limited availability of pediatric PK data. In some studies, but not others, correlations have been shown between vincristine PK parameters and clinical outcome, as well as risk of the dose-limiting toxicity, peripheral neuropathy[5–7]. Therefore, we believe that it is important to develop an adult mechanistic PBPK model of vincristine that can be validated using available clinical PK data and adapt it to a pediatric PBPK model that can guide dosing of the drug in pediatric patients with ALL and solid tumors.

Simulations with the initial adult model revealed that the distribution phase was not well predicted. Hence, we reasoned that since vincristine exerts its anti-mitotic effects by binding to intracellular β-tubulin subunits, this intracellular binding may also impact the overall distribution of vincristine. By incorporating the binding of vincristine to β-tubulin, simulated plasma concentrations were adequately described in comparison to the observed concentration data, with the majority of observed data points falling within the 95% prediction interval. The improved PBPK model was able to predict adult PK parameters of vincristine (AUC, $t_{1/2}$, V_D, CL) within a 2-fold margin of the observed parameters from three published PK studies (**Table 2-2**). These results suggested that binding to β-tubulin might have a key role in vincristine distribution.

Sensitivity analyses were performed to evaluate the relevance of the key processes that were incorporated in the PBPK model as determinants of the PK behavior of vincristine. These analyses demonstrated that CYP3A4 V_{max} and expression influenced simulated adult vincristine clearance and exposure (AUC), consistent with the reported predominantly CYP3A4-mediated metabolism of vincristine[25]. For example, a 100% increase in CYP3A4 relative expression decreased AUC and $t_{1/2}$, and increased CL by greater than 25% (**Table 2-4**). Although it has been reported that CYP3A5 plays a larger role than CYP3A4 in the metabolism of vincristine, changes in CYP3A5 V_{max} and expression showed less impact on vincristine PK parameters. This may be due to low or no CYP3A5 expression in the patient population providing the observed concentration data and PK parameters. Based on the location of the studies, the pediatric population and the adult populations in the two published studies were presumed to be majority Caucasian and East Asian[19,28]. The frequency of the non-functional variant, *CYP3A5*3* allele (CYP3A5 non-expresser), is 92-94% and 71-75% for a Caucasian European and East Asian population, respectively[29]. Contrary to expectations, sensitivity analyses of P-gp K_m and J_{max} in

the adult PBPK model indicated that AUC, CL, or V_D parameters did not change even upon a 100% increase in these kinetic parameters. Thus, it appears that biliary efflux *via* P-gp may not be the critical factor in defining vincristine hepatic clearance. Studies utilizing suspended cryopreserved human hepatocytes also indicate that the rate-limiting factor is not efflux *via* P-gp, which is consistent with the conclusion reached based on the sensitivity analyses, but suggests a possible role of BL organic anion transporter proteins (OATP transporters)[27] in rate-limiting uptake into hepatocytes.

The importance of intracellular binding of vincristine to tubulin is supported by the sensitivity of PK parameters to changes in the K_D and TUBB values. Theoretical increases in the affinity for binding of vincristine to tubulin subunits (by decreasing K_D) or in the expression of TUBB would lead to increased intracellular binding. In both cases, sensitivity analyses suggest that an increase in intracellular binding would result in more extensive distribution (increase in V_D) and decreased plasma levels of vincristine (AUC). *In vitro*, the intracellular accumulation of vincristine is strongly correlated with β-tubulin expression[30]. In mice and dogs, tissue concentrations of vincristine and tissue-to-plasma partition coefficients were also highly correlated with β-tubulin binding capacity, suggesting that β-tubulin could also play an important role in tissue distribution and accumulation of vincristine in humans[31]. Further corroboration of the importance of β-tubulin binding to the distribution of vincristine is provided by mechanistic modeling of the taxane docetaxel, which binds to a different site of the β-tubulin subunit. Published mouse PBPK models of docetaxel incorporated the specific binding of docetaxel to β-tubulin (K_D) and an estimated tubulin binding capacity[32,33]. When tubulin binding capacity was adjusted for organ size, the mouse PBPK model was successfully adapted to predict docetaxel PK in adult humans[33]. Although the ontogeny of β-tubulin expression is unknown, its expression

and content vary by organ, as well as organ sizes which are age-dependent. Therefore, in addition to hepatic efflux by P-gp and metabolism by CYP3A enzymes, it is possible that the extent of intracellular binding to β-tubulin could differ in children *vs* adults, either due to differences in β-tubulin expression or in organ sizes.

The pediatric PBPK model was adapted from the adult model by incorporating age-related physiological differences, including the ontogeny of CYP3A4 expression (CYP3A5 expression is not age-dependent[12]). Although the sensitivity analyses indicated that P-gp might not play a significant role in determining PK parameters of vincristine, the ontogeny of P-gp was also considered, as protein expression of P-gp is approximately 60% and 80% of adult levels in infants and children respectively[14]. We also considered the binding of vincristine to the plasma protein α-1-acid glycoprotein (AAG)[34], as AAG levels increase with age[35]**.** Since vincristine is not extensively bound to AAG (f_u 0.51) and AAG levels are lower in young children, this was not expected to explain the distribution of vincristine in children[36]. Surprisingly, model optimization suggested that simulating a higher relative expression of TUBB in children (4.9-fold higher than adult expression) improved predictions of vincristine concentrations. To our knowledge, the effect of age on tubulin expression has not previously been studied. We hypothesize that the greater extent of vincristine distribution observed in children compared to adults was likely due to the pediatric PK samples being sourced from patients with large solid tumors, *i.e.*, Wilms tumor. Gene expression of β-tubulin subunits in 15 pediatric patients with Wilms tumor was at least 2-fold greater as compared to noncancerous adult kidney tissue[37]. Further *in silico* and *in vitro* studies are needed to understand the physiological basis for possible differences in tubulin binding that are associated with age.

There are two limitations of this study pertaining to the incorporation of β-tubulin into the PBPK models. First, published values for vinblastine were used as the initial estimates for *in vitro* binding of vincristine to β-tubulin, since binding parameters for vincristine have not been reported in the literature. Vincristine and vinblastine are structurally similar vinca alkaloids (**Figure 2-1**), with similar thermodynamics and binding parameters to several β-tubulin isotypes[38]. The vinblastine and vincristine equilibrium constants (K) for binding to tubulin subunits are similar (1.5×10^5 M^{-1} and 1.4×10^5 M^{-1}, respectively)[22]. Published estimates of k_{off} for vinblastine binding to β-tubulin range from 0.006 to 0.0083 $1/s$[22,39]. In simulations with the adult PBPK model of vincristine, decreases in k_{off} by orders of magnitude were required to impact the simulation, and decreased accuracy of the model predictions. Furthermore, a sensitivity analysis of k_{off} indicates that increasing this value by 100% does not impact simulated PK parameters of vincristine (**Table 2-4**). The value obtained for vincristine by parameter estimation, 0.00193 1/s, appears to be a reasonable estimate based on the published vinblastine k_{off} values. Second, expression of only one isotype of β-tubulin, TUBB, was used in the PBPK models due to its ubiquity in human tissues, although there are eight human β-tubulin isotypes. Expression of these isotypes varies widely in the body; for example, isotypes IIa (TUBB2A) and IVa (TUBB4) are expressed almost exclusively in neural issue[21]. Further adaptation of the model to include additional isotypes of β-tubulin may be useful in understanding vincristine distribution to specific organs and tissues.

In summary, the mechanistic PBPK models developed in this study predicts vincristine PK in adults and children upon IV administration. Notably, the models yield interesting mechanistic information about the key determinants of the PK parameters of vincristine that could not have been obtained through clinical studies. Specifically, the PBPK models suggests

that CYP3A5 and P-gp, which were implicated in the clearance of vincristine from *in vitro* studies, are not limiting factors in the clearance of vincristine in either adults or children. This is presumably because CYP3A5 expression is very low, in comparison with CYP3A4 expression, in the simulated patient populations; and P-gp expression and activity are not rate-limiting for hepatobiliary trafficking of vincristine. Further, we found that intracellular binding had to be invoked in building the model to describe and predict the distribution phase of vincristine PK. In retrospect, the rationale for the importance of intracellular binding in vincristine PK is clear, since binding to β-tubulin is the mechanistic basis for the anticancer activity of this drug. To our knowledge, this is the first example in which intracellular binding has been incorporated into a pediatric PBPK model. Additionally, this study raises an interesting possibility that there may be age-related differences in the extent of intracellular binding to β-tubulin, leading to the corresponding differences in vincristine PK in these two populations. We believe that PBPK modeling of vincristine disposition in children will improve the prediction of PK parameters in pediatric patients, providing a useful tool to investigate the relationship between vincristine exposure and clinical outcomes without invasive monitoring of plasma drug concentrations.

Table 2-1: Vincristine parameters used for the adult and pediatric PBPK models

Parameter	Value			Source
Molecular Weight (g/mol)	824.958			PubChem
Solubility (mg/L)	2.27 mg/L			
LogP	2.82			Hansch *et al.*, 1995[39]
pKa	5.00 and 7.4			Owellen *et al.*, 1977[40]
f_u	0.51 (α-1-acid glycoprotein)			Mayer and St-Onge, 1995[35]
Metabolism		**rhCYP3A4**	**rhCYP3A5**	Dennison *et al.*, 2006[25]
	V_{max} (pmol/min/pmol enzyme)	0.9	8.1	
	K_m (µM)	19.8	14.3	
P-gp Transport	**J_{max} (pmol/mL/min)**	**Initial**	**Optimized**	Experimental
		416.1	416.1	
	K_m (µM)	17.1	17.1	
Specific Binding to β-tubulin		**Initial**	**Optimized**	Initial estimates for vinblastine-tubulin binding by Lobert *et al.*, 1996[22]
	k_{off} (1/s)	8.30×10^{-3}	1.93×10^{-3}	
	K_D (µM)	0.05	0.05	
	Relative TUBB Expression (µM)	1.00	1.00 (Adult) 4.90 (Pediatric)	UNIGENE and E-GEOD (PK-Sim database query)

f_u, unbound fraction; LogP, partition coefficient; rhCYP3A4 and rhCYP3A5, recombinant human CYP3A4 and CYP3A5; V_{max}, maximal reaction rate for CYP3A-mediated metabolism of vincristine; K_m, Michaelis-Menten constant; J_{max}, maximal rate of transport mediated by P-gp; k_{off}, dissociation rate constant for binding of vincristine to β-tubulin; K_D, dissociation constant for binding of vincristine to β-tubulin

Table 2-2: Comparison of experimental mean vs. simulated PK parameters of vincristine in the adult population.

Source	Patient Population	N	Dose	$AUC_{0-\infty}$ (ng*hr/mL)			$t_{1/2}$ (h)			V_D (L/kg)			CL (L/hr)		
					Fold Difference	% Error[a]		Fold Difference	% Error		Fold Difference	% Error		Fold Difference	% Error
Model Simulation[b]	**Adult, virtual population**	**100**	**2 mg, 15 min IV infusion**	**76.5**	**.**	**.**	**19.6**	**.**	**.**	**6.4**	**.**	**.**	**29.1**	**.**	**.**
Villikka *et al.* 1999	Malignant brain tumors	6	2 mg, 15 min IV infusion	65.1	1.2	-17%	12.7	1.5	-54%	12.9	0.5	50%	34.1	0.9	15%
Fedeli *et al.* 1989[c]	Solid tumors	14	2 mg, IV bolus	48.3	1.6	-58%	21.7	0.9	10%	11.4	0.6	44%	35.4	0.8	18%
Model Simulation[b]	**Adult, virtual population**	**100**	**2 mg, 60 min IV infusion**	**116.1**	**.**	**.**	**17.9**	**.**	**.**	**5.8**	**.**	**.**	**24.1**	**.**	**.**
Yan *et al.* 2012[d]	Advanced solid tumors	6	2 mg, 60 min IV infusion	140.3	0.8	17%	16.0	1.1	-12%	5.0	1.2	-16%	14.6	1.7	-65%

[a]% error = (observed - simulated) / observed * 100. [b]V_D and CL values for model simulation calculated based on average virtual population body mass of 77 kg. [c]V_D and CL values from Fideli *et al.* converted based on mean patient BSA of 1.67m^2 and weight (65.21 kg). [d]V_D value from Yan *et al*. converted based on median patient weight of 64 kg (mean not reported).

Table 2-3: Comparison of experimental mean vs. simulated PK parameters of vincristine in the pediatric population.

Source	Patient Population	N	Dose (mg/m^2)	$AUC_{0-\infty}$ (ng*hr/mL)			$t_{1/2}$ (h)			V_D (L/kg)			CL (L/hr)		
					Fold Difference	% Error[a]		Fold Difference	% Error		Fold Difference	% Error		Fold Difference	% Error
Model Simulation,Adult TUBB Expression	Pediatric (0-12 yrs) virtual population	100	1	149.6	.	.	12.5	.	.	5.6	.	.	8.7	.	.
Final Model Simulation, 4.9-fold increase in TUBB Expression	**Pediatric (0-12 yrs) virtual population**	**100**	**1**	**118.6**	**.**	**.**	**15.6**	**.**	**.**	**8.6[b]**	**.**	**.**	**10.7**	**.**	**.**
Pediatric patients with Wilms tumor	Pediatric (0-12 yrs)	23[c]	1.5[d]	186.4[e]	0.6	36.4%	16.0[e]	1.0	2.5%	9.8[e,f]	0.9	12.2%	10.4[e]	1.0	-2.9 %

[a]% error = (observed - simulated) / observed * 100. [b]V_D value calculated based on average pediatric body mass of virtual subjects, 26.4 kg (N=100). [c]Plasma concentration data were available for 25 pediatric subjects. However, PK analyses could not be completed for 2 subjects due to insufficient number of concentrations. [d]Dose reduced by ⅓ if under 12 kg. [e]Calculated using plasma concentrations normalized to dose (mg). [f]V_D value converted based on average pediatric body mass of study subjects, 16.4 kg (N=25)

Table 2-4: Sensitivity analysis effect of CYP3A4, CYP3A5, P-gp, and β-tubulin binding parameters on vincristine PK in adults.

		$AUC_{0-\infty}$	$t_{1/2}$	V_D	CL
CYP3A4	rhCYP V_{max}	-0.35	-0.36	-0.01	0.34
	Relative Expression	-0.26	-0.26	-0.00139	0.25
CYP3A5	rhCYP V_{max}	-0.04	-0.04	0.00599	0.04
	Relative Expression	-0.02	-0.02	-0.0002	0.02
P-gp	K_m	-0.05	-0.00958	0.04	0.05
	V_{max}	0.05	0.0095	-0.04	-0.05
	Relative Expression	-0.05	-0.00943	0.04	0.05
Binding to β-tubulin	K_D	0.20	-0.13	-0.34	-0.21
	k_{off}	-0.00043	-0.00243	-0.002	0.000429
	TUBB Relative Expression	-0.20	0.30	0.50	0.19

Sensitivity analyses using the built-in PK-Sim tool were performed to evaluate effect of input parameters on performance of the adult PBPK model. Input values were evaluated over a 100% variation range to determine impact on simulated adult PK parameters, *e.g.*, a 100% increase in CYP3A4 relative expression decreased $AUC_{0-\infty}$ and $t_{1/2}$ by greater than 25%. Overall, the analyses demonstrated that PK parameters are sensitive to changes in CYP3A4 relative expression, K_D of β-tubulin binding to vincristine, and relative expression of TUBB.

Figure 2-1: Whole-body PBPK model structure simulated by PK-Sim® software package

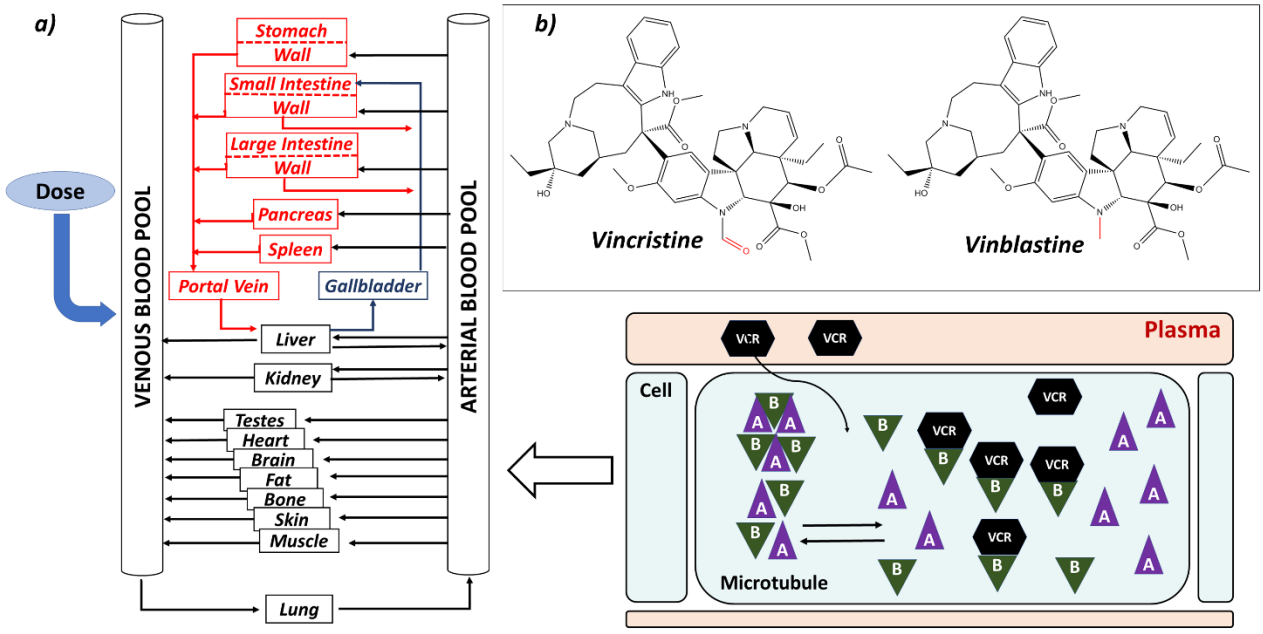

(a). Adapted from Willmann *et al.*[41] The model includes simulation of the specific protein binding of vincristine to β-tubulin within the cellular compartment. Microtubule structures within the cell, comprising units of α-tubulin (represented by the triangles marked A) and β-tubulin subunits (represented by the triangles marked B), exchange subunits with an intracellular pool of unbound α- and β-tubulin (<u>also shown in **Figure 1-4** in Chapter 1, Introduction</u>). Vincristine enters the cell by passive diffusion, and binds to the free intracellular β-tubulin[42]. The chemical structures of vincristine and vinblastine are inset in **(b)**, with differences between structures noted in red.

Figure 2-2: Simulation of vincristine plasma concentration *vs.* time curve from 0 to 24 hours following a single intravenous dose of vincristine (2 mg) in a virtual adult population (N=100).

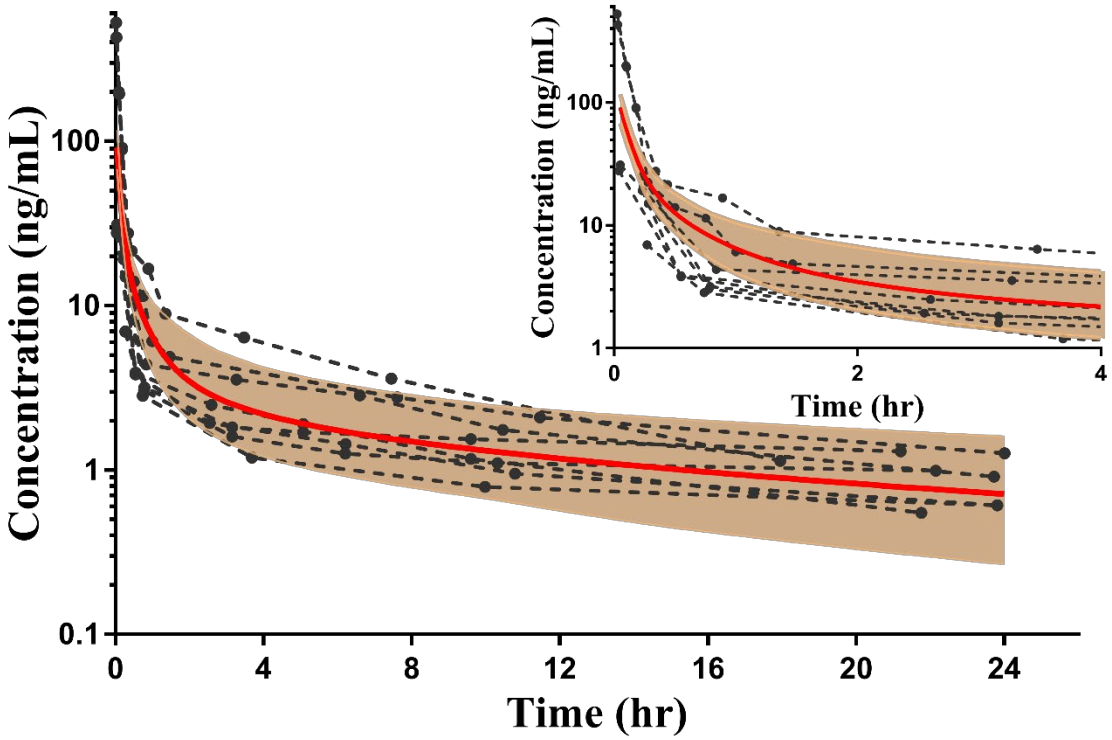

The solid red line represents the simulated mean and the shaded area is the 95% prediction interval. The dotted lines represent the observed vincristine concentration vs. time profiles for 10 adults, extracted from publications by GetData[17,43]. The inset panel shows the concentration vs. time curve from 0 to 4 hours only.

Figure 2-3: Simulations of vincristine plasma concentration vs. time in the virtual pediatric population (N=100) with observed concentration data of 25 children, aged 0 to 12 years.

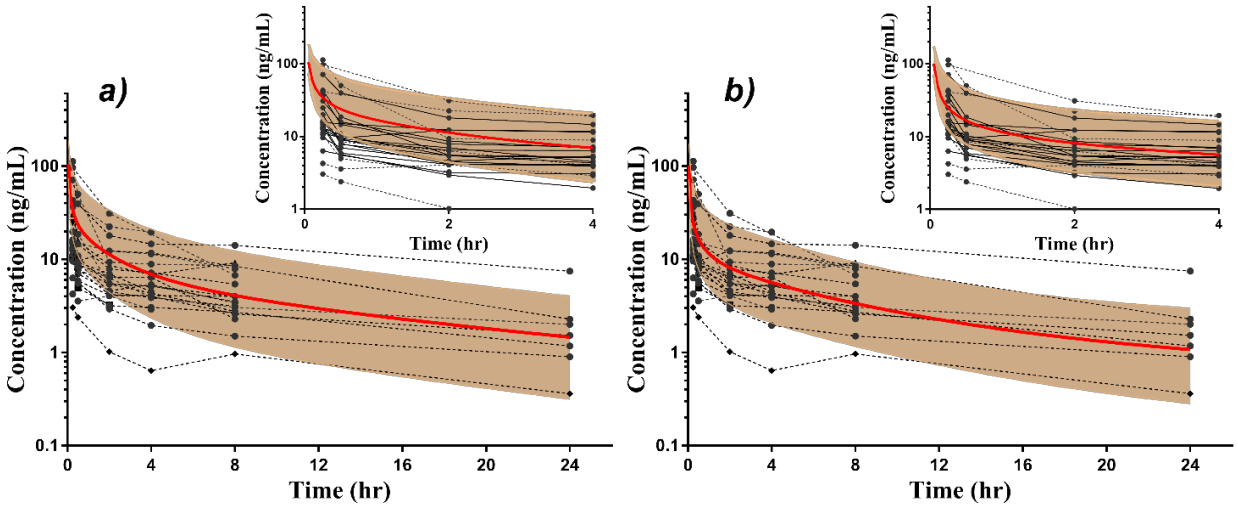

The solid red lines represent the simulated mean and shaded areas represent the 95% prediction interval. Observed concentrations (circles connected by dotted lines) have been normalized to the dose (mg) received. Panel a) represents the pediatric population simulation with PBPK model, using adult expression levels of TUBB. Relative TUBB expression in the virtual pediatric population was optimized by parameter estimation. As shown in Panel b), a higher expression of TUBB (4.9-fold increase relative to adult expression) improved predictions of pediatric vincristine concentrations and more fall within the 95% prediction interval compared to Panel a), particularly in the first 4 hours post-dose. The inset panels in a) and b) show the concentration vs. time curves from 0 to 4 hours only.

.

Supplementary Table

Table 2-5: Vincristine Compound File (PK Sim 7.3.0.42)

Basic Physicochemistry	
Is small molecule	Yes
Molecular Weight	824.96 g/mol
Effective Molecular Weight	824.96 g/mol
pKa value	5
Compound Type	Acid
Lipophilicity	2.82
Fraction Unbound	0.51 (Human)
Solubility	2.27
Solubility Reference pH	7.00
Solubility gain per charge	1000.00
Absorption	
Specific Intestinal Permeability	7.93×10^{-7}
Specific Organ Permeability	6.03×10^{-5}
Distribution	
Partition Coefficients	Schmitt
Cellular Permeabilities	PK-Sim Standard
Specific binding	
k_{off}	1.93×10^{-3} 1/s
K_D	0.05 µmol/L
Metabolism	
CYP3A4	
Process Type	*In vitro* metabolic rate in the presence of recombinant CYPs/enzymes - Michaelis-Menten
In vitro V_{max} / recombinant enzyme	0.90 pmol/min/pmol rec. enzyme
K_m	19.70 µmol/L
k_{cat}	0.90 1/min
CYP3A5	
Process Type	*In vitro* metabolic rate in the presence of recombinant CYPs/enzymes - Michaelis-Menten
In vitro V_{max} / recombinant enzyme	8.10 pmol/min/pmol rec. enzyme
K_m	14.30 µmol/L
k_{cat}	8.10 1/min
Transport and Excretion	
MDR1	
Process Type	Specific active transport – Michaelis-Menten
Transporter concentration	1.00 µmol/L
V_{max}	416.10 pmol/mL/min
K_m	17.10 µmol/L
k_{cat}	0.42 1/min

REFERENCES

1. Ward E, DeSantis C, Robbins A, *et al*. Childhood and Adolescent Cancer statistics, 2014. *CA Cancer J Clin*. 2014;64(2):83-103.

2. Inaba H, Greaves M, Mullighan C. Acute Lymphoblastic Leukemia. *Lancet*. 2013;381(9881):1-27.

3. Gidding CEM, Kellie SJ, Kamps W a., De Graaf SSN. Vincristine Revisited. *Crit Rev Oncol Hematol*. 1999;29(3):267-287.

4. Carlson K, Ocean AJ. Peripheral Neuropathy with Microtubule-targeting Agents: Occurrence and Management Approach. *Clin Breast Cancer*. 2011;11(2):73-81.

5. Crom WR, de Graaf SS, Synold T, *et al*. Pharmacokinetics of Vincristine in Children and Adolescents with Acute Lymphocytic Leukemia. *J Pediatr*. 1994;125(4):642-9.

6. Egbelakin A, Ferguson MJ, MacGill EA, *et al*. Increased Risk of Vincristine Neurotoxicity Associated with Low CYP3A5 Expression Genotype in Children with Acute Lymphoblastic Leukemia. *Pediatr Blood Cancer*. 2012;56(3):361-367.

7. Lönnerholm G, Frost BM, Abrahamsson J, *et al*. Vincristine Pharmacokinetics is Related to Clinical Outcome in Children with standard risk acute lymphoblastic leukemia. *Br J Haematol*. 2008;142(4):616-621.

8. Moriyama B, Henning S a., Leung J, *et al*. Adverse Interactions Between Antifungal Azoles and Vincristine: Review and analysis of cases. *Mycoses*. 2012;55(4):290-297.

9. Israels T, Damen CWN, Cole M, *et al*. Malnourished Malawian Patients Presenting with Large Wilms Tumours Have a Decreased Vincristine Clearance rate. *Eur J Cancer*. 2010;46(10):1841-1847.

10. Zane NR, Thakker DR. A Physiologically Based Pharmacokinetic Model for Voriconazole Disposition Predicts Intestinal First-pass Metabolism in Children. *Clin Pharmacokinet*. 2014;53(12):1171-1182.

11. Zane NR. Predicting Pharmacokinetic Behavior and Dose of Sildenafil and Voriconazole in Neonatal and Pediatric Populations by In Vitro Metabolism and PBPK Modeling (Doctoral dissertation). *Retrieved from Carolina Digit Repos*. 2015.

12. Stevens JC, Hines RN, Gu C, *et al*. Developmental Expression of the Major Human Hepatic CYP3A Enzymes. *J Pharmacol Exp Ther*. 2003;307(2):573-582.

13. Gidding CE, Meeuwsen-de Boer GJ, Koopmans P, *et al*. Vincristine Pharmacokinetics After Repetitive Dosing in Children. *Cancer Chemother Pharmacol*. 1999;44(3):203-9.

14. Prasad B, Gaedigk A, Vrana M, *et al*. Ontogeny of Hepatic Drug Transporters as Quantified by LC-MS/MS Proteomics. *Clin Pharmacol Ther*. 2016;100(4):362-370.

15. Troutman MD, Thakker DR. Efflux Ratio Cannot Assess P-Glycoprotein-Mediated Attenuation of Absorptive Transport: Asymmetric Effect of P-Glycoprotein on Absorptive and Secretory Transport across Caco-2 Cell Monolayers. *Pharm Res*. 2003;20(8):1200.

16. Gao J, Murase O, Schowen RL, Aube J, Borchardt RT. A Functional Assay for Quantitation of the Apparent Affinities of Ligands of P-Glycoprotein in Caco-2 Cells. *Pharm Res*. 2001;18(2).

17. Sethi VS, Jackson D V, White DR, *et al*. Pharmacokinetics of Vincristine Sulfate in Adult Cancer Patients. *Cancer Res*. 1981;41(September):3551-3555.

18. Yan Z, Zhu Z, Qian Z, *et al*. Pharmacokinetic Characteristics of Vincristine Sulfate Liposomes in Patients with Advanced Solid Tumors. *Acta Pharmacol Sin*. 2012;33:852-858.

19. Villikka K, Kivistö KT, Mäenpää H, *et al*. Cytochrome P450-inducing Antiepileptics Increase the Clearance of Vincristine in Patients with Brain Tumors. *Clin Pharmacol Ther*. 1999;66(April 1997):589-593.

20. Valentin J. Basic Anatomical and Physiological Data for Use in Radiological Protection. *Ann ICRP*. 2002;32.

21. Leandro-García LJ, Leskelä S, Landa I, *et al*. Tumoral and Tissue-specific Expression of the Major Human Beta-tubulin Isotypes. *Cytoskeleton*. 2010;67(4):214-223.

22. Lobert S, Vulevic B, Correia JJ. Interaction of Vinca Alkaloids with Tubulin: A Comparison of Vinblastine, Vincristine, and Vinorelbine. *Biochemistry*. 1996;35(21):6806-14.

23. Peters SP, Kunselman SJ, Icitovic N, *et al*. Tiotropium Bromide Step-up Therapy for Adults with Uncontrolled Asthma. *N Engl J Med*. 2010;363(18):1715-1726.

24. Schmitt W. General Approach for the Calculation of Tissue to Plasma Partition Coefficients. *Toxicol Vitr*. 2008;22(2):457-467.

25. Dennison JB, Kulanthaivel P, Barbuch RJ, *et al*. Selective Metabolism of Vincristine In Vitro by CYP3A5. *Drug Metab Dispos*. 2006;34(8):1317-1327.

26. Giacomini KM, Huang S, Tweedie DJ, *et al*. Membrane Transporters in Drug Development. *Nat Rev Drug Discov*. 2010;9(3):215-236.

27. Nicolaï J, Thevelin L, Bing Q, *et al*. Role of the OATP Transporter Family and a Benzbromarone-SensitiveEfflux Transporter in the Hepatocellular Disposition of Vincristine. *Pharm Res*. 2017;34(11):2336-2348.

28. Fedeli L, Colozza M, Boschetti E, *et al*. Pharmacokinetics of Vincristine in Cancer Patients Treated with Nifedipine. *Cancer*. 1989;64(9):1805-1811.

29. Xie H-G, Wood AJ, Kim RB, *et al*. Genetic Variability in CYP3A5 and its Possible Consequences. *Pharmacogenomics*. 2004;5(3):243-272.

30. Reichle A, Diddens H, Altmayr F, *et al*. Beta-tubulin and P-glycoprotein: Major Determinants of Vincristine Accumulation in B-CLL cells. *Leuk Res*. 1995;19(11):823-829.

31. Wierzba K, Sugiyama Y, Okudaira K, *et al*. Tubulin as a Major Determinant of Tissue Distribution of Vincristine. *J Pharm Sci*. 1987;76(12):872-875.

32. Hudachek SF, Gustafson DL. Incorporation of ABCB1-mediated Transport Into a Physiologically-based Pharmacokinetic Model of Docetaxel in Mice. *J Pharmacokinet Pharmacodyn*. 2013;40(4):437-449.

33. Bradshaw-Pierce EL, Eckhardt SG, Gustafson DL. A Physiologically Based Pharmacokinetic Model of Docetaxel Disposition: From Mouse to Man. *Clin Cancer Res*. 2007;13(9):2768-2776.

34. Donigian DW, Owellen RJ. Interaction of Vinblastine, Vincristine, and Colchicine with Serum Proteins. *Biochem Pharmacol*. 1973;22:2113-2119.

35. Maharaj AR, Gonzalez D, Cohen-Wolkowiez M, *et al*. Improving Pediatric Protein Binding Estimates: An Evaluation of α1-Acid Glycoprotein Maturation in Healthy and Infected Subjects. *Clin Pharmacokinet*. 2017:1-13.

36. Mayer LD, St.-Onge G. Determination of Free and Liposome-associated Doxorubicin and Vincristine Levels in Plasma Under Equilibrium Conditions Employing Ultrafiltration Techniques. *Anal Biochem*. 1995;232(2):149-157.

37. Takahashi M, Yang XJ, Lavery TT, *et al*. Gene Expression Profiling of Favorable Histology Wilms Tumors and its Correlation with Clinical Features. *Cancer Res*. 2002;62(22):6598-6605.

38. Lobert S, Frankfurter A, Correia JJ. Energetics of Vinca Alkaloid Interactions with Tubulin Isotypes: Implications for Drug Efficacy and Toxicity. *Cell Motil Cytoskeleton*. 1998;39(2):107-121.

39. Gigant B, Wang C, Ravelli RBG, *et al*. Structural Basis for the Regulation of Tubulin by Vinblastine. *Nature*. 2005;435(7041):519-522.

40. Hansch C. *Exploring QSAR - Hydrophobic, Electronic, and Steric Constants*. Washington DC: American Chemical Society; 1995.

41. Owellen RJ, Donigian DW, Hartke CA, *et al*. Correlation of Biologic Data with Physico-chemical Properties Among the Vinca Alkaloids and Their Congeners. *Biochem Pharmacol*. 1977;26(13):1213-1219.

42. Wilson L, Jordan MA. New Microtubule / Tubulin-Targeted Anticancer Drugs and Novel Chemotherapeutic Strategies. *J Chemother*. 2014;16(sup4):83-85.

43. Villikka K, Kivistö KT, Mäenpää H, *et al*. Cytochrome P450-inducing Antiepileptics Increase the Clearance of Vincristine in Patients with Brain Tumors. *Clin Pharmacol Ther*. 1999;66(6):589-593.

44. Willmann S, Lippert J, Sevestre M, *et al*. PK-Sim®: A Physiologically Based Pharmacokinetic 'Whole-body' Model. *Biosilico*. 2003;1(4):121-124.

CHAPTER 3 : ABSORPTIVE TRANSPORT OF AMOXICILLIN ACROSS CACO-2 CELL MONOLAYERS AND ADULT HUMAN INTESTINAL EPITHELIA: CONTRIBUTION OF PEPT1 AND PARACELLULAR TRANSPORT

Introduction

The β-lactam antibiotic amoxicillin is one of the most frequently prescribed drugs in infants and children as a first-line treatment for AOM, a common childhood disease that affects over 80% of children under 5 years of age[1]. Amoxicillin is hydrophilic (logD -2.3, pH 7.4) and zwitterionic at physiological pH, and thus is expected to have poor membrane permeability[2]. In children, amoxicillin oral bioavailability and penetration into the MEF are highly variable, leading to poor outcomes[3]. In adults, amoxicillin oral bioavailability is dose-dependent, ranging from 22% to 90%, suggesting transporter-mediated absorption[4,5], although the mechanism of its intestinal absorption is not well understood. Furthermore, amoxicillin has a short elimination half-life after intravenous administration (1.31 hrs) that is approximately twice as long after oral administration, suggesting that amoxicillin demonstrates "flip-flop" kinetics in which absorption, rather than elimination, is the rate-limiting step in its disposition[6,7].

Amoxicillin is a substrate for the intestinal and kidney transporter PEPT1, a proton-coupled symporter[8]. Therefore, the intestinal absorption of amoxicillin is likely to involve AP enterocytic uptake by PEPT1, potentially other AP uptake and BL efflux transporters, and a yet unknown contribution of the paracellular route[8]. Significant contribution of the paracellular route to amoxicillin absorption is likely due to its hydrophilicity and relatively small size.

The aim of this work is to elucidate the kinetics and mechanisms of amoxicillin absorptive transport across Caco-2 cell monolayers and adult human intestinal epithelium, and determine the rate-limiting step in its intestinal absorption. Understanding the basis of the "flip-flop" kinetics of amoxicillin will assist in future exploration of the highly variable oral PK of amoxicillin and its penetration into the MEF in pediatric patients. Caco-2 cell monolayers are a well-recognized cellular model for intestinal epithelium, and have been used in conjunction with three-compartment kinetic models to describe the absorptive transport of the cationic hydrophilic drugs ranitidine and metformin[9–11]. However, Caco-2 cell monolayers are derived from human colon carcinoma, and are less reflective of the human jejunum where a majority of drug absorption occurs. Thus, amoxicillin transport was studied in a second relevant *in vitro* model, *i.e.,* adult intestinal epithelium, harvested from fresh intestinal tissue that is discarded during bariatric surgery of obese patients, in which the dose-dependent absorption of amoxicillin *in vivo* could be recapitulated and intestinal transporter expression and activity would be preserved[12]. In this study, the contribution of PEPT1 and other uptake transporters in the intestinal absorptive transport of amoxicillin has been evaluated, and a three-compartmental kinetic model has been used to determine the relative contributions of the transporter-assisted transcellular pathway and diffusion across the paracellular pathway to the overall absorptive transport of amoxicillin.

Methods

Materials

The Caco-2 cell line was obtained from the American Type Culture Collection (ATCC). MEM media, nonessential amino acids (NEAA), antibiotic antimycotic (anti-anti), fetal bovine serum (FBS), Krebs Ringer buffer (KRB), Hank's balanced salt solution (HBSS), and HEPES buffer were obtained from Gibco. Amoxicillin, valacyclovir, and glysar were purchased from

Toronto Research Chemicals. [N-(4-[2-(1,2,3,4-tetrahydro-6,7-dimethoxy-2-isoquinolinyl)ethyl]-phenyl)-9,10-dihydro-5-methoxy-9-oxo-4-acridine carboxamide] (GW918) was a gift from GlaxoSmithKline (Research Triangle Park, NC, USA). [^{3}H]Amoxicillin (5 Ci/mmol), [^{3}H]glysar (3 Ci/mmol) and [^{14}C]mannitol (55.5 mCi/mmol) were purchased from American Radiolabeled Chemicals, Inc. Adult human jejunal tissue was collected from the Division of Gastrointestinal Surgery, UNC Chapel Hill during roux-en-y gastric bypass operations under an IRB-exempt protocol (#14-1165). Liquid scintillation fluid (Ultima Gold^{TM} XR) was obtained from Perkins Elmer**.** The Ussing chamber apparatus (EasyMount diffusion chamber system) was purchased from Physiologic Instruments.

Cell Culture

Caco-2 cells were cultured in MEM with 10% FBS, 1% NEAA, and 1% anti-anti in 5% CO_2. Cells were passaged at 90% confluency and plated in T-75 flasks. Cells were seeded in 12-well plates on Transwell^{TM} polycarbonate filters of 1.12 cm^2 growth area and 0.4 μM pore size (Corning). Medium was changed the day after seeding, then every other day. Cell monolayers were used for experiments between 21 to 28 days after seeding. To ensure integrity of the monolayer, transepithelial electrical resistance (TEER) was determined using an EVOM II voltohmeter prior to the start of the experiment. Cell monolayers with TEER values greater than 300 Ω were used for experimentation.

Human Intestinal Epithelia

Fresh jejunal tissue was obtained from adult patients undergoing bariatric surgery at the Division of Gastrointestinal Surgery at UNC Hospitals. To maximize tissue viability, tissues were washed with ice cold KRB containing protease inhibitor, and studies were completed

within 6 hours of tissue harvest[13]. The tissue was first resected and stripped of the outer serosa and muscularis externa layer, then mounted on slides with an exposed surface area of 0.3 cm^2 for the epithelial tissue. Resection and mounting were performed on ice using KRB containing protease inhibitor, and slides were placed in ice cold KRB containing protease inhibitor until ready to mount in the Ussing chamber system. The slides were sandwiched between AP and BL compartments in the Ussing chamber apparatus and incubated in 37ºC KRB with protease inhibitor at pH 6.0 (AP) or 7.4 (BL) for 30 minutes prior to initiating experiments. During tissue incubation and throughout the experiment, the Ussing chamber system was maintained at 37ºC using heated water from a water bath, and each chamber was oxygenated to maintain tissue viability.

Transport and Accumulation Studies

Absorptive (AP to BL) and secretory (BL to AP) transport of amoxicillin was determined across Caco-2 cell monolayers and across fresh adult human intestinal epithelia in the Ussing diffusion chamber system. These studies were conducted as described previously, with minor modifications[9,14,15]. In transport experiments, the appearance of amoxicillin in the receiver compartment was determined over time in the linear region of transport and under sink conditions, *i.e.*, in the presence of a concentration gradient wherein less than 10% of the donor concentration was expected to be transported to the receiver compartment by the end of the study.

Transport buffer for Caco-2 cell monolayers was prepared as HBSS (25 mM D-glucose, 10 mM HEPES); for human intestinal epithelia, KRB containing protease inhibitor was used. Unless otherwise stated, buffers and dosing solutions (*i.e.*, transport buffer containing [^{3}H]amoxicillin) for transport experiments were prepared at pH 6.0 and 7.4 for AP and BL

compartments, respectively, to maintain a pH gradient for optimal PEPT1 activity. [^{14}C]Mannitol (10 μM) was included in dosing solutions as a marker of paracellular transport and confirmation of epithelial monolayer integrity.

Caco-2 cell monolayers were preincubated with transport buffer for 30 minutes at 37ºC, then washed with fresh buffer. To determine absorptive transport, 0.4 mL dosing solutions of [^{3}H]amoxicillin were added to the AP donor compartment. Samples (200 μL) were taken from the BL receiver compartment (1.5 mL) every 15 minutes over a period of 60 minutes; the collected samples were immediately replaced with 200 μL of fresh buffer to maintain sample volume. For secretory transport, 1.5 mL dosing solutions were added to the BL donor compartment and sequential samples were taken from the AP receiver compartment with replacement with fresh buffer. Cellular accumulation was determined at the end of the experiment by first washing the monolayers three times with ice cold transport buffer and then drying the monolayers. The polycarbonate filters were removed from the Transwell™ inserts and incubated at room temperature in 400 μL of 1% Triton-X for 4 hours on an orbital shaker. The filters were then gently scraped with a pipet tip and discarded. The remaining cell lysate solution was mixed by vortexing and reserved for analysis by liquid scintillation counting (LSC) and for determination of protein content by the bicinchoninic acid assay (BCA) assay.

Transport and accumulation studies with human intestinal epithelia were conducted in an Ussing chamber system as described above, with minor changes as follows. Volumes of 3.0 mL dosing solution and 3.0 mL transport buffer were used in the donor and receiver compartments, respectively. To determine intracellular accumulation of amoxicillin at the end of the experiment, epithelial tissue was washed in KRB and incubated for 4 hours in 0.5 mL 1 N NaOH in a water bath maintained at 42ºC. The lysate was vortex mixed to ensure dissolution, and neutralized with

0.5 mL 1N HCl solution before LSC analysis. [^{14}C]mannitol, [^{3}H]glysar, and [^{3}H]amoxicillin in transport study samples and in cell lysates were quantified by LSC.

Uptake Studies

AP and BL uptake studies in Caco-2 cell monolayers and human intestinal epithelia were conducted as previously described[14,15]. For all experiments, the pH in the AP compartment was 6.0 and the pH in the BL compartment was 7.4.

Caco-2 cell monolayers were preincubated with transport buffer for 30 minutes at 37ºC, then washed with fresh buffer. To initiate uptake experiments, transport buffer in the donor compartment was replaced with varying concentrations of [^{3}H]amoxicillin (0.5 mL for AP and 1.5 mL for BL compartments), and uptake of the drug was determined at time points within the linear range of uptake. Cell monolayers were washed in both compartments with ice cold transport buffer to stop transport and terminate the experiment. The cellular accumulation of amoxicillin and protein content were then determined as described above. Uptake studies using human intestinal epithelia were conducted similarly, with the exception that the volume in the AP and BL compartments was 3.0 mL each. The accumulation of amoxicillin in the tissue was determined as described above.

Efflux Studies

Caco-2 cell monolayers were preincubated with transport buffer at 37ºC for 30 minutes, then preloaded for 60 minutes with [^{3}H]amoxicillin by incubating with 1 mM dose solution in the AP (0.4 mL) and BL (1.5 mL) compartments. Cell monolayers were then washed 3 times with ice cold transport buffer. To initiate the experiment, the AP and BL compartments were refilled with fresh 37ºC transport buffer (pH 6.0 AP, pH 7.4 BL). Appearance of [^{3}H]amoxicillin

in AP and BL chambers was determined at several time points over a period of 10 minutes and monitored as a function of time. Cell monolayers were washed 3 times with ice cold transport buffer for determination of cellular accumulation at the end of the study. The total amount of [^{3}H]amoxicillin preloaded at the start of the experiment was calculated by adding the mass of amoxicillin in the cell lysate and the total mass of amoxicillin effluxed into each compartment over time. To calculate the initial intracellular concentration (C_o), the total amount of amoxicillin that was preloaded was divided by the cellular volume for Caco-2 cells (3.66 µL/mg protein[16]). Efflux clearance was calculated in the linear range of efflux *vs* time.

Human intestinal epithelia were preincubated with transport buffer (KRB with protease inhibitor) at 37ºC for 30 minutes, then preloaded for 60 minutes by incubating with 1 mM dose solution in the AP and BL compartments (3 mL each). The epithelial tissue was then washed 3 times with ice cold transport buffer to stop accumulation. To initiate the experiment, the AP and BL compartments were refilled with fresh 37ºC transport buffer (pH 6.0 AP, pH 7.4 BL). Appearance of [^{3}H]amoxicillin was determined in AP and BL chambers at several time points over a period of 10 minutes and monitored as a function of time. Epithelial tissue was washed 3 times with ice cold transport buffer for determination of amoxicillin accumulation in the tissue at the end of the study. The total amount of [^{3}H]amoxicillin preloaded at the start of the experiment was calculated by adding the mass of amoxicillin in the tissue lysate and the total mass of amoxicillin effluxed into each compartment over time. Efflux clearance was calculated in the linear range of efflux *vs* time.

Data Analysis

Transport of amoxicillin across Caco-2 cell monolayers or across human intestinal epithelia is reported as apparent permeability (P_{app}), calculated by equation (1) below:

$$P_{app} = \frac{dX/dt}{(A * C_0)} \quad (1)$$

where dX/dt is the mass of amoxicillin (X) transported over time (t), A is the surface area of the Transwell^{TM} insert or the surface area of the human intestinal epithelia, and C_o is the initial concentration in the donor compartment. Transport of amoxicillin can also be expressed as flux (*J*) using equation (2) below:

$$J = \frac{dX/dt}{A} \quad (2)$$

To obtain the kinetic constants (J_{max}, K_m, K_d) for amoxicillin transport, uptake data were fitted to a model describing one saturable and one nonsaturable component, using equation (3) below:

$$J = \frac{(J_{max} * C)}{(K_m + C)} + K_{d,transport} * C \quad (3)$$

where C is the amoxicillin concentration, J_{max} is the maximal flux, K_m Michaelis-Menten constant, and $K_{d,transport}$ is the rate constant for nonsaturable component of amoxicillin transport. These kinetic constants were used in a model of amoxicillin uptake, in equation (4) below:

$$\text{Uptake Rate} = \frac{(V_{max} * C)}{(K_m + C)} + K_{d,uptake} * C \quad (4)$$

where C is the amoxicillin concentration, V_{max} is the maximal velocity, K_m is the Michaelis-Menten constant, and $K_{d,uptake}$ is the rate constant for nonsaturable component of amoxicillin uptake.

To calculate the clearance (CL) for amoxicillin efflux across the AP and BL membranes after preloading, equation (5) was used:

$$CL = \frac{dX/dt}{C_0} \quad (5)$$

To determine the initial intracellular concentration C_o for efflux, the total amount of amoxicillin at preloading was calculated. This was determined by adding the total mass of amoxicillin effluxed into the AP and BL compartments over the time course of the experiment to the amount of amoxicillin remaining in the cells at the end of the experiment. For Caco-2 cell monolayers, a cellular volume of 3.66 μL/mg protein was used for concentration calculations[16].

Compartmental Model of Amoxicillin Transport

Compartmental modeling has been used previously to determine cellular accumulation, and transcellular and paracellular transport of compounds in Caco-2 cells, including the cationic hydrophilic drugs metformin and ranitidine[9–11]. In brief, a three-compartmental model was implemented to describe the accumulation and transport of amoxicillin in Caco-2 cell monolayers and in human intestinal epithelia (**Figure 3-1**). To describe the transfer of amoxicillin between the three compartments, the following differential equations (6, 7, 8) were used:

$$\frac{dX_1}{dt} = -(k_{12} + k_{13}) * X_1 + k_{21} * X_2 \quad (6)$$

$$\frac{dX_2}{dt} = k_{12} * X_1 - (k_{21} + k_{23}) * X_2 + k_{32} * X_3 \quad (7)$$

$$\frac{dX_3}{dt} = k_{23} * X_2 + k_{13} * X_1 - k_{32} * X_3 \quad (8)$$

where X_1, X_2, and X_3 represent the mass of amoxicillin in the AP, cellular, and BL compartments, respectively. The differential equations include first-order rate constants for the

AP uptake (k_{12}), AP efflux (k_{21}), BL uptake (k_{32}), and BL efflux (k_{23}) parameters. Paracellular transport is represented by the first-order rate constant k_{13}. Reverse paracellular transport (k_{31}) was excluded from the model as it is assumed to be negligible under sink conditions. In the presence of a large AP to BL concentration gradient, passive transport in the reverse direction against the gradient is not expected.

To obtain the parameter estimates, cellular accumulation and transport of amoxicillin were modeled using nonlinear regression (Phoenix WinNonlin, Certara, USA), using a 1/Y weighting and Gauss-Newton minimization. Experimentally derived values for AP efflux (k_{21}), BL efflux (k_{23}), and BL uptake (k_{32}) were fixed during the modeling process to improve estimations of the remaining parameters. Initial estimates for the BL efflux rate constant were calculated using equation 9:

$$k_{23} = \frac{dX/dt}{(X_0)} \tag{9}$$

The rate of initial AP or BL uptake was calculated using equation 10:

$$\frac{dX_2}{dt_{initial}} = k_{12\ (or\ 32)} * X_{1\ (or\ 3)} \tag{10}$$

Since the initial rate of amoxicillin uptake into the cellular compartment ($dX_2/dt_{initial}$) can also be described by an equation that incorporates a saturable and nonsaturable component, the initial AP uptake rate may also be calculated using equation 11:

$$\frac{dX_2}{dt_{initial}} = \frac{V_{max} * X_{1\ (or\ 3)}}{K_m * V_{AP\ (or\ BL)} + X_{1\ (or\ 3)}} + \frac{K_{d,uptake} * X_{1\ (or\ 3)}}{V_{AP\ (or\ BL)}} \tag{11}$$

Using equations 10 and 11, the rate constants k_{12} and k_{32} for initial AP or BL uptake can also be calculated as follows using the experimentally determined Michaelis-Menten kinetic parameters (12):

$$k_{12\ (or\ 32)} = \frac{V_{max}}{K_m * V_{AP\ (or\ BL)} + X_{1\ (or\ 3)}} + \frac{K_d}{V_{AP\ (or\ BL)}} \qquad (12)$$

Validation of the three-compartmental model and goodness of fit to experimental data were assessed by evaluating the %CV values for each parameter estimate, as well as the parameter sensitivity.

Simulation of Transcellular and Paracellular Transport

The contribution of transcellular and paracellular transport to the absorptive transport of amoxicillin was determined by simulating the appearance of amoxicillin in the BL compartment after AP dosing, using differential equations describing transcellular or paracellular transport only. These equations were as follows:

Paracellular:

$$\frac{dX_1}{dt} = -k_{13} * X_1 \qquad (13)$$

$$\frac{dX_3}{dt} = k_{13} * X_1 \qquad (14)$$

Transcellular:

$$\frac{dX_1}{dt} = -k_{12} * X_1 + k_{21} * X_2 \qquad (15)$$

$$\frac{dX_2}{dt} = k_{12} * X_1 - (k_{21} + k_{23}) * X_2 + k_{32} * X_3 \qquad (16)$$

$$\frac{dX_3}{dt} = k_{23} * X_2 - k_{32} * X_3 \qquad (17)$$

To validate the estimates of relative contributions of paracellular and transcellular transport, P_{app} values were calculated for simulated transcellular and paracellular transport and compared to the experimentally determined P_{app} for absorptive transport of amoxicillin.

Results

Absorptive Transport and Cellular Accumulation of Amoxicillin in Caco-2 Cell Monolayers

The absorptive transport across Caco-2 cell monolayers and cellular accumulation of amoxicillin are shown in **Figure 3-2**. Absorptive transport (*i.e.*, AP to BL transport) of amoxicillin across Caco-2 cell monolayers was linear with respect to time, up to 60 minutes. Less than 5% of the total starting dose of amoxicillin was transported over the course of the experiment. The absorptive and secretory (*i.e.*, BL to AP) permeabilities of amoxicillin at 50 µM were similar (80 nm/s) and not significantly different. At 100 µM and 8 mM of amoxicillin, the permeability of amoxicillin was similar (P_{app} of 49.21 nm/s and 51.28 nm/s, respectively). In ice cold buffer conditions (4ºC), the absorptive transport of amoxicillin (100 µM) decreased by 1.8-fold (P_{app} of 27.29 nm/s) and was significantly different compared to the P_{app} at 37ºC ($p=0.01$), suggesting that while there is evidence for a role of a transporter(s) in the translocation of amoxicillin across Caco-2 cell monolayers, a component of amoxicillin's transport is *via* passive processes. Furthermore, the cellular accumulation of amoxicillin in Caco-2 cell monolayers was negligible compared to transport into the BL compartment over 60 minutes (**Figure 3-2b**) at both concentrations evaluated, indicating that efflux of amoxicillin from the cell across the BL membrane is unlikely to be the rate-limiting step in amoxicillin transport.

Amoxicillin AP to BL permeability across human intestinal epithelia was similar to that across Caco-2 cell monolayers (P_{app} of 66.9 nm/s). Interestingly, the secretory transport of amoxicillin (BL to AP) was significantly greater than that in the AP to BL direction (P_{app} of 153.9 nm/s, $p<0.01$), a 2.3-fold difference (**Figure 3-2c**). The higher BL to AP transport compared to AP to BL was not observed in Caco-2 cell monolayers. At the termination of the absorptive transport experiment, there was greater mass of amoxicillin in the recipient chamber (BL, 1328 pmol) than in the tissues (614 pmol or <1% of the starting dose), suggesting that BL efflux of amoxicillin is not rate-limiting in the absorptive transport of amoxicillin across human intestinal epithelium.

Concentration-dependent AP and BL Uptake of Amoxicillin in Caco-2 Cell Monolayers.

In Caco-2 cell monolayers, the uptake of amoxicillin across the AP membrane was a nonlinear and saturable process with respect to concentration, and fit a model with one saturable and one nonsaturable component (**Figure 3-3**). A V_{max} of 560.2 pmol/mg protein/min, K_m of 0.67 mM, and $K_{d,uptake}$ of 0.243 µL/min/mg protein were obtained, indicative of a relatively low affinity but high capacity active transport mechanism for amoxicillin. Comparison of the nonsaturable $K_{d,uptake}$ value (0.243 µL/min/mg) and the uptake CL value (*i.e.*, V_{max}/K_m ratio - 0.836 µL/min/mg) suggests that at low concentrations (*i.e.*, concentrations well below the K_m), approximately 80% of the AP uptake of amoxicillin likely occurs *via* a saturable process in Caco-2 cell monolayers.

In contrast, the uptake of amoxicillin across the BL membrane was linear with respect to concentration up to 10 mM (**Figure 3-4**). The BL uptake data did not support a model of saturable and nonsaturable components; this may be due to uptake of amoxicillin across the BL membrane that is mediated by a transporter that cannot be saturated at concentrations up to

10 mM, or due to non-specific binding when amoxicillin approaches the cells from the BL chamber, or both..

Efflux of Amoxicillin from AP and BL Membranes of Preloaded Caco-2 Cell Monolayers and Human Intestinal Epithelia

Efflux of amoxicillin to the AP and BL compartments was determined as a function of time after preloading Caco-2 cell monolayers with amoxicillin (100 μM dosing solution, **Figure 3-5**). A mean of 500 pmol amoxicillin was preloaded into Caco-2 cell monolayers (*i.e.*, the sum of cumulative amoxicillin effluxed during the experiment and the mass in cell or tissue at the termination of the experiment). At each time point, BL efflux was greater than AP efflux, with 21% and 41% of the preloaded amount egressed in 10 minutes across the AP and BL membranes, respectively. The results suggest a contribution of one or more BL efflux transporters to the overall absorptive transport of amoxicillin across Caco-2 cell monolayers, and that BL efflux is unlikely to be rate-limiting in the absorptive transport of amoxicillin. Greater BL efflux compared to AP efflux was observed in adult human intestinal epithelia that were preloaded with amoxicillin (100 μM dosing solution, **Figure 3-5**). A mean of 3294 pmol amoxicillin was preloaded into tissues, of which 39% and 40% were egressed in 10 minutes across the AP and BL membranes, respectively. Amoxicillin absorptive transport across human intestinal epithelia is also likely to involve an efficient BL efflux transporter.

Kinetic Modeling of Amoxicillin Absorptive Transport in Caco-2 Cell Monolayers and Human Intestinal Epithelia

Experimental transport of amoxicillin (100 μM) and cellular accumulation data (**Figure 3-2, Figure 3-3, Figure 3-5**) were simultaneously modeled using the differential equations

described in the Methods Section (Equations 6, 7, and 8). For Caco-2 cell monolayers, the rate constants k_{21} and k_{23} representing AP efflux and BL efflux, respectively, were fixed to experimentally derived parameters as these processes were linear with respect to time (**Figure 3-5**). Since BL uptake in Caco-2 cell monolayers was shown to be nonsaturable and possibly due to an experimental artifact, the rate constant k_{32} representing BL uptake was assumed to be negligible and fixed to a small number (**Table 3-1**). BL uptake is also expected not to contribute to the overall absorptive transport of amoxicillin because of the sink conditions present (*i.e.*, less than 5% of amoxicillin transported from AP to BL compartments over the course of the experiment) and the consequently low concentrations of amoxicillin in the BL compartment. Similarly, for human intestinal epithelia, rate constants for k_{21} and k_{23} were fixed at experimental values (**Table 3-1**).

Simulation of amoxicillin absorptive transport across Caco-2 cell monolayers with the kinetic models provided an estimate of amoxicillin absorptive P_{app} of 104 nm/s, which is within 15% of the experimental absorptive P_{app} value of 92 nm/sec, providing validation of the model. The model provided an estimate of the relative contribution of transcellular and paracellular transport across Caco-2 cell monolayers to be approximately 80% and 20%, respectively. For human intestinal epithelia, the estimated value of absorptive P_{app} was 67 nm/s, which was approximately twice the experimental value of 32 nm/s, but was closer to the estimated value of absorptive P_{app} in the Caco-2 cell model. It is important to note that the experimental value of absorptive P_{app} in the intestinal epithelia was 72% of the absorptive P_{app} (43 nm/s) of mannitol, a paracellular transport marker, which is a surprising result considering that the model estimates 73% of the overall absorptive transport of amoxicillin across human intestinal epithelium to be transcellular (27% paracellular). Thus, the predominant absorption mechanism for amoxicillin in

both *in vitro* models is primarily transcellular, with a significant paracellular contribution (>20%). This is consistent with the experimental data that demonstrate saturable (transporter-mediated) AP uptake of amoxicillin into Caco-2 cell monolayers and human intestinal epithelium, and efficient BL efflux. However, the predominant transcellular transport of amoxicillin across human intestinal epithelium is not consistent with the published experimental absorptive P_{app} value that is lower than that of the paracellular marker mannitol[17]. Given that amoxicillin is a zwitterionic and hydrophilic molecule and thus expected to have poor membrane permeability, it is reasonable that both AP uptake and BL efflux require drug transporters.

Inhibition of Cellular Accumulation of Amoxicillin in Caco-2 Cell Monolayers by Transporter Inhibitors

To investigate the possible role of potential AP uptake and BL efflux transporters in the absorptive transport of amoxicillin across Caco-2 cell monolayers, the cellular accumulation of amoxicillin was determined at 60 minutes after AP dosing in the absence or presence of known chemical inhibitors of several drug transporters.

Inhibition of PEPT1 with a known inhibitor of this transporter, valacyclovir[18], decreased cellular accumulation of amoxicillin by 3.3-fold ($p<0.001$) (**Figure 3-6**), providing evidence that PEPT1 plays a significant role in AP uptake and absorptive transport of amoxicillin across Caco-2 cell monolayers. A 2.7-fold decrease ($p<0.001$) was also observed in amoxicillin accumulation into Caco-2 cell monolayers across the AP membrane in the presence of estrone-3-sulfate (E3S), a known inhibitor of OATP transporters (**Figure 3-6**)[19]. This was further investigated in a second *in vitro* system of HEK293 cells overexpressing OATP2B1, the OATP transporter that is highly expressed in the human intestine[20]. Inhibition of OATP2B1 by high concentrations of (unlabeled) E3S in this system did not impact the accumulation of amoxicillin but did reduce

accumulation of the radiolabeled E3S (positive control) (**Figure 3-7**), suggesting that amoxicillin is likely not a substrate of OATP2B1 and that this transporter does not contribute to the intestinal absorption of amoxicillin.

There was no statistically significant difference in amoxicillin accumulation after AP dosing in the presence of GW918, a chemical inhibitor of the AP efflux transporters P-gp and BCRP, providing evidence that AP efflux does not impede amoxicillin absorptive transport across Caco-2 cell monolayers (data not shown). In the presence of MK571, an inhibitor of MRPs, including the AP efflux transporter MRP2 and the BL efflux transporters MRP3 and MRP4, there was also no difference in amoxicillin accumulation after 60 minutes (data not shown). Thus, it can be concluded that MRP2 does not impede amoxicillin absorptive transport across Caco-2 cell monolayers and that MRP transporters in the BL membrane do not facilitate amoxicillin egress across this membrane.

Discussion

Amoxicillin has dose-dependent oral bioavailability and demonstrates "flip-flop" kinetics wherein absorption, rather than elimination, appears to be the rate-limiting step in its disposition. Thus, its intestinal absorption is likely the rate-limiting step in its disposition and its absorption is saturable and likely mediated by transporters[4,5,6,7]. Amoxicillin oral bioavailability decreases with dose from 90% for a 50 mg dose and 22% at 10 g[5]. At oral doses above 850 mg, it is likely that solubility limitations are the reason for the apparent decrease in amoxicillin oral bioavailability; however, the dose-dependency of absorption has been observed even across a range of lower doses between 250 and 875 mg[2]. Under typical experimental conditions (pH 7.4 in AP and BL compartments) reported in the literature, amoxicillin (100 μM) has poor passive diffusion across two *in vitro* transport models, MDCK and Caco-2 cell monolayers[17] with P_{app}

values of 2.4 and 0.21 nm/s respectively. The previously reported P_{app} value is surprising, given that it is 27-fold lower than that of the paracellular marker mannitol (5.7 nm/s) obtained within the same experiment[17]. Such low P_{app} values are not consistent with the reported human oral bioavailability of >90%. Previous studies have suggested that amoxicillin is a substrate for PEPT1 as well as the renal peptide transporter PEPT2, but not for organic anion transporter 1 (OAT1)[8].

To elucidate the dose-dependency of amoxicillin oral bioavailability and its "flip-flop" kinetics, a relevant *in vitro* model was required in which the dose-dependent oral absorption of amoxicillin could be recapitulated and in which the transporter expression profile, particularly of PEPT1, would be similar to that in human intestinal epithelium. Two *in vitro* models were used in these studies, the Caco-2 cell monolayers and fresh adult human intestinal epithelia mounted in an Ussing chamber diffusion system. Caco-2 cell monolayers are a common *in vitro* model for studying drug transport and permeability across intestinal epithelium. However, Caco-2 cell monolayers have a smaller average pore radius and higher TEER compared to human intestinal (jejunal) epithelium[21]. Expression of some transporters such as PEPT1 can be highly variable between laboratories and culture conditions, and may not reflect *in vivo* conditions[22]. Therefore, a second *in vitro* model, fresh adult human intestinal epithelia, was used to generate uptake and transport kinetic data that are more relevant to *in vivo* conditions of amoxicillin intestinal absorption and overall disposition. Fresh adult human intestinal epithelia, when mounted in Ussing chambers, have been used to perform drug metabolism and transport studies[12].

Interestingly, the dose-dependent absorptive transport of amoxicillin observed in the *in vitro* model of intestinal transport/absorption, Caco-2 cell monolayers, was not reflective of the dose-dependent absorption observed in human subjects. P_{app} values observed in Caco-2 cell

monolayers decreased from 80 nm/s to 49 nm/s when the amoxicillin AP concentration was increased from 50 μM to 100 μM, but there was no further change in P_{app} at concentrations up to 8 mM amoxicillin. In this study, in contrast to previously published work[17], transport experiments were conducted at pH 6 in the AP compartment and pH 7.4 in the BL compartment to assess the role of PEPT1, a proton-symporter, in the absorptive transport of amoxicillin across Caco-2 cell monolayers and human intestinal epithelia. Under these conditions, and at the same dosing concentration of 100 μM, amoxicillin exhibited a P_{app} value of approximately 50 nm/s, consistent with transporter-mediated (*e.g.*, PEPT1) absorptive transport. The role of PEPT1 in amoxicillin absorptive transport was confirmed by the observation that an inhibitor of PEPT1, valacyclovir, significantly decreased AP accumulation of amoxicillin into Caco-2 cells (**Figure 3-6**). Inhibition studies in Caco-2 cell monolayers indicate that most β-lactam antibiotics, including amoxicillin, have low affinity for PEPT1 (K_i > 7 mM)[23,24], an observation that is consistent with the AP uptake kinetics determined in this study.

Interestingly, increases in C_{max} and AUC of amoxicillin in healthy adults are less than proportional to the increase in doses, indicating saturation starting 750 mg[85] (**Figure 1-6**), a dose that corresponds to an intestinal luminal concentration of 8.2 mM (assuming dissolution in 250 mL). AP uptake studies performed in Caco-2 cell monolayers suggested a saturable component which contributed predominantly to amoxicillin uptake up to a concentration of 0.67, with a non-saturable component predominating at higher concentrations. It is conceivable that the saturable component of the amoxicillin transport across Caco-2 cell monolayers, which may play a major role at low concentrations (< K_m of 0.67 mM), is not discernable in studies with human subjects because sufficiently low doses were not evaluated. Interestingly, studies performed using human intestinal epithelia showed that AP uptake of amoxicillin increased

linearly with respect to concentration up to 8 mM. Thus, at concentrations of amoxicillin within the limits of its solubility (approximately 8 mM at a pH of 6.0)[2], it appears to be difficult to saturate the amoxicillin AP uptake process in the human intestinal epithelia model. Based on these results obtained with Caco-2 cell monolayers and human intestinal epithelium, and consistent with the saturation of amoxicillin absorption in human subjects occurring at luminal concentrations near its solubility limit (750 mg dose, 8.2 mM luminal concentration), one can pustulate that PEPT1, a likely AP uptake transporter for amoxicillin, is highly expressed and thus difficult to saturate. This is consistent with mass spectrometric analyses which indicate that PEPT1 is highly expressed in the small intestine and comprises up to 50% of total transporter protein[20,26]. Interestingly, the permeability of amoxicillin across Caco-2 cell monolayers in ice cold transport buffer decreased. Under ice cold conditions, active uptake and efflux by transporters is halted, and only transport by passive diffusion can occur (although the decrease in temperature can also decrease the rate of passive diffusion). Thus, the decrease in permeability observed in ice cold conditions suggests that amoxicillin transport across Caco-2 cell monolayers is transporter-mediated, with a significant passive transport component, which may be due to paracellular transport.

While inhibition of PEPT1 by valacyclovir reduced the accumulation of amoxicillin in Caco-2 cell monolayers, this inhibition is incomplete and there is a possible role for other yet unknown AP uptake transporters. Amoxicillin is an inhibitor of OATP1B1, OATP2B1, and OATP1B3[25], suggesting an affinity for OATP uptake transporters. E3S, a substrate and competitive inhibitor of OATP transporters, reduced accumulation of amoxicillin in Caco-2 cell monolayers across the AP membrane by 2.7-fold ($p<0.01$), suggesting that AP uptake of amoxicillin, at least in part, is mediated by an OATP transporter (**Figure 3-6b**), assuming that

E3S does not inhibit PEPT1. Interestingly, E3S did not affect amoxicillin (10 μM) uptake into OATP2B1-transfected HEK293 cells (**Figure 3-7**). In contrast, uptake of radiolabeled E3S (1 μM), the positive control substrate, was significantly ($p<0.0001$) reduced with excess concentrations of E3S in this *in vitro* model. OATP2B1 was selected in this study because it is the OATP transporter present in the human intestine, comprising 6% of total transporter proteins in the small intestine[20,26]. It is possible that amoxicillin is a substrate of one of the other OATP transporters. However, OATP1B1 and 1B3 mRNA and protein were not detectable in the small intestines of 9 adults[26], suggesting that these are not major transporters in the human intestine. Whether another transporter inhibited by E3S, *e.g.*, a MATE transporter[27] or OSTα/β[28], plays a role in amoxicillin absorption, remains to be investigated.

Comparison of the intracellular and tissue disposition of amoxicillin to transported amoxicillin in the receiver compartment (BL) shows very little accumulation of amoxicillin in Caco-2 cell monolayers and human intestinal epithelia, suggesting that BL efflux is not rate-limiting in amoxicillin absorption. Efflux studies performed in both *in vitro* models also suggest efficient BL efflux of amoxicillin.

As amoxicillin remains charged upon uptake into the cell, a BL efflux transporter is required to assist its egress across the BL membrane of the enterocyte into the blood. The BL transporters include MRP3[29], MRP4[30], BL peptide transporters[31], and OSTα/β[32]. A BL peptide efflux transporter is implicated in a physiological role in effluxing dietary peptides, although it has not been characterized to date[31,33,34]. In contrast to the AP PEPT1 transporter, the BL peptide efflux transporter appears to be a bidirectional facilitative transport system[31,35]. MRP transporters typically transport anionic or zwitterionic compounds[36], and are known to transport cephalosporin β-lactam antibiotics[37,38]; however, the results in this study did not support a role

for them in facilitating BL egress of amoxicillin in the Caco-2 cell monolayer model. OSTα/β is a bidirectional intestinal bile acid transporter with broad substrate specificity, but primarily transports bile acids and is unlikely to be involved in amoxicillin BL efflux[39]. Preliminary experiments (data not shown) confirmed that amoxicillin is not a substrate for OSTα/β[2]. The BL peptide efflux transporter is likely to also efflux amoxicillin as it is a peptidomimetic compound. Although this transporter has not been characterized, it appears to be a facilitative transport mechanism[31,35]. Thus, the BL peptide efflux transporter may explain, in part, the efficient BL efflux of amoxicillin and also the significant passive transport that has been observed in Caco-2 cell monolayers.

Since the relative contribution of transcellular *vs* paracellular transport cannot be experimentally determined *in vitro*, a three-compartment kinetic model was used to estimate the contribution of transcellular and paracellular pathways to the absorptive transport of amoxicillin. A similar kinetic modeling approach has been used in conjunction with data obtained from Caco-2 cell monolayers to identify the relative contribution of these pathways for the hydrophilic cations ranitidine and metformin[9,10]. As with amoxicillin, the low lipophilicity and positive charge of these compounds would indicate low passive permeability and thus, poor oral bioavailability in the absence of transporter-mediated processes. However, in all cases, oral bioavailability is higher than would be expected based on these physicochemical properties alone: over 50% for ranitidine[40] and 50-60% for metformin[41]. Kinetic modeling suggests that the absorptive transport of amoxicillin across Caco-2 cell monolayers is predominantly transcellular but the paracellular route contributes 20%. Compared to the cationic drugs ranitidine and

[2] Courtesy of Dr. Dong Fu and the Brouwer Laboratory, UNC Eshelman School of Pharmacy, UNC Chapel Hill.

metformin (~60%[10] and 10%[9] transcellular, respectively), amoxicillin has a greater transcellular component (~80% transcellular) to its absorptive transport.

In the case of ranitidine and metformin, AP cation-selective uptake transporters are available for entry into the enterocyte. However, BL efflux is inefficient and appears to be the rate-limiting step in the transcellular pathway of absorption for these cations[9,10]. Efflux studies suggest that for these hydrophilic cations, traversing the BL membrane after entering the cell is an inefficient passive process, and in fact, there may not be BL efflux transporters for cationic compounds at all[42]. The lack of cation-selective transporters to efflux ranitidine and metformin across the BL membrane results in BL efflux being a rate-limiting step in the absorption of these compounds *via* the transcellular pathway. Consequently, the paracellular pathway plays a key role in the absorptive transport of metformin and a significant role in the absorptive transport of ranitidine. In contrast to ranitidine and metformin, amoxicillin is a zwitterion rather than a cation, and like some of the penicillin and cephalosporin β-lactam antibiotics, has a peptidomimetic structure that increases its likelihood of transport by peptide transporters[43]. Unlike ranitidine and metformin, amoxicillin is able to utilize AP uptake and BL efflux transport mechanisms in the small intestine (*i.e.*, AP PEPT1 and a BL peptide facilitative transport system) that have important dietary roles and are highly efficient. As a zwitterion, the BL efflux transporters MRP3 and MRP4 are also possible options for efficient BL efflux, although the accumulation studies performed suggest that MRPs are unlikely to be involved. Therefore, it is not surprising that transcellular processes would have greater contribution to the absorptive transport of amoxicillin compared to hydrophilic cationic drugs.

Prior to this study, there was little knowledge or evidence about the contribution of paracellular transport to the absorption of amoxicillin and the mechanism(s) underlying the

unexpectedly high oral bioavailability of amoxicillin despite a long-hypothesized role of PEPT1. Both amoxicillin and ampicillin are zwitterions with low passive permeability, but the oral bioavailability of amoxicillin is at least 2-fold higher than that of ampicillin (34%)[44]. Ampicillin, like amoxicillin, is a penicillin and substrate of PEPT1, but in an everted rat gut sac model, was transported without significant contribution of PEPT1[45]. Transport of ampicillin was increased 3-fold[45] in the presence of ethylenediaminetetraacetic acid (EDTA), a chelator of intracellular calcium that increases diffusion by the paracellular route[46,47], suggesting a significant role of the paracellular pathway in its absorptive transport. However, this experimental approach could not provide an estimate of the relative contribution of the paracellular pathway *vs* the transcellular pathway in the absorptive transport of ampicillin. The tight junction proteins are selective for size and charge[48]; there is an upper radius size limit of 6-10 Å to travel through the pores of the tight junctions ("pore pathway")[48]. A paracellular “leak pathway” permits the passage of uncharged molecules up to 60 Å[48]. As a small hydrophilic charged molecule, amoxicillin also undergoes significant paracellular transport in addition to transporter-mediated transcellular transport.

In conclusion, the experimental results from two different *in vitro* models of human intestinal transport provide significant new insights into the mechanisms underlying the oral absorption of amoxicillin, an important antibiotic agent used to treat bacterial infections in adult and pediatric populations. The study supports the role of PEPT1, the peptide transporter in the AP membranes of human enterocytes, in the oral absorption of amoxicillin; notably, it also provides evidence that in addition to PEPT1, an AP transporter of the OATP family may play a role in amoxicillin absorption, although a role by other transporters (*e.g.*, MATE) cannot be ruled out. The results provide evidence that egress across the BL membrane is fairly efficient and not

rate-limiting to the intestinal absorption of amoxicillin. While a specific BL transporter that is responsible for egress of amoxicillin from enterocytes into the portal blood was not identified, preliminary data do not support a role for MRPs or OSTα/β, leaving a bidirectional peptide transporter as a likely candidate transporter that assists the egress of amoxicillin across the BL membrane of enterocytes. Finally, modeling studies provided evidence that paracellular transport across the tight junctions likely plays an important role in the oral absorption of amoxicillin. The new information generated in this work lays a strong foundation for conducting PBPK modeling studies to assess optimum doses of amoxicillin in pediatric populations in which this drug is a front-line therapy for bacterial infections.

Table 3-1. Estimated kinetic constants for AP uptake, BL uptake, and absorptive (AP to BL) transport of amoxicillin in Caco-2 cell monolayers and adult human intestinal epithelia.

Parameter	Amoxicillin Donor Concentration	
	Caco-2 Estimate (1/min; %CV)	Human Intestinal Epithelia (1/min; %CV)
	100 µM	100 µM
k_{12}	0.00375908 (19.7%)	0.00007 (12.2%)
k_{21}	0.07128 (N/A)[a]	0.012606 (N/A)[a]
k_{23}	0.14214 (N/A)[a]	0.016428 (N/A)[a]
k_{32}	0.000001 (N/A)[b]	0.00004 (330%)
k_{13}	0.000298911 (69.7%)	0.000009 (44%)

[a]Fixed to experimental value

[b]Fixed and assumed to have negligible contribution as experiments suggested high degree of nonspecific binding in this experiment.

Table 3-2. Experimental and model-simulated absorptive transport of amoxicillin in Caco-2 cell monolayers and human intestinal epithelia to assess relative contribution of transcellular and paracellular transport.

Experimental $P_{app,total}$ (%CV)			**Model Prediction, Caco-2 Cell Monolayers**				
Mannitol (10 μM)	**Amoxicillin**		**$P_{app,\ total}$**	**$P_{app,trans}$**	**$P_{app,para}$**	**% Transcellular**	**% Paracellular**
12.8 (5%)	100 μM	92.17 (11%)	103.98	83.64	22.04	80%	21%
			Model Prediction, Human Intestinal Epithelia				
			$P_{app,\ total}$	**$P_{app,trans}$**	**$P_{app,para}$**	**% Transcellular**	**% Paracellular**
42.7 (16%)	100 μM	66.9 (10%)	31.50	23.00	8.50	73%	27%

P_{app} values are expressed as nm/sec

Figure 3-1. Representative Ussing chamber and schematic of three-compartment kinetic model of amoxicillin intestinal absorption[10].

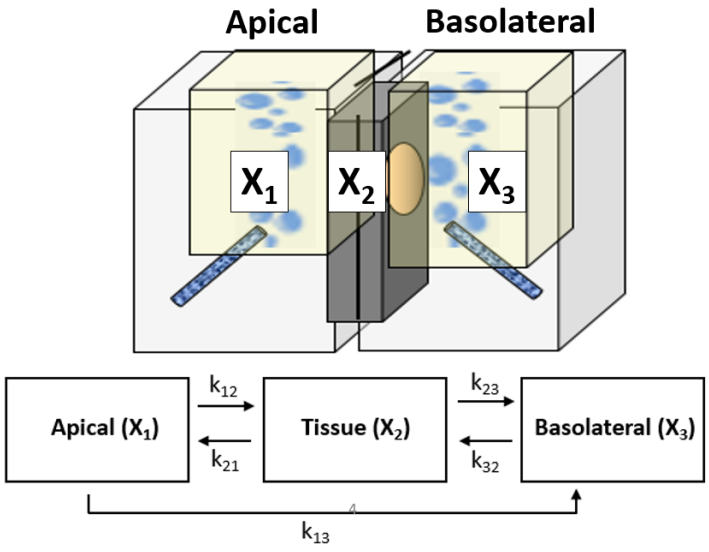

The three compartments represent the AP (X_1), cellular or tissue compartments (X_2), and BL (X_3) chambers. The rate constants represent AP uptake (k_{12}), AP efflux (k_{21}), BL uptake (k_{32}), BL efflux (k_{23}), and paracellular transport (k_{13}). Reverse paracellular flux (k_{31}) was assumed to be negligible under sink conditions, and thus is not included in the model.

Figure 3-2. Amoxicillin transport and cellular accumulation as a function of time after dosing.

a)

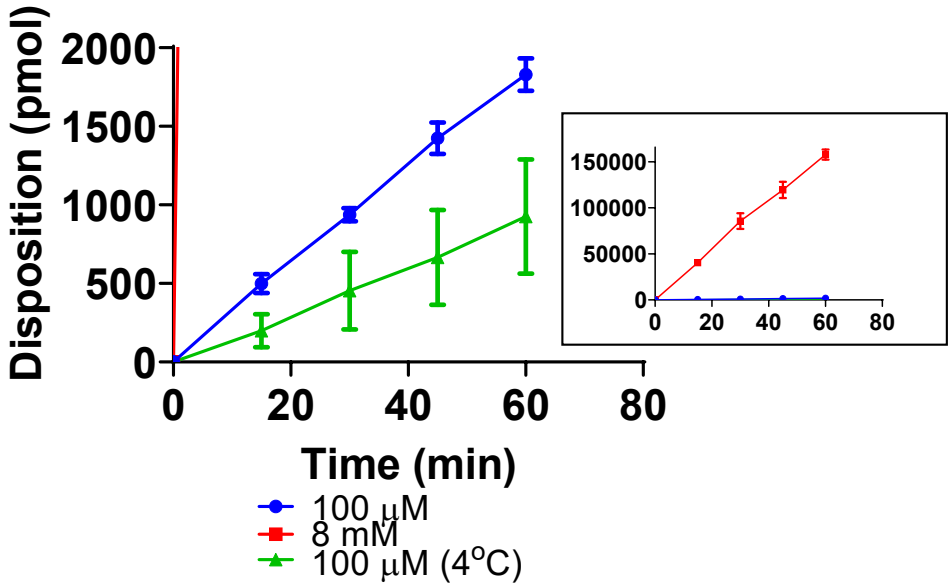

b)

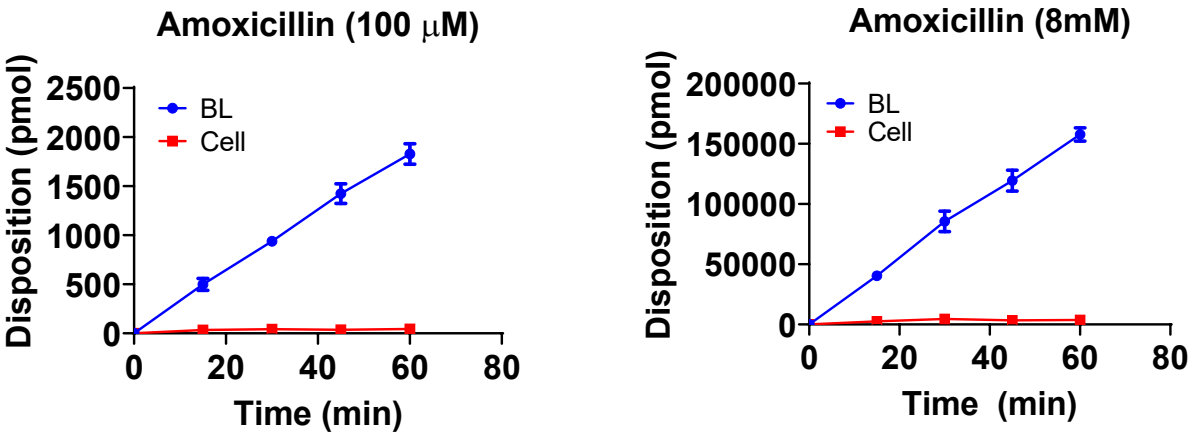

c)

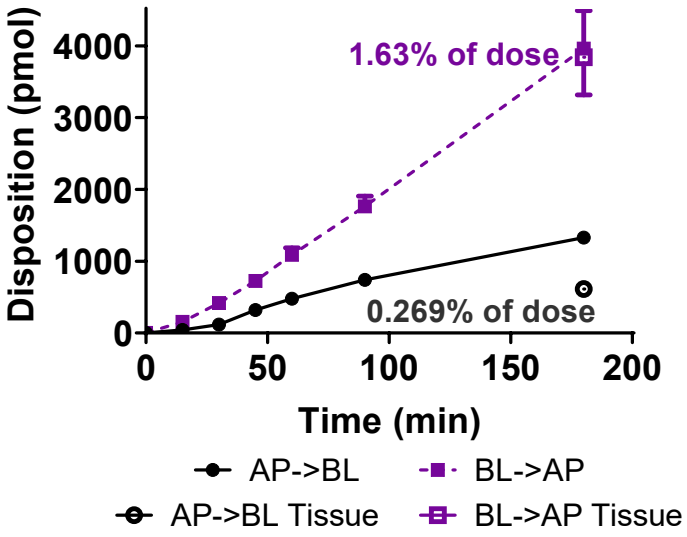

(a) Amoxicillin appearance in the BL compartment in Caco-2 cell monolayers (100 µM or 8mM) after AP dosing. (b) Amoxicillin cellular accumulation in relation to its appearance in the BL compartment in Caco-2 cell monolayers as a function of time. c) Amoxicillin (100 µM) appearance in the recipient chamber and in tissue following absorptive (AP to BL) and secretory (BL to AP) transport across human intestinal epithelia. Data represent mean ± S.D., n=3.

Figure 3-3. Concentration-dependent AP uptake of amoxicillin in a) Caco-2 cell monolayers and b) human intestinal epithelia.

a)

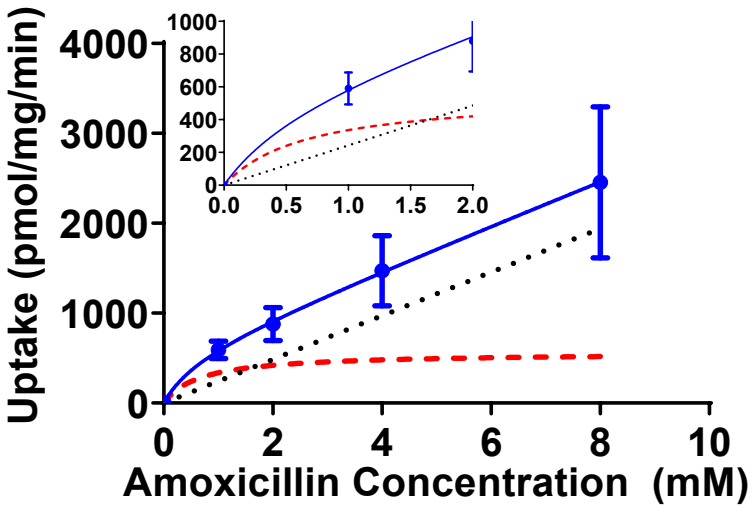

AP uptake of amoxicillin was fit to Equation 4, where the dotted black line represents the nonsaturable component and the dashed red line represents the saturable component. The inset panel in a) represents concentrations up to 2 mM to better visualize uptake below the k_m. Data represent mean ± S.D., n=3.

b)

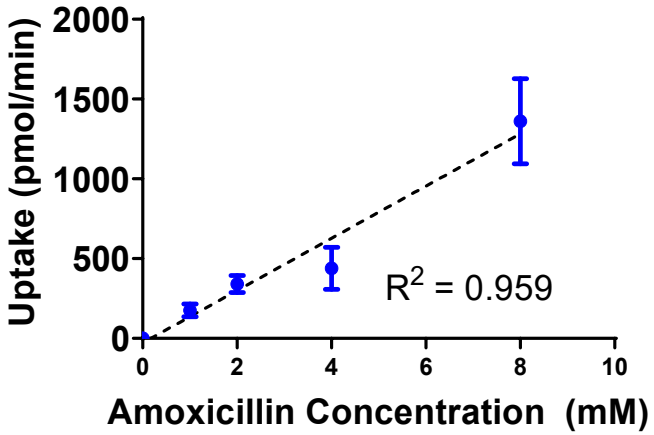

AP uptake of amoxicillin in human intestinal epithelia did not support a model of saturable and nonsaturable components. Rather, AP uptake increased linearly with concentration (linear regression line shown by black dashed line). Data represent mean ± S.D., n=3.

Figure 3-4. Concentration-dependent BL uptake of amoxicillin in Caco-2 cell monolayers.

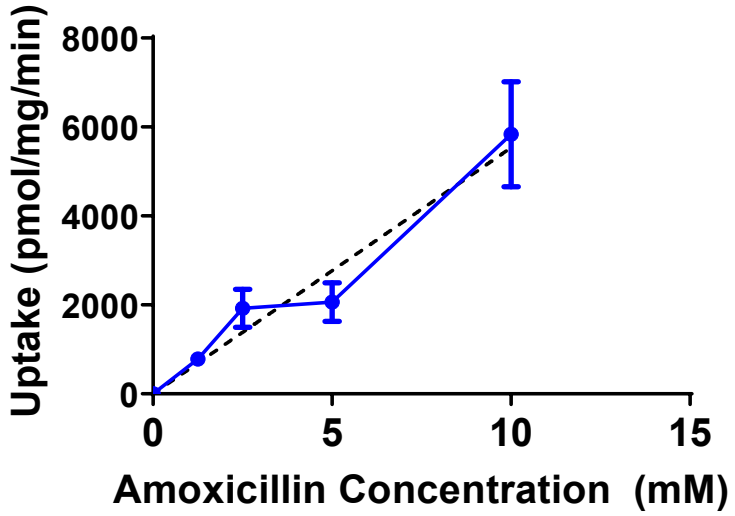

BL uptake of amoxicillin in Caco-2 cell monolayers did not support a model of saturable and nonsaturable components. Instead, BL uptake increased linearly with concentration (linear regression line shown by black dashed line). Data represent mean ± S.D., n=3.

Figure 3-5. Efflux of amoxicillin across AP and BL membranes from Caco-2 cell monolayers and adult human intestinal epithelia after preloading from AP and BL compartments with amoxicillin (100 µM).

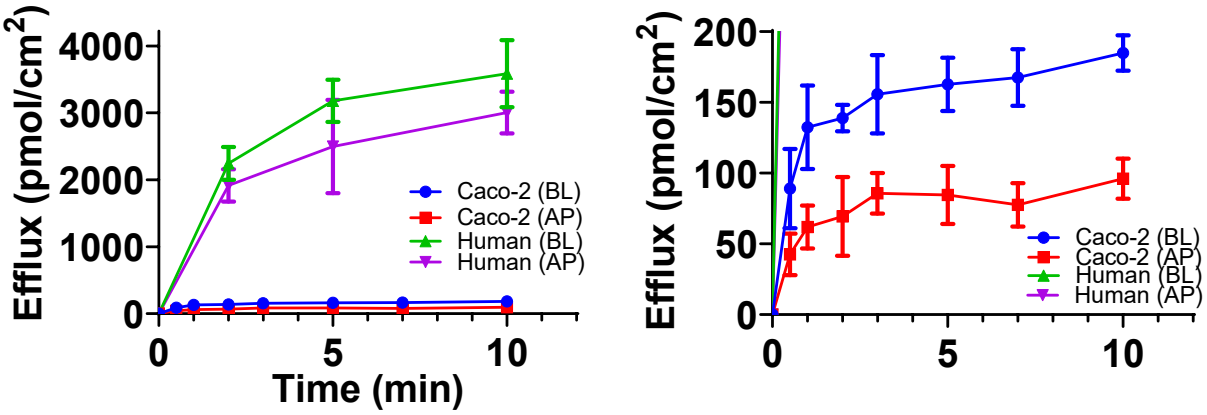

Efflux data have been normalized to the surface area available for permeation (1.15 cm^2 for Caco-2 cell monolayers in a Transwell™, and 0.3 cm^2 for adult human intestinal epithelia mounted in Ussing chamber slides). An average of 500 pmol amoxicillin was preloaded in Caco-2 cells and 3294 pmol in human intestinal epithelia (*i.e.*, the sum of the cumulative mass of amoxicillin effluxed during the experiment and the mass in cells or in tissue at the termination of the experiment). Right panel represents the same data on a different scale. Data represent mean ± S.D., n=4 for Caco-2 cell monolayers, and n=3 for human intestinal epithelia.

Figure 3-6. Accumulation and uptake of amoxicillin in Caco-2 cell monolayers in the presence of chemical inhibitors of uptake transporters.

a)

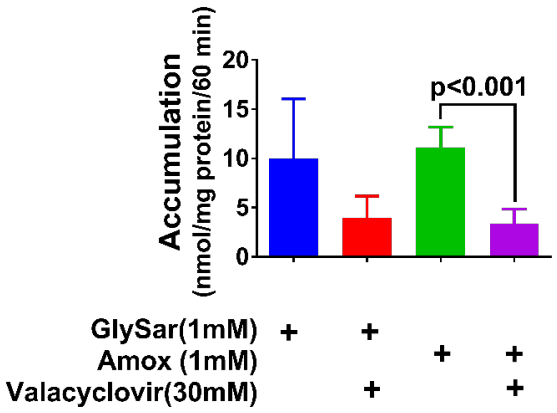

b)

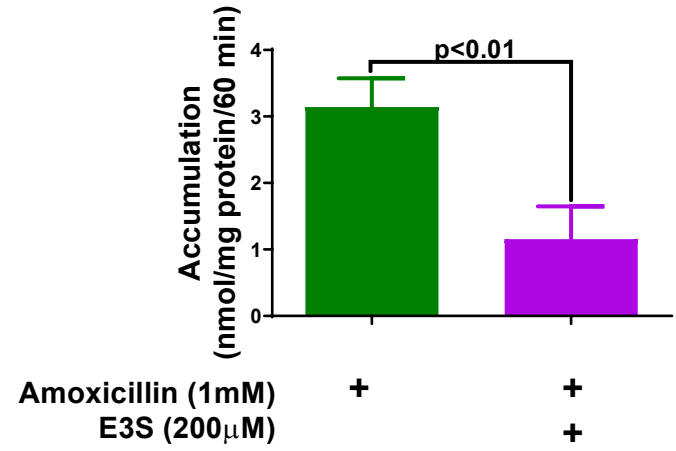

a) Cellular accumulation of amoxicillin and glysar at 60 minutes upon AP dosing (1 mM) in the presence of the PEPT1 inhibitor, valacyclovir (30mM). b) Cellular accumulation of amoxicillin upon AP dosing (1 mM) in the presence of an inhibitor of OATP transporters, estrone-3-sulface (E3S, 200 μM). The experiments depicted in (a) and (b) were conducted in different batches of Caco-2 cells. Data represent mean ± S.D., n=3.

Figure 3-7. Accumulation of E3S and amoxicillin in HEK293-OATP2B1 Corning TransportoCells™ in the presence of excess E3S.

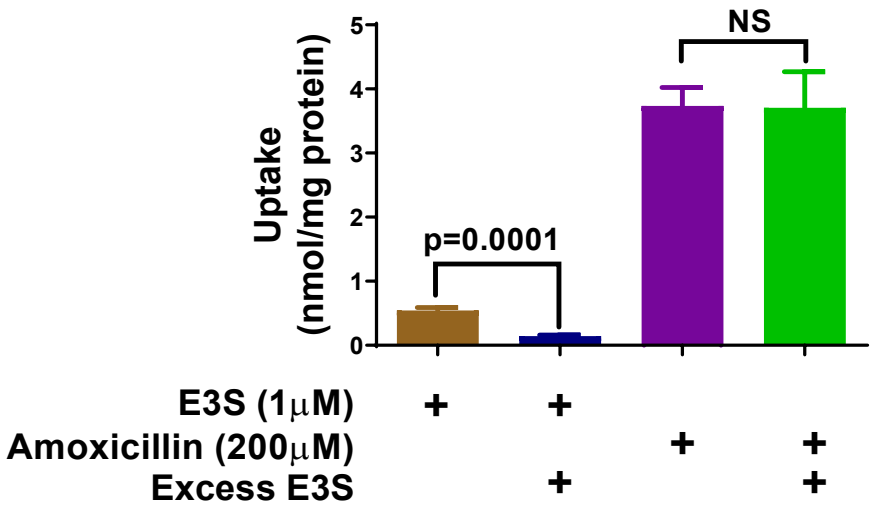

Cellular accumulation of E3S and amoxicillin and glysar in HEK293 cells overexpressing OATP2B1, in the presence of excess amounts of the OATP inhibitor, E3S. Data represent mean ± S.D., n=3.

REFERENCES

1. Lieberthal AS, Carroll AE, Chonmaitree T, *et al*. The Diagnosis and Management of Acute Otitis Media. *Pediatrics*. 2013;131(3):e964-99.

2. Thambavita D, Galappatthy P, Mannapperuma U, *et al*. Biowaiver Monograph for Immediate-Release Solid Oral Dosage Forms : Amoxicillin Trihydrate. *J Pharm Sci*. 2017;106(10):2930-2945.

3. Pichichero ME, Reed MD. Variations in Amoxicillin Pharmacokinetic/pharmacodynamic Parameters May Explain Treatment Failures in Acute Otitis Media. *Pediatr* Drugs. 2009;11(4):243-249.

4. Spyker D a., Rugloski RJ, Vann RL, *et al.* Pharmacokinetics of Amoxicillin: Dose Dependence After Intravenous, Oral, and Intramuscular Administration. *Antimicrob Agents Chemother*. 1977;11(1):132-141.

5. Piotrovskij VK, Paintaud G, Alván G, *et al.* Modeling of the Saturable Time-Constrained Amoxicillin Absorption in Humans. *Pharm Res*. 1994;11(9):1346-1351.

6. Paintaud G, Alván G, Dahl ML, *et al*. Nonlinearity of Amoxicillin Absorption Kinetics in Human. *Eur J Clin Pharmacol*. 1992;43(3):283-288.

7. Garrison KL, Sahin S, Benet LZ. Few Drugs Display Flip-Flop Pharmacokinetics and These Are Primarily Associated with Classes 3 and 4 of the BDDCS. *J Pharm Sci*. 2015:3229-3235.

8. Li M, Anderson GD, Phillips BR, *et al*. Interactions of Amoxicillin and Cefaclor with Human Renal Organic Anion and Peptide Transporters. *Drug Metab Dispos*. 2006;34(4):547-555.

9. Proctor WR, Bourdet DL, Thakker DR. Mechanisms Underlying Saturable Instestinal Absorption of Metformin. *Drug Metab Dispos*. 2008;36(8):1650-1658.

10. Bourdet DL, Pollack GM, Thakker DR. Intestinal Absorptive Transport of the Hydrophilic Cation Ranitidine: A Kinetic Modeling Approach to Elucidate the Role of Uptake and Efflux Transporters and Paracellular vs. Transcellular Transport in Caco-2 Cells. *Pharm Res*. 2006;23(6):1178-1187.

11. Ming X, Knight BM, Thakker DR. Vectorial Transport of Fexofenadine Across Caco-2 Cells: Involvement of Apical Uptake and Basolateral Efflux Transporters. *Mol Pharm*. 2011;8(5):1677-1686.

12. Kisser B, Mangelsen E, Wingolf C, *et al*. The Ussing Chamber Assay to Study Human Intestine. *Curr Protoc Pharmacol*. 2017;77(June):1-19.

13. Söderholm JD, Hedman L, Artursson P, *et al*. Integrity and Metabolism of Human Ileal Mucosa In Vitro in the Ussing Chamber. *Acta Physiol Scand*. 1998;162(1):47-56.

14. Bourdet DL, Thakker DR. Saturable Absorptive Transport of the Hydrophilic Organic Cation Ranitidine in Caco-2 cells: Role of pH-dependent Organic Cation Uptake System and P-glycoprotein. *Pharm Res*. 2006;23(6):1165-1177.

15. Dufek MB, Knight BM, Bridges AS, *et al*. P-glycoprotein Increases Portal Bioavailability of Loperamide in Mouse By Reducing First-pass Intestinal Metabolism. *Drug Metab Dispos*. 2013;41(March):642-650.

16. Blais A, Bissonnette P, Berteloot A. Common Characteristics for Na + -Dependent Sugar Transport in Caco-2 Cells. *J Membr Biol*. 1987;99:113-125.

17. Irvine JD, Takahashi L, Lockhart K, *et al*. MDCK (Madin − Darby Canine Kidney) Cells: A Tool for Membrane Permeability Screening. *J Pharm Sci*. 1999;88(1):28-33.

18. Pak YA, Long AJ, Annes WF, *et al*. In Vitro and Clinical Evaluations of the Drug-Drug Interaction Potential of a Metabotropic Glutamate 2/3 Receptor Agonist Prodrug with Intestinal Peptide Transporter 1. *Drug Metab Dispos*. 2017;45(2).

19. Ishiguro N, Maeda K, Kishimoto W, *et al*. Predominant Contribution of OATP1B3 to the Hepatic Uptake of Telmisartan, an Angiotension II Receptor Antagonist, in Humans. *Drug Metab Dispos*. 2006;34(7):1109-1115.

20. Drozdzik M, Gro C, Penski J, *et al*. Protein Abundance of Clinically Relevant Multidrug Transporters Along the Entire Length of the Human Intestine. *Mol Pharm*. 2014;11(10):3547-3555.

21. Tavelin S. *New Approaches to Studies of Paracellular Drug Transport in Intestinal Epithelial Cell Monolayers*. Vol 285.; 2003.

22. Behrens I, Kamm W, Dantzig AH, *et al.*. Variation of Peptide Transporter (PepT1 and HPT1) Expression in Caco-2 Cells as a Function of Cell Origin. *J Pharm Sci*. 2004;93(7):1743-1754.

23. Brandsch M, Knütter I, Leibach FH. The Intestinal H+/peptide Symporter PEPT1: Structure-affinity Relationships. *Eur J Pharm Sci*. 2004;21(1):53-60.

24. Brandsch M. Transport of Drugs by Proton-coupled Peptide Transporters: Pearls and Pitfalls. *Expert Opin Drug Metab Toxicol*. 2009;5(8):887-905.

25. Parvez MM, Jung JA, Shin HJ, *et al.* Characterization of 22 Antituberculosis Drugs for Inhibitory Interaction Potential on Organic Anionic Transporter Polypeptide (OATP)-Mediated Uptake. *Antimicrob Agents Chemother*. 2016;60(5):3096-3105.

26. Drozdzik M, Busch D, Lapczuk J, *et al*. Protein Abundance of Clinically Relevant Drug Transporters in the Human Liver and Intestine: A Comparative Analysis in Paired Tissue Specimens. *Clin Pharmacol Ther*. 2019;105(5):1204-1212.

27. Tanihara Y, Masuda S, Sato T, *et al.* Substrate Specificity of MATE1 and MATE2-K, Human Multidrug and Toxin Extrusions/H+ -Organic Cation Antiporters. *Biochem Pharmacol*. 2007;74:359-371.

28. Seward DJ, Koh AS, Boyer JL, *et al.* Functional Complementation Between a Novel Mammalian Polygenic Transport Complex and an Evolutionarily Ancient Organic Solute Transporter, OSTalpha-OSTbeta. *J Biol Chem*. 2003;278(30):27473-27482.

29. Rost D, Mahner S, Sugiyama Y, *et al*. Expression and Localization of the Multidrug Resistance- Associated Protein 3 in Rat Small and Large Intestine. *Am J Physiol Gastrointest Liver Physiol*. 2001;282:720-726.

30. Ming X, Thakker DR. Role of Basolateral Efflux Transporter MRP4 in the Intestinal Absorption of the Antiviral Drug Adefovir Dipivoxil. *Biochem Pharmacol*. 2010;79(3):455-462.

31. Irie M, Terada T, Okuda M, *et al*. Efflux Properties of Basolateral Peptide Transporter in Human Intestinal Cell Line Caco-2. *Pflugers Arch Eur J Physiol*. 2004;449(2):186-194.

32. Dawson PA, Hubbert M, Haywood J, *et al*. The Heteromeric Organic Solute Transporter α-β, Ostα-Ostβ, Is an Ileal Basolateral Bile Acid Transporter□. *J Biol Chem*. 2005;280(8):6960-6968.

33. Berthelsen R, Nielsen CU, Brodin B. Basolateral Glycylsarcosine (Gly-Sar) Transport in Caco-2 Cell Monolayers is pH Dependent. *J Pharm Pharmacol*. 2013;65(7):970-979.

34. Rohm F, Daniel H, Spanier B. Transport Versus Hydrolysis: Reassessing Intestinal Assimilation of Di- and Tripeptides by LC – MS / MS Analysis. *Mol Nutr Food Res*. 2019;1900263:1-10.

35. Terada T, Sawada K, Saito H, *et al*. Functional Characteristics of Basolateral Peptide

Transporter in the Human Intestinal Cell Line Caco-2. *Am J Physiol*. 1999;276(6 Pt 1):G1435-G1441.

36. Hillgren KM, Keppler D, Zur a a, *et al*. Emerging Transporters of Clinical Importance: An Update from the International Transporter Consortium. *Clin Pharmacol Ther*. 2013;94(1):52-63.

37. De Waart DR, Van De Wetering K, Kunne C, *et al*. Oral Availability of Cefadroxil Depends on ABCC3 and ABCC4. *Drug Metab Dispos*. 2012;40(3):515-521.

38. Akanuma S, Uchida Y, Ohtsuki S, *et al*. Molecular-weight-dependent, Anionic-substrate-preferential Transport of β-Lactam Antibiotics via Multidrug Resistance-associated Protein 4. *Drug Metab Pharmacokinet*. 2011;26(6):602-611.

39. Rao A, Haywood J, Craddock AL, *et al*. The Organic Solute Transporter Alpha-Beta, Ost Alpha-Ost Beta, is Essential for Intestinal Bile Acid Transport and Homeostasis. *PNAS*. 2008;105(10):3891-3896.

40. Lin JH. Pharmacokinetic and Pharmacodynamic Properties of Histamine H2-receptor Antagonists. Relationship Between Intrinsic Potency and Effective Plasma Concentrations. *Clin Pharmacokinet*. 1991;20(3):218–236.

41. Tucker GT, Casey C, Phillips PJ, *et al*. Metformin Kinetics in Healthy Subjects and in Patients with Diabetes Mellitus. *Br J Clin*. 1981;12:235-246.

42. Proctor WR, Ming X, Bourdet D, *et al*. Why Does the Intestine Lack Basolateral Efflux Transporters for Cationic Compounds? A Provocative Hypothesis. *J Pharm Sci*. 2016;105(2):484-496.

43. Nakashima E, Tsuji A, Mizuo H, *et al*. Kinetics and Mechanism of In Vitro Uptake of Amino-Beta-Lactam Antibiotics by Rat Samll Intestine and Relation to the Intact-Peptide Transport System. *Biochem Pharmacol*. 1984;33(21):3345-3352.

44. Gordon RC, Regamey C, Kirby WMM. Comparative Clinical Pharmacology of Amoxicillin and Ampicillin Administered Orally. *Antimicro*. 1972;1(6):504-507.

45. Lafforgue G, Arellano C, Vachoux C, *et al*. Oral Absorption of Ampicillin: Role of Paracellular Route vs. PepT1 Transporter. *Fundam Clin Pharmacol*. 2008;22(2):189-201.

46. Tomita M, Hayashi M, Awazu S. Absorption-Enhancing Mechanism of EDTA, Caprate, and Decanoylcarnitine in Caco-2 Cells. *J Pharm Sci*. 1996;85(6):12-15.

47. Takizawa Y, Kishimoto H, Nakagawa M, *et al*. Effects of Pharmaceutical Excipients on Membrane Permeability in Rat Small Intestine. *Int J Pharm*. 2013;453(2):363-370.

48. Shen L, Weber CR, Raleigh DR, *et al*. Tight Junction Pore and Leak Pathways : A Dynamic Duo. *Annu Rev Physiol*. 2011;73:283-309.

CHAPTER 4 : PHYSIOLOGICALLY-BASED PHARMACOKINETIC MODELS TO PREDICT PHARMACOKINETICS AND INTESTINAL ABSORPTION OF AMOXICILLIN IN CHILDREN

Introduction

The β-lactam antibiotic amoxicillin is a broad-spectrum penicillin that is the first-line treatment for AOM. Amoxicillin is well tolerated, and is effective against the two most common AOM isolates, *Streptococcus pneumoniae* and *Haemophilus influenza*[1]. AOM is a common childhood disease that affects over 80% of children under 5 years of age[2], and disproportionately affects children under two years of age, who make up 48% of the children diagnosed with AOM[2]. Even after failure of initial antibiotic treatment for AOM, amoxicillin is still a first-line treatment when given in combination with the β-lactamase inhibitor clavulanate. As a result, amoxicillin is one of the most frequently prescribed drugs in infants and children[3,4].

While amoxicillin is generally considered to be well tolerated and does not have a narrow therapeutic index, understanding its disposition and predicting PK in pediatric populations is important in evaluating the recommended doses and its efficacy in AOM. Distribution to the middle ear space is by passive diffusion and generally increases with dose and exposure[5], yet pediatric MEF concentrations of amoxicillin are highly variable and in some cases the antibiotic is undetectable (15% to 35%[5]) despite high oral doses[6,7]. Infants have especially poor penetration of amoxicillin into the MEF[7]. In 2013 (reaffirmed in 2019), the daily dose of amoxicillin recommended by the American Academy of Pediatrics for AOM was increased from 40 mg/kg/day to 60 mg/kg/day in infants and 80-90 mg/kg/day in children, given as divided doses,

twice (b.i.d.) or thrice (t.i.d.) daily[4,8]. However, the rates of treatment failure and relapse of AOM in children have not been reduced by doses above 70 mg/kg/day, suggesting that these higher doses did not improve MEF penetration or efficacy[6,7]. Thus, an arbitrary increase in the dose to improve treatment outcome in this population is not appropriate, considering the risk of oral antibiotic-associated diarrhea, for which the incidence is highest in children under two years of age[9]. For children treated with amoxicillin, the rate of antibiotic-associated diarrhea is 8.1% and increases to 19.8% if given in combination with clavulanate[9]. Thus, inappropriate selection of antibiotics and doses could increase the risk of diarrhea and its severity, especially in infants and young children, burdening caretakers and putting patients at risk of adverse effects such as dehydration.

It has been hypothesized that the AOM treatment failures are due to high variability in pediatric PK parameters, and that this variability is in large part due to variable intestinal absorption of amoxicillin[5]. In pediatric patients, up to a 30-fold difference in serum concentrations and 20-fold difference in MEF concentrations has been observed for a given dose[5]. Because amoxicillin demonstrates "flip-flop" kinetics in which absorption, rather than elimination, is the rate-limiting step in its disposition, one must conclude that the variability in plasma and MEF concentrations are caused by differences in oral absorption of the antibiotic[10,11]. Amoxicillin is hydrophilic (logP 0.61, logD -2.21 at pH 7[12]), and it is zwitterionic at physiological pH. Thus, it is expected to have poor membrane permeability. However, high and dose-dependent oral bioavailability has been observed in adults, which has been attributed to a role of intestinal transporters in its absorption; it is likely that the transporter-mediated absorption contributes to the variability in PK observed *in vivo*[13,14].

In Chapter 3, PEPT1 and a transporter of the OATP family were implicated in the absorptive transport of amoxicillin. Further, by modelling cellular kinetic data in two *in vitro* models of the intestinal epithelium, it was estimated that approximately 80% of amoxicillin transport across intestinal epithelium occurs transcellularly (with the assistance of transporters) and the remaining 20% of the absorptive transport occurs *via* the paracellular route. In order to arrive at safe and effective doses of amoxicillin in children (< 2 years of age), the age group most disproportionately affected by AOM, PBPK modeling of amoxicillin disposition is critically important. The mechanistic information obtained in the studies described in Chapter 3 regarding intestinal absorption of amoxicillin was used to develop a "bottom-up" PBPK model for adults and children as described here.

Methods

Pharmacokinetic data

The PK of amoxicillin and clavulanate have been studied extensively alone and in combination, and are not different when administered together[15,16]. Therefore, the observed PK data used in this study included PK data from studies in which amoxicillin was administered as a combination formulation with clavulanate. PK studies were selected on the basis of availability of amoxicillin plasma concentration data and PK parameters. Publications with healthy adult or AOM PK data and pediatric patients with AOM were preferred (no pediatric PK studies were identified with healthy pediatric patients).

Individual adult and pediatric amoxicillin concentration-time data for model optimization and evaluation were obtained by digitizing published PK profiles (GetData Graph Digitizer, v2.26)[17]. Noncompartmental analysis (NCA) was performed on the digitized adult and pediatric

amoxicillin concentration data using Phoenix 8.0 (Certara USA, Inc., Princeton NJ). Figures for simulated *vs* observed PK data were generated in GraphPad Prism 8.2.1 (La Jolla, CA).

Modelling workflow

A whole-body adult PBPK model (**Figure 4-1**, left) for IV administration of amoxicillin was first developed using PK-Sim® software (Open Systems Pharmacology Suite, v7.1) that incorporated amoxicillin physicochemical parameters (**Table 4-1**). The IV PBPK model was first developed in order to evaluate model assumptions of amoxicillin distribution and elimination prior to incorporating oral absorption parameters. Tissue to plasma partition coefficients were determined in PK-Sim® using a method described by Rodgers and Rowland[18,19]. Initial values for LogD and f_u for plasma protein binding to albumin were obtained from the literature and optimized using the built-in PK-Sim® parameter identification tool, using a Monte-Carlo algorithm and multiple optimization with randomized start values.

The IV adult model was then adapted (**Figure 4-2**) to an oral PBPK model (**Figure 4-1**, right) to simulate the oral administration of amoxicillin in adults, incorporating solubility and intestinal permeability values. To model absorption of oral drugs, PK-Sim® uses a compartmentalized transit model in which each segment of the GI tract is described as a series of compartments (stomach, duodenum, jejunum, ileum, cecum, and colon), each with region-specific pH, volume, transit rate, and surface area[20,21].The oral adult model was adapted to the pediatric model by incorporating the pediatric virtual population (described below).

Population simulation

Population-based PK simulations in PK-Sim® were performed for adults (18 to 65 years old) using a virtual population of 100 subjects and for children (see age-range below) using a

virtual pediatric population of 200 subjects, comprising an equal proportion of male and female subjects. Age ranges for virtual populations were set based on the demographics of the published PK studies; for the pediatric populations, two virtual population ranges were generated to match the publications; the first comprised 200 virtual subjects between 3 and 23 months of age[22], and the second comprised 200 virtual subjects 3 months to 5 years of age[23]. The physiologic parameters for the virtual adult and pediatric populations were generated based on the 1997 National Health and Nutrition Examination Survey. Pediatric virtual populations generated in PK-Sim® accounted for the age dependence of anatomy and physiology (*e.g.*, organ size, blood flow rates, body composition), including ontogeny factors for albumin and GFR. For the GI tract, this included age-appropriate surface area, lengths, volumes, and transit time.

Model evaluation

Model performance was evaluated by comparing simulated plasma concentration-time profiles (population mean and 95% prediction interval) to observed concentration data available in the literature. Models were accepted if (i) simulated concentration-time profiles fit the overall shape of observed profiles, (ii) the majority of observed concentration data fell within the 95% prediction interval for simulated data, and (iii) the simulated PK parameters were within 2-fold of the observed parameters.

Mean simulated adult PK parameters also were compared to published PK parameters of 5 adults with bronchitis that were given 500 mg IV amoxicillin[17] and 16 healthy adults given 500 mg amoxicillin as a powder for suspension[24]. Mean simulated pediatric PK parameters were compared to the published PK parameters from 40 infants (aged 6 to 23 months) with AOM treated with 80 mg/kg/day amoxicillin orally (given as 40 mg/kg twice daily)[22], and 34 infants with AOM following a single oral dose of 25 mg/kg amoxicillin[23].

Sensitivity analyses

Sensitivity analyses were performed using the PK-Sim® tool to evaluate the effect of estimated fraction GFR and intestinal permeability on performance of the adult PBPK model. The two parameters were selected because renal clearance is the major clearance mechanism for amoxicillin, and intestinal absorption is expected to be a rate-limiting step in amoxicillin disposition. Input values were evaluated with over a 100% variation range and change to determine the impact on the simulated PK parameters pertaining to absorption (C_{max}, T_{max}, AUC).

Results

PBPK Model for Amoxicillin in Adults after IV Administration

For initial model building and optimization, a preliminary IV model of amoxicillin was first developed as described in the Methods Section. Observed concentration data were obtained from a PK study of 5 adults with chronic bronchitis given 500 mg amoxicillin by IV bolus[17].

The renal clearance of amoxicillin, which undergoes tubular reabsorption (by PEPT1 and PEPT2) but has net tubular secretion was implemented in the model as the estimated fraction relative to GFR using a method described by Maharaj and Edginton[20]. This approach was used in the absence of detailed mechanistic data about amoxicillin transporter-mediated renal clearance, and the lack of ontogeny data for renal transporters. Incorporating renal clearance as a tubular secretion process (first-order or Michaelis-Menten) was also considered. However, in the absence of supporting clinical data or *in vitro* parameters for these processes, the estimated GFR fraction was preferred as a surrogate parameter.

Briefly, observed adult clinical renal clearance data was used to estimate the fraction relative to GFR (estimated GFR fraction)[25]. In PK-Sim®, the GFR fraction parameter was used as a surrogate input parameter to implement active reabsorption (GFR fraction <1) or active secretion (GFR fraction >1) in the absence of known tubular secretion or reabsorption rates[26]. Renal clearance in a healthy adult (2.6 mL/min/kg) was approximately 1.5 to 2-fold that of the GFR[25]. This estimated fraction GFR (1.5 to 2) was incorporated into the IV model and used to simulate the fraction excreted into the urine (f_e) and the results were compared to mass balance data[25] to optimize the estimated GFR fraction parameter. The estimated GFR fraction after fitting was 1.5, indicating net secretion of amoxicillin, which was consistent with published reports of renal clearance that exceeds GFR[25,27]. The renal clearance of amoxicillin is constant for oral doses up to 3 g[10,28], suggesting that this parameter is not dose-dependent.

GFR reaches adult values after the first year of life, but continues to increase above the adult values, and peaks between 2 and 5 years of age before decreasing to typical adult levels[29]. In contrast, tubular secretion reaches adult levels after the first year of life and remains steady to adulthood[25]. The ontogeny of tubular reabsorption processes is not well known and appears to increase through adolescence.[30] Thus, to facilitate adaptation of the adult PBPK model to a pediatric PBPK model, amoxicillin renal clearance was incorporated as the input parameter, GFR fraction, so that it could be scaled with age. The advantage of using the estimated GFR fraction as a surrogate input parameter is that this can be scaled by age using renal ontogeny functions that describe the development of GFR by age and weight (*e.g.*, the method described by Rhodin *et al.*)[29,31].

A single IV dose of 500 mg amoxicillin was simulated in 100 virtual adults (**Figure 4-4**). The adult PBPK model for IV amoxicillin adequately described the observed concentration data,

with most of the concentration-time points falling within the 95% prediction interval. The $AUC_{0-\infty}$, $t_{1/2}$, V_D, and CL were predicted well within 2-fold of observed parameters[17]. There was a tendency towards overestimation of the V_D, but CL parameters were well predicted (8.93 L/hr predicted *vs* 9.00 L/hr observed).

PBPK Model for Amoxicillin in Adults after Oral Administration

The pH-dependent solubility, intestinal permeability, and other GI physiological parameters values were incorporated into the IV PBPK model to simulate PK behavior of amoxicillin after oral administration in adults. An *in vitro* intestinal P_{app} value was obtained experimentally from adult human intestinal epithelia and from Caco-2 cell monolayers (Chapter 3). The *in vitro* P_{app} values and an *in vivo* P_{eff} value were first evaluated as initial estimates for intestinal permeability in two different simulations: 1) 500 mg amoxicillin, and 2) 875 mg amoxicillin. However, the *in vitro* P_{app} and *in vivo* P_{eff} values could not be directly incorporated into the PBPK model because experimental apparent permeability values are not directly translatable without the use of additional calibration and scaling factors[32]. Within the PK-Sim® modeling software, a permeability coefficient P_{int} is determined on the basis of physicochemical properties of drugs (*e.g.*, molecular weight, lipophilicity, diffusion coefficients in water and lipid bilayer membrane). The algorithm is empirically determined and was developed using a library of 126 compounds that are primarily permeability-limited and absorbed by passive processes (transcellular or paracellular)[32]. Thus, the model P_{int} value is specific to each PBPK model and does not directly correlate to experimental values. This is best seen in the ~150-fold difference between the initial estimate (67 nm/s) and the model optimized value (0.47 nm/s, **Table 4-1**). Hence, the *in vitro* P_{app} value derived from adult human intestinal epithelia (Chapter 3) was used as an initial estimate, then simultaneously fit to both the 500 mg and the 875 mg simulations

using the built-in PK-Sim® parameter estimation tool as described, resulting in an optimized value of 0.47 nm/s. The value from adult human intestinal epithelia was chosen over Caco-2 cell monolayers (67 nm/s *vs* 90 nm/s) for this purpose as it was a slightly better initial estimate; however, the arbitrary P_{int} values required by the model is so different that the choice of initial estimates was not expected to have an impact on the model. This approach was utilized to obtain an estimated parameter of intestinal permeability appropriate for use in PK-Sim®.

The majority of concentration-time points were captured within the 95% prediction interval in both the 500 mg and 875 mg simulations (**Figure 4-5, Figure 4-6**). The model was able to predict amoxicillin PK parameters (C_{max}, T_{max}, $AUC_{0-\infty}$, and CL) within 2-fold of observed parameters in simulations of 500 mg amoxicillin as well as 875 mg amoxicillin (**Table 4-2**).

PBPK Model for Amoxicillin in Children after Oral Administration

To adapt the adult oral PBPK model, pediatric physiology was incorporated and simulations were performed in two virtual pediatric populations (N=200 each). The pediatric virtual populations were generated based on the demographics of the observed pediatric populations, one with children aged 3 to 23 months[23], the second with children aged 3 months to 5 years of age[22]. GFR was scaled in PK-Sim® using the Rhodin ontogeny equation[31].

Two pediatric doses were evaluated; the first, 25 mg/kg, represents a single oral dose of amoxicillin that would be given twice daily (50 mg/kg/day)[23]. The second dose is a single 40 mg/kg dose intended to be given twice daily (80 mg/kg/day)[22], representing the higher daily doses of amoxicillin recommended by the American Academy of Pediatrics for AOM in 2013[4,8]. The simulations of the 25 mg/kg and 40 mg/kg doses are shown in **Figure 4-6** and **Figure 4-7**.

The majority of concentration-time points were captured within the 95% prediction interval in both the 25 mg/kg and 40 mg/kg simulations, though high variability in the observed data is noted. The model was able to predict amoxicillin PK parameters (C_{max}, T_{max}, $AUC_{0-\infty}$, and CL) within 2-fold of observed parameters in both simulations (**Table 4-3**).

For β-lactam antibiotics, the time above the MIC is a key efficacy parameter, with the goal to maintain 70% of the dosing interval above MIC[33,34]. Evaluation of MEF isolates from children with AOM has demonstrated that of the two most common pathogens in AOM, *Haemophilus influenza* and *Streptococcus pneumoniae*, amoxicillin has greater efficacy against the latter[33]. Although MIC_{50} and MIC_{90} levels for *S. pneumoniae* are attainable at these oral doses (**Figure 4-7, Figure 4-8**), the MIC_{90} for *Haemophilus influenza* (64 μg/mL) greatly exceeds the expected C_{max} (<20 μg/mL) *in vivo.*

Sensitivity Analyses

Sensitivity analyses demonstrated that simulated adult amoxicillin C_{max}, T_{max}, and $AUC_{0-\infty}$ are sensitive to changes in the estimated GFR fraction parameter as well as the intestinal permeability parameter (**Table 4-4**). Increasing the estimated GFR fraction by 100%, for example, decreased the C_{max}, T_{max}, and $AUC_{0-\infty}$ by 32%, 9%, and 71% respectively, underscoring the role that net secretion of amoxicillin plays in its renal clearance. Intestinal permeability, not surprisingly, was also an important parameter, increasing C_{max}, and $AUC_{0-\infty}$ by 74%, and 71%, respectively, and decreasing the T_{max} by 9%.

Discussion

Amoxicillin is one of the most frequently prescribed pediatric drugs[3,4] due to its efficacy in treating the common childhood disease AOM. Although amoxicillin is widely used and well

tolerated, its PK is highly variable in children and penetration into the MEF is poor[6,7]. Furthermore, due to the increase in antibiotic resistance, the recommended daily doses of amoxicillin for AOM treatment have increased up to 80 to 90 mg/kg/day in children[4,8]. The increased doses, however, have not reduced the rates of AOM treatment failure or relapse[6,7], nor has it improved penetration of amoxicillin into the MEF[5]. The variability in amoxicillin PK and treatment failures with this antibiotic have been attributed to amoxicillin's intestinal absorption, which is thought to be the rate-limiting step in its disposition[5]. At least a part of the variability in absorption is believed to be due to the necessary role of intestinal transporters in the oral absorption of amoxicillin[10,11]. The rate-limiting intestinal absorption may also explain in part why treatment failure and relapse rates in AOM treatment have not improved with higher doses of amoxicillin. Since it would be challenging to conduct clinical research with pediatric populations to understand the role of intestinal transporters and other factors on the variability in amoxicillin oral absorption and its PK, the goal of the present study was to apply PBPK modeling using the knowledge about the intestinal absorption of amoxicillin, and predict its PK in young children with AOM; however, there were limitations in incorporating the *in vitro* data directly into the PBPK model.

Historically, the mechanism underlying the intestinal absorption of amoxicillin has not been well understood, although PEPT1 was implicated in its AP uptake in the intestinal epithelia. The hydrophilicity and zwitterionic nature of amoxicillin at physiological pH suggest that in the absence of transporters, amoxicillin would have poor membrane permeability; however, high oral bioavailability is observed *in vivo,* likely due to the contribution of transporters, including PEPT1. Intestinal permeability in the PK-Sim® modeling software is incorporated using an empirically determined algorithm for *in vitro* to *in vivo* extrapolation that is dependent upon

calibration of *in vitro* values from a large training set. Thus, the P_{int} values used in the model cannot be directly correlated to the *in vitro* values determined in Chapter 3. As a result, intestinal permeability in this study was incorporated by using an initial *in vitro* estimate of amoxicillin P_{app} determined in human intestinal epithelia (Chapter 3). An alternate approach considered was to use an estimated passive permeability value based on the physicochemical properties of amoxicillin alone, which would be expected to be low in the absence of intestinal transporters, and to incorporate amoxicillin AP uptake and BL efflux by intestinal transporters. This approach of combining an estimate of passive permeability with intestinal transport kinetics was not used in this study because the kinetics of amoxicillin uptake by PEPT1 have not been determined.

The studies described in Chapter 3 also demonstrated that approximately 20% of the absorptive transport of amoxicillin can be attributed to the paracellular pathway and 80% to the transcellular pathway. Although paracellular and transcellular intestinal permeability can be implemented in PBPK models using the PK-Sim® software, a limitation is that the GI transit and absorption processes were developed with the assumption that paracellular transport is only a minor route of intestinal absorption as it accounts only for 0.01% of the small intestinal surface area[32,35,36]. Paracellular transport, transporter-mediated uptake, and efflux can be incorporated into the PBPK model; and data are available for adult transporter expression. However, at present, commercial PBPK modeling software is limited in the capacity to implement more complex transporter-mediated absorption mechanisms, especially for drugs with significant paracellular contribution[32].

As with intestinal transport, an alternate approach was required to address the active renal secretion of amoxicillin, where drug transporters are also likely to play an important role. Up to 80% of amoxicillin is eliminated unchanged in the urine[12]. Amoxicillin undergoes active renal

secretion that exceeds GFR, with some reabsorption from the urine at the AP membrane of the renal epithelial layer due to PEPT1 and PEPT2[27]. Amoxicillin has higher affinity for PEPT2 (K_i 733 μM) than for PEPT1 (K_i 66 mM), suggesting that PEPT2 is primarily responsible for the reabsorption of amoxicillin at the AP membrane rather than PEPT1 despite the importance of PEPT1 in its intestinal absorption[27]. To date, the renal transporters at the proximal tubules responsible for the net secretion of amoxicillin, *i.e.*, BL uptake from the blood and AP efflux into the urine, have not been identified. Amoxicillin has pK_a values of 2.67, 7.48, 9.98[37] and would be expected to be zwitterionic at a typical blood pH and in the urine, where typical urine pH values are around pH 6.0 but range from 5.5 to 7.0 in a healthy adult[38]. Notably, the renal clearance of amoxicillin is significantly reduced by probenecid, an inhibitor of renal organic anion transporters (OATs)[39], suggesting that these are involved in the BL uptake and tubular secretion of amoxicillin in the kidney proximal tubules. In Madin-Darby canine kidney cells overexpressing OAT1, amoxicillin was shown to be a weak inhibitor, but not a substrate for OAT1[27]. It is possible that at the BL membrane, the other OAT transporters OAT2, 3, or 4 are responsible for uptake; the OCT transporters OCT2 and OCTN2 are also highly expressed in the kidney[40], but their role in amoxicillin transport is unknown. However, the kinetics of uptake and efflux for amoxicillin by these transporters has not been determined. Thus, an alternate approach previously described[20] was used by inputting GFR fraction as a surrogate parameter, accounting for net active secretion (GFR fraction >1) in the absence of known tubular secretion or reabsorption rates[26].

Amoxicillin PK is not altered by coadministration with clavulanate, with which it is commonly coformulated[15,16]. Thus, the PK studies used for PBPK model development and validation included studies in which amoxicillin was administered alone, and also where

amoxicillin was administered with clavulanate. Critically ill children treated with amoxicillin/clavulanate show augmented renal clearance rate, contributing to treatment failure, though the mechanism for this is not understood[41]. Therefore, pediatric PK data used in this study were limited to children with AOM. As a broad-spectrum antibiotic, amoxicillin is a commonly used antibiotic for other pediatric indications such as respiratory tract infections, urinary tract infections, skin and tissue infections[12], and future work with this model may also include alternate dosing regimens for other pediatric indications.

The development of oral PBPK models for pediatric drugs such as amoxicillin may also assist in simulations of future drug-drug interactions or food effects, with the proper pediatric physiological data. Amoxicillin is not known to have food-drug interactions in adults. However, infants may theoretically be at increased risk of food effects compared to adults due to reliance on breast milk or formula, a higher dietary fat intake compared to adults, and frequent feeding (up to 10 times per day)[42]. Food intake can change GI pH, delay gastric emptying, stimulate bile flow, increase GI blood flow, and affect drug solubility. Changes in these physiological processes are not well understood for children or infants; however, high fat and high calorie meals have the greatest impact on GI physiology in adults, and the fat content and frequent feeding schedule in infants presents a very different scenario. Furthermore, where oral liquid formulations are not available or where a caretaker desires to mask the taste of a drug, antibiotics may sometimes be mixed with formula or with milk for infants[24]. While an amoxicillin powder for suspension was demonstrated to be bioequivalent in adults under fasted conditions when prepared in water *vs.* human milk, it is not known whether the same results would be observed with infant physiology[24]. In addition to physiological changes induced by food, breast milk and cow's milk-based infant formula contain small dipeptides and tripeptides[43] that may compete

with amoxicillin for uptake by peptide transporters such as PEPT1. A significant reduction in oral bioavailability and delay in T_{max} has been reported in a rat model with vigabatrin, a substrate for proton-coupled amino acid transporter (PAT1), when administered with infant formula[44]. In adults, coadministration with milk reduced the C_{max} of the PEPT1 substrate oseltamivir to 0.69-fold of the C_{max} when administered with water[45], presenting an example of a food interaction with a PEPT1 substrate that may be mediated by dietary peptides.

In summary, the PBPK models developed in this study were able to predict the PK of amoxicillin in adults upon IV and oral administration, and in children under five years of age upon oral administration. A major limitation of this study is the implementation of intestinal absorption in oral PBPK models. A permeability parameter was optimized simultaneously for multiple simulations in order to obtain a value that would be appropriate at more than one dose level. Evaluation of the models and simulated PK parameters indicated that at the oral doses simulated, the PBPK models were able to predict amoxicillin PK in adults and in children with the optimized parameter.

Figure 4-1. Whole-body PBPK model structure simulated by PK-Sim® software package.

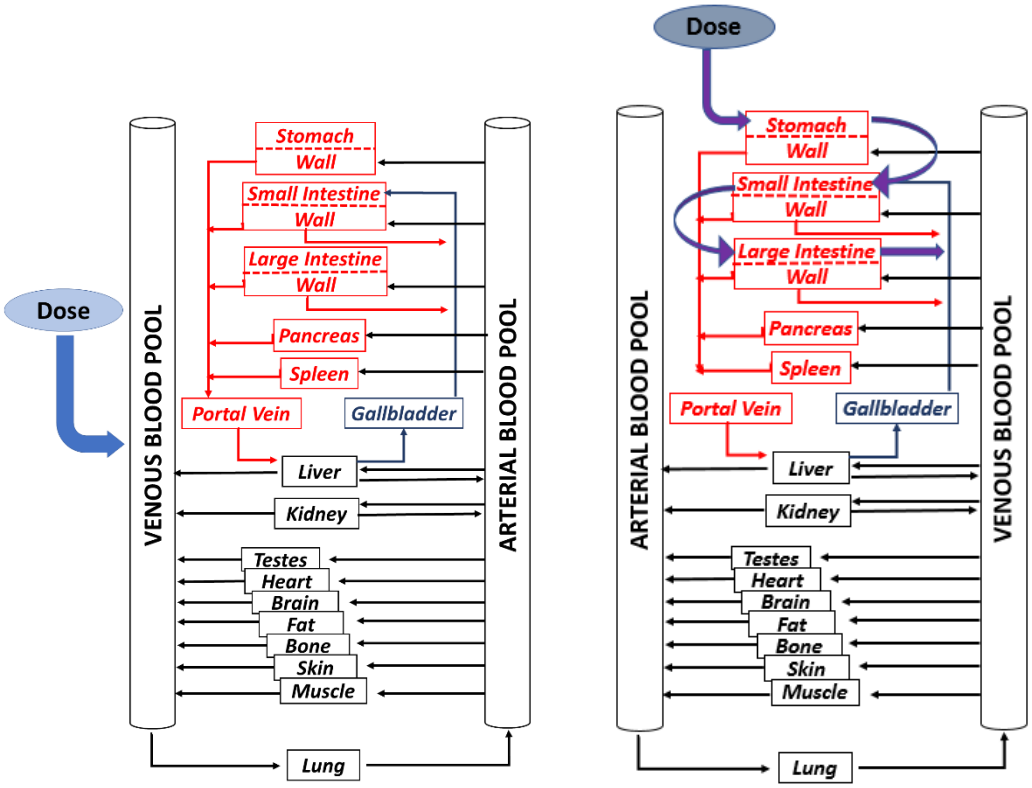

Intravenous (left) and oral (right), adapted from Willmann *et al.*[26] The models include physicochemical parameters of amoxicillin, renal clearance, and tissue to plasma partition coefficients as determined by a method described by Rodgers and Rowland[18,19]. The oral model also includes parameters for the solubility and intestinal permeability of amoxicillin.

Figure 4-2. Flowchart of developing adult intravenous, adult oral, and pediatric oral PBPK models.

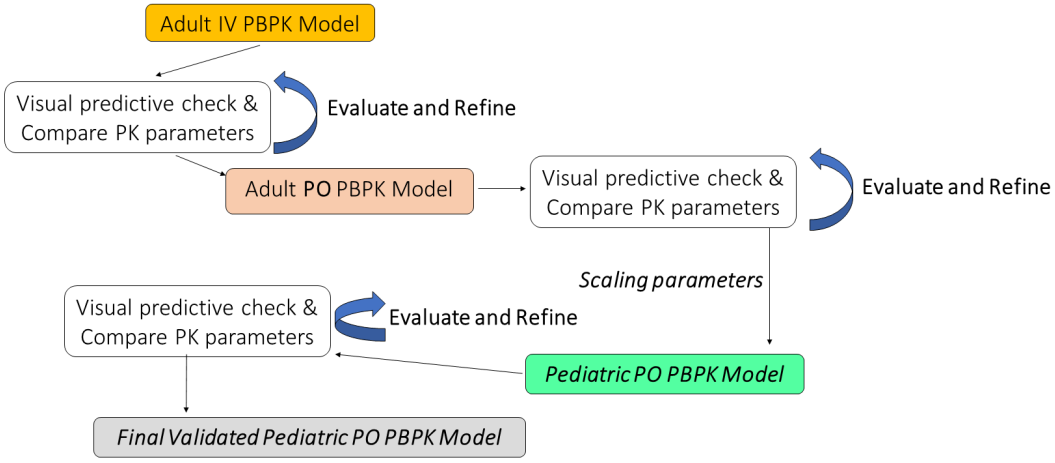

A flowchart is shown for the development of the adult intravenous, adult oral, and pediatric oral PBPK models of amoxicillin. The adult intravenous model is first developed in order to evaluate model assumptions of amoxicillin distribution and elimination. The intravenous model is evaluated and refined by visual predictive check and comparison of clinical PK parameters prior to adaptation to the adult oral model. The adult oral model is also evaluated and refined using clinical PK data, then scaled to the pediatric oral PBPK model. The pediatric oral PBPK model is also evaluated and refined using clinical PK data, resulting in a final validated pediatric oral PBPK model.

Figure 4-3. Molecular structure of amoxicillin.

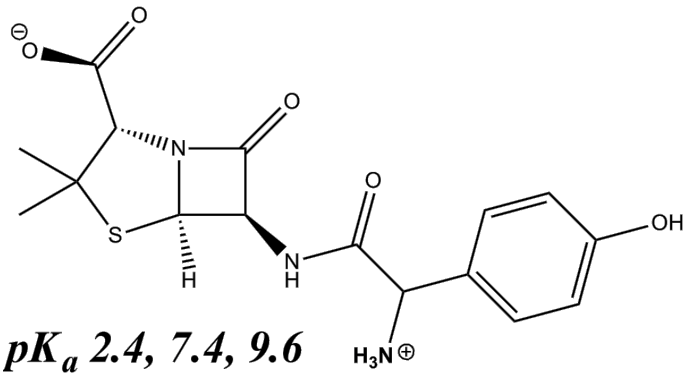

pK_a 2.4, 7.4, 9.6

Table 4-1. Amoxicillin parameters used for the adult and pediatric PBPK models.

Parameter	Value			Source
Molecular Weight (g/mol)	365.4			Thambavita *et al*., 2017[12]
LogD	**Initial**	**Optimized**		Thambavita *et al*., 2017[12]
	-2.21	-2.3		
pKa	2.67, 7.48, 9.98			Felix *et al*., 2016[37]
f_u (Albumin)	**Initial**	**Optimized**		
	0.77, 0.85	0.80		Wise *et al*., 1980[46]; Bergan *et al*., 1987[47]
Solubility (mg/L)	**pH**	**Solubility (mg/mL)**		Thambavita *et al*., 2017[12]
	1.20	7690		
	4.50	3550		
	5.00	4400		
	5.50	5000		
	6.80	5400		
GFR Fraction	2.00 (Secretion)			Estimated using adult clinical data from Horber *et al.*, 1986[25]
Intestinal Permeability (nm/s)	**PK-Sim Calculated**	**Experimental**	**Optimized**	
	0.000029	67	0.47	Experimental (Human intestinal epithelia)

f_u, unbound fraction; GFR, glomerular filtration rate; LogP, lipid/aqueous fluid partition coefficient.

Parameter estimation was used to optimize the LogD, pKa, f_u, and intestinal permeability, using published data or experimental data for initial estimates.

Figure 4-4. Simulation of amoxicillin plasma concentration *vs.* time curve from 0 to 6 hours following a single intravenous dose of amoxicillin (500 mg) in a virtual adult population (N=100).

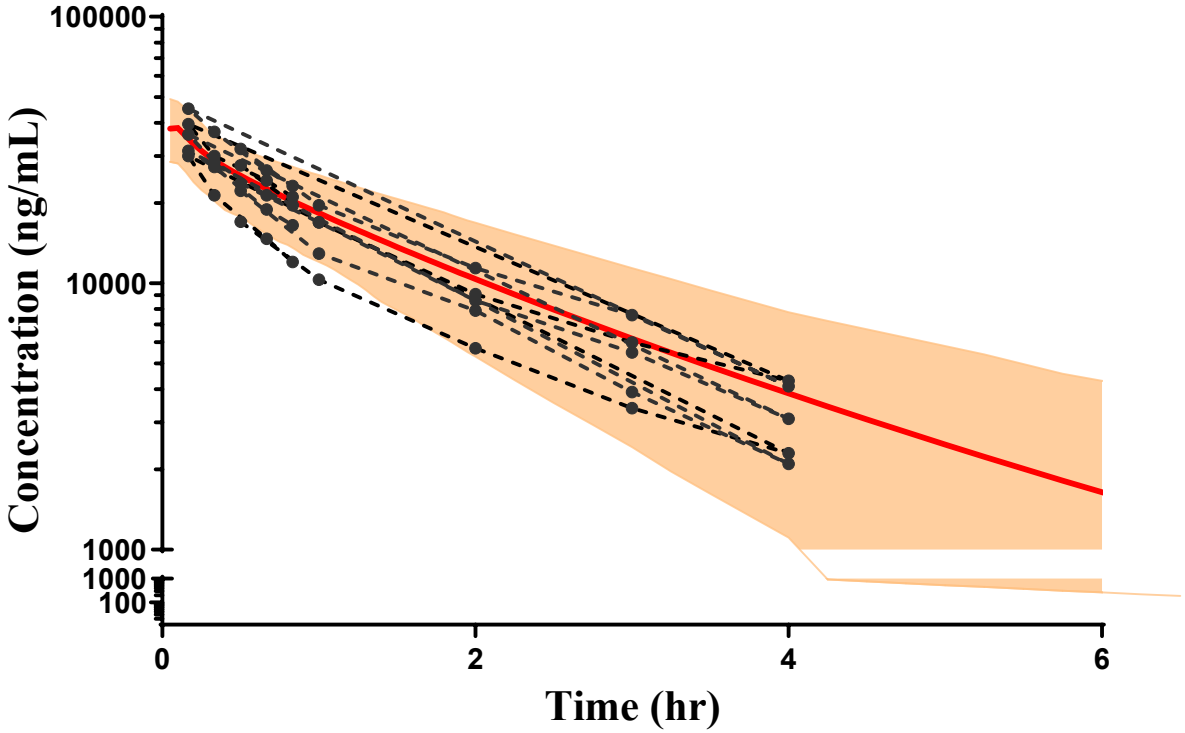

The solid red line represents the simulated mean and the shaded area is the 95% prediction interval. The dotted lines represent the observed amoxicillin concentration *vs.* time profiles for 5 adults, extracted from Lovering *et al.* by GetData[17].

Figure 4-5. Simulation of amoxicillin plasma concentration vs. time curve from 0 to 12 hours following a single oral dose of amoxicillin (500 mg, oral suspension) in a virtual adult population (N=100).

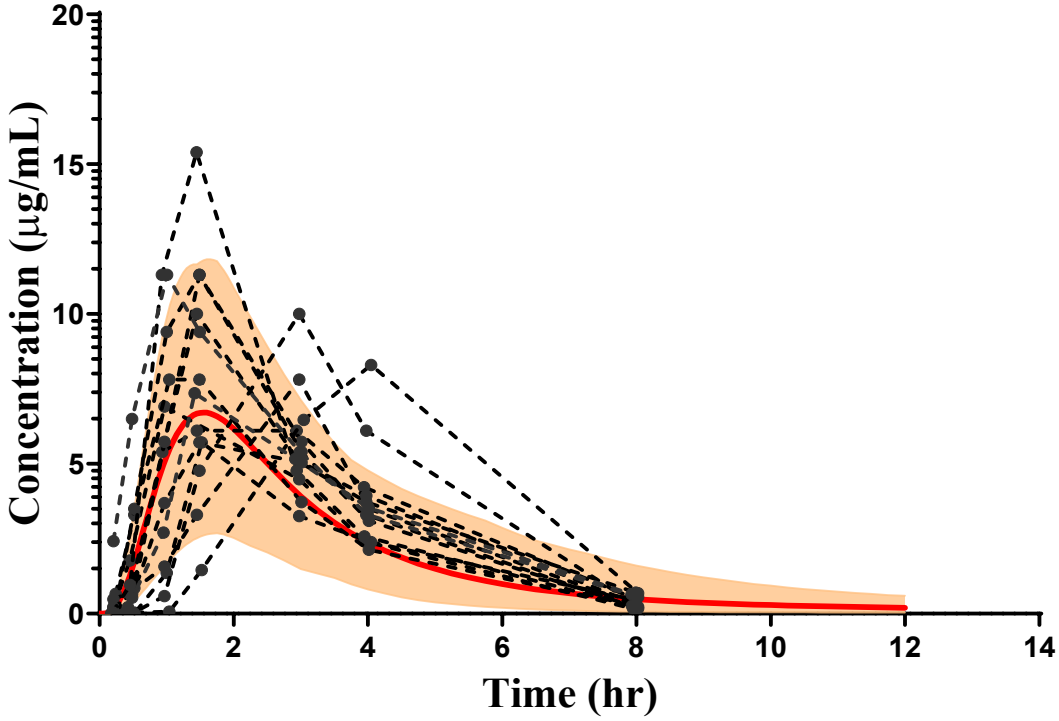

The solid red line represents the simulated mean and the shaded area is the 95% prediction interval. The dotted lines represent the observed amoxicillin concentration *vs.* time profiles for 16 adults, extracted from Yazdani-Brojeni *et al.* by GetData[24].

Figure 4-6. Simulation of amoxicillin plasma concentration *vs.* time curve from 0 to 12 hours following a single oral dose of amoxicillin (875 mg, administered as oral amoxicillin/clavulanic acid tablets) in a virtual adult population (N=100).

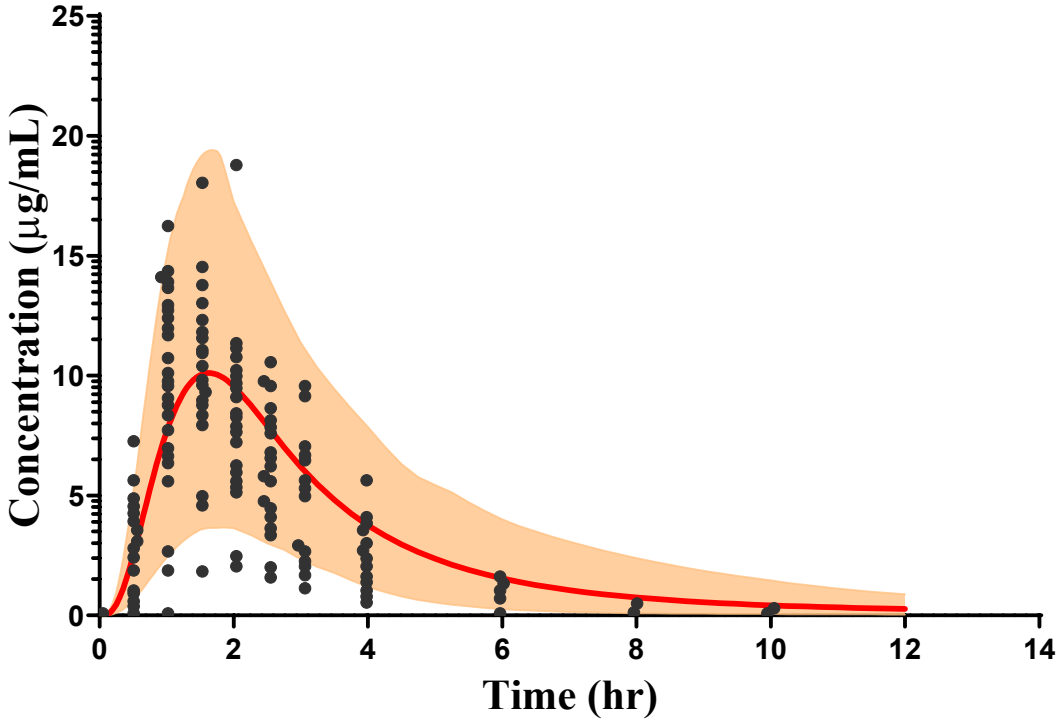

The solid red line represents the simulated mean and the shaded area is the 95% prediction interval. The solid circles represent the observed amoxicillin pooled concentrations (individual profiles are not available) for 14 healthy adults, extracted from de Velde *et al.* by GetData[48].

Figure 4-7. Simulation of plasma amoxicillin concentration *vs.* time curve from 0 to 12 hours following a single oral dose of amoxicillin (25 mg/kg, administered as an oral amoxicillin formulation) in a virtual pediatric population (N=200, 3 months to 5 years).

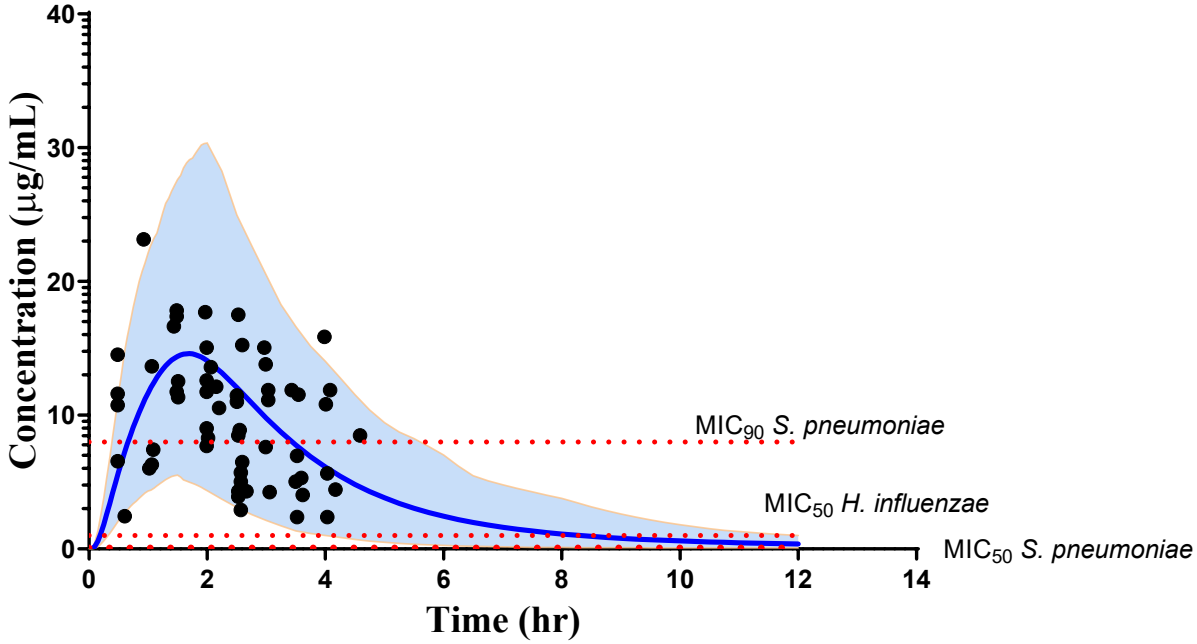

The solid blue line represents the simulated mean and the shaded area is the 95% prediction interval. The solid circles represent the observed amoxicillin concentrations for 34 children (3 months to 5 years of age) with AOM, extracted from Canafax *et al.* by GetData[23]. MIC_{50} and MIC_{90} for *Streptococcus pneumoniae* (0.064 and 8 µg/mL, respectively) are shown in dotted lines along with the MIC_{50} for *Haemophilus influenzae* (1 µg/mL; the MIC_{90} of 64 µg/mL is not shown).

Figure 4-8. Simulation of plasma amoxicillin concentration *vs.* time curve from 0 to 12 hours following a 40 mg/kg oral dose of amoxicillin (administered twice daily as an oral amoxicillin/clavulanate formulation in a 80 mg/kg/day regimen) in a virtual pediatric population (N=200, 3 to 23 months of age).

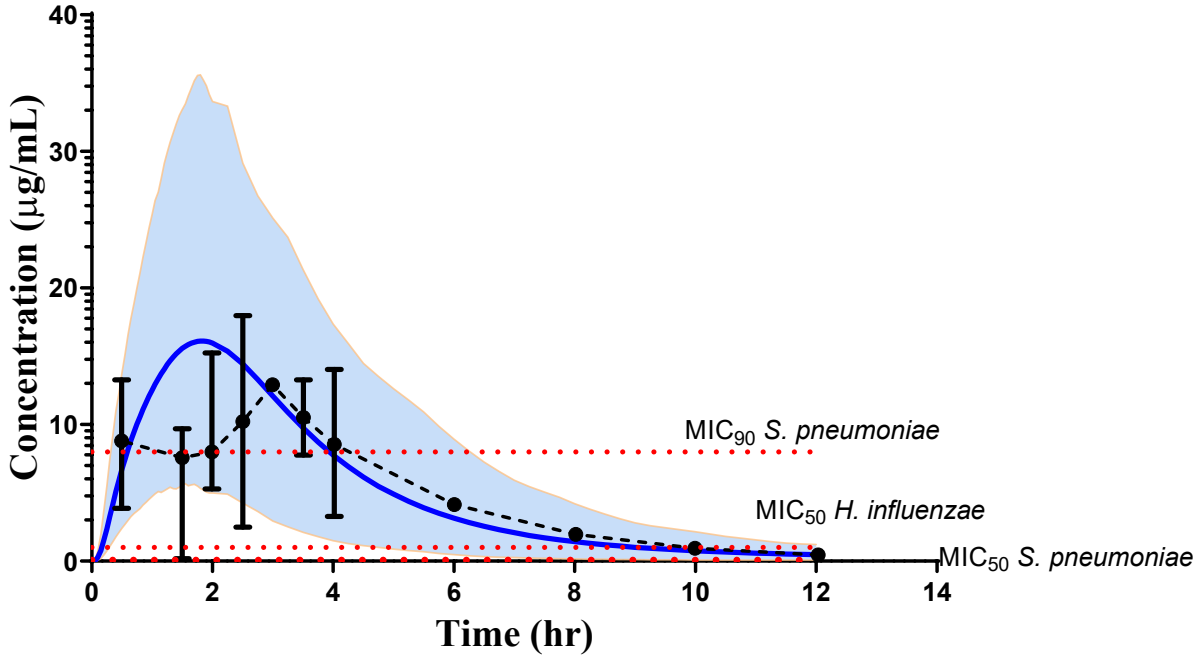

The solid blue line represents the simulated mean and the shaded area is the 95% prediction interval. The solid circles represent the mean observed amoxicillin concentrations (± SD) for 40 children (3 to 23 months of age) with AOM, extracted from Hoberman *et al.*[22]. Where error bars are not present, concentration data were available only for one child. MIC_{50} and MIC_{90} for *Streptococcus pneumoniae* (0.064 and 8 µg/mL, respectively) are shown in dotted lines along with the MIC_{50} for *Haemophilus influenzae* (1 µg/mL; the MIC_{90} of 64 µg/mL is not shown).

Table 4-2. Comparison of experimental mean *vs*. simulated PK parameters of amoxicillin in the adult population.

Source		**Model Simulation**	Lovering *et al.*, 1990	**Model Simulation**	Yazdani-Brojeni *et al.*, 2014	**Model Simulation**	de Velde *et al.*, 2016
Patient Population		**Adult, virtual population**	Healthy adult	**Adult, virtual population**	Healthy adult	**Adult, virtual population**	Healthy adult
N		**100**	5	**100**	**16**	**100**	14
Dose		**500 mg IV**	500 mg IV	**500 mg PO**	500 mg PO	**875 mg PO**	875 mg PO
C_{max} (µg/mL)		**.**	**.**	**6.79**	8.65	**10.22**	11.21
	Fold Difference	**.**	**.**	**1.27**	**.**	**1.10**	**.**
	% Error[a]	**.**	**.**	**27%**	**.**	**10%**	**.**
T_{max} (hr)		**.**	**.**	**1.60**	1.68	**1.685**	1.52
	Fold Difference	**.**	**.**	**1.05**	**.**	**0.90**	**.**
	% Error[a]	**.**	**.**	**5%**	**.**	**-10%**	**.**
$AUC_{0-\infty}$ (µg*hr/mL)		**63.03**	57.15	**23.87**	28.18	**35.52**	55.04
	Fold Difference	**0.91**	**.**	**1.18**	**.**	**1.55**	**.**
	% Error[a]		**.**	**18%**	**.**	**55%**	**.**
$t_{1/2}$ (hr)		**2.65**	1.55	**4.68**	**1.28**	**5.07**	1.14
	Fold Difference	**0.58**	**.**	**0.27**	**.**	**0.22**	**.**
	% Error		**.**	**-73%**	**.**	**-78%**	**.**
V_D (L)		**35.64**	17.00	**29.99**	**37.08**	**25.82**	NC
	Fold Difference	**0.48**	**.**	**1.24**	**.**	**.**	**.**
	% Error		**.**	**24%**	**.**	**.**	**.**
CL (L/hr)		**8.93**	9.00	**28.14**	**22.63**	**33.54**	NC
	Fold Difference	**1.01**	**.**	**0.80**	**.**	**.**	**.**
	% Error		**.**	**-20%**	**.**	**.**	**.**

NC = PK parameter not calculated or reported in the published study.

[a] % error = (observed - simulated) / observed * 100

[b] AUC_{0-24} calculated and reported for comparison to literature value

Table 4-3. Comparison of experimental mean *vs*. simulated PK parameters of amoxicillin in the pediatric population.

Source		**Model Simulation[b]**	**Model Simulation**	Hoberman *et al.*, 2017
Patient Population		**Children (3 to 23 months)**	**Children (3 months to 5 years)**	Children (3 to 23 months) with AOM
N		**200**	**200**	**40**
Dose		25 mg/kg	40 mg/kg	40 mg/kg
C_{max} (µg/mL)		**15.53**	17.29	13.00
	Fold Difference	**.**	**0.75**	**.**
	% Error[a]	**.**	**-25%**	**.**
T_{max} (hr)		**1.76**	1.92	2.9
	Fold Difference	**.**	**1.51**	**.**
	% Error[a]	**.**	**51%**	**.**
$AUC_{0-\infty}$ (µg*hr/mL)		53.21	66.31	55.30
	Fold Difference	**.**	**0.83**	**.**
	% Error[a]	**.**	**-17%**	
$t_{1/2}$ (hr)		**4.06**	2.96	1.90
	Fold Difference	**.**	**0.64**	**.**
	% Error	**.**	**-36%**	**.**
V_D (L/kg)		**12.37**	11.68	**NC**
	Fold Difference	**.**	**.**	**.**
	% Error	**.**	**.**	
CL (mL/hr/kg)		**628.10**	864.82	690.00
	Fold Difference	**.**	**0.80**	**.**
	% Error	**.**	**-20%**	**.**

NC = PK parameter not calculated or reported in the published study.

[a] % error = (observed - simulated) / observed * 100

[b] Simulated based on Canafax *et al.*[23]; however, only sparse concentration data available in this publication without PK data for parameters.

Table 4-4. Sensitivity analysis of the effect of estimated fraction GFR and intestinal permeability on amoxicillin PK in adults.

	C_{max}	T_{max}	$AUC_{0-\infty}$
Estimated Fraction GFR	-0.32	-0.09	-0.71
Intestinal Permeability	0.74	-0.09	0.71

Sensitivity analyses using the built-in PK-Sim® tool were performed to evaluate effect of input parameters on performance of the adult PBPK model. The two parameters were selected because renal clearance is the major clearance mechanism for amoxicillin, and intestinal absorption was expected to be a rate-limiting step in amoxicillin disposition. Input values were evaluated over a 100% variation range to determine impact on simulated adult PK parameters, *e.g.*, a 100% increase in the intestinal permeability parameter increased $AUC_{0-\infty}$ by 74%.

REFERENCES

1. Mather MW, Drinnan M, Perry JD, *et al*. A Systematic Review and Meta-analysis of Antimicrobial Resistance in Paediatric Acute Otitis Media. *Int J Pediatr Otorhinolaryngol*. 2019;123(May):102-109.

2. Coco A, Vernacchio L, Horst MA, *et al*. Management of Acute Otitis Media After Publication of the 2004 AAP and AAFP Clinical Practice Guideline. *Pediatrics*. 2010;125(2):214-220.

3. Chai G, Governale L, McMahon AW, *et al*. Trends of Outpatient Prescription Drug Utilization in US Children, 2002-2010. *Pediatrics*. 2012;130(1):23-31.

4. Lieberthal AS, Carroll AE, Chonmaitree T, *et al*. The Diagnosis and Management of Acute Otitis Media. *Pediatrics*. 2013;131(3):e964-99.

5. Pichichero ME, Reed MD. Variations in Amoxicillin Pharmacokinetic/pharmacodynamic Parameters May Explain Treatment failures in Acute Otitis Media. *Pediatr Drugs*. 2009;11(4):243-249.

6. Harrison CJ, Welch DF. Middle Ear Effusion Amoxicillin Concentrations in Acute Otitis Media. *Pediatr Infect Dis J*. 1988;17(7):657-658.

7. Sox CM, Finkelstein JA, Yin R, *et al*. Trends in Otitis Media Treatment Failure and Relapse. *Pediatrics*. 2008;121(4):674-679.

8. Lister PD, Pong A, Chartrand SA, *et al*. Rationale Behind High-dose Amoxicillin Therapy For Acute Otitis Media Due to Penicillin-nonsusceptible Pneumococci: Support From In Vitro Pharmacodynamic Studies. *Antimicrob Agents Chemother*. 1997;41(9):1926-1932.

9. Kuehn J, Ismael Z, Long PF, *et al*. Reported Rates of Diarrhea Following Oral Penicillin Therapy in Pediatric Clinical Trials. *J Pediatr Pharmacol Ther*. 2015;20(2):90-104.

10. Paintaud G, Alván G, Dahl ML, *et al*. Nonlinearity of Amoxicillin Absorption Kinetics in Human. *Eur J Clin Pharmacol*. 1992;43(3):283-288.

11. Garrison KL, Sahin S, Benet LZ. Few Drugs Display Flip-Flop Pharmacokinetics and These Are Primarily Associated with Classes 3 and 4 of the BDDCS. *J Pharm Sci*. 2015:3229-3235.

12. Thambavita D, Galappatthy P, Mannapperuma U, *et al*. Biowaiver Monograph for

Immediate-Release Solid Oral Dosage Forms : Amoxicillin Trihydrate. *J Pharm Sci*. 2017;106(10):2930-2945.

13. Spyker D a., Rugloski RJ, Vann RL, *et al*. Pharmacokinetics of Amoxicillin: Dose Dependence After Intravenous, Oral, and Intramuscular Administration. *Antimicrob Agents Chemother*. 1977;11(1):132-141.

14. Piotrovskij VK, Paintaud G, Alván G, *et al*. Modeling of the Saturable Time-Constrained Amoxicillin Absorption in Humans. *Pharm Res*. 1994;11(9):1346-1351.

15. Berlin TU, Steglitz K. Pharmacokinetic Studies of Amoxicillin , Potassium Clavulanate and their Combination. *Eur J Clin Microbiol*. 1982;1(4):233-237.

16. Navarro AS. New Formulations of Amoxicillin/clavulanic acid: A Pharmacokinetic and Pharmacodynamic Review. *Clin Pharmacokinet*. 2005;44(11):1097-1115.

17. Lovering AM, Pycock CJ, Harvey JE, *et al*. The Pharmacokinetics and Sputum Penetration of Ampicillin and Amoxycillin Following Simultaneous IV Administration. *J Antimicrob Chemother*. 1990;25(3):385-392.

18. Rodgers T, Rowland M. Physiologically Based Pharmacokinetic Modelling 2: Predicting the Tissue Distribution of Acids, Very Weak Bases, Neutrals and Zwitterions. *J Pharm Sci*. 2006;95(6):1238-1257.

19. Rodgers T, Leahy D, Rowland M. Physiologically Based Pharmacokinetic Modeling 1 : Predicting the Tissue Distribution of Moderate-to-Strong Bases. *J Pharm Sci*. 2005;94(6):1259-1276.

20. Maharaj A, Edginton A. Physiologically Based Pharmacokinetic Modeling and Simulation in Pediatric Drug Development. *CPT Pharmacometrics Syst Pharmacol*. 2014;3(11):e148.

21. Yu LX, Crison JR, Amidon GL. Compartmental Transit and Dispersion Model Analysis of Small Intestinal Transit Flow in Humans. *Int J Pharm*. 1996;140:111-118.

22. Hoberman A, Paradise JL, Rockette HE, *et al*. Reduced-concentration Clavulanate for Young Children with Acute Otitis Media. *Antimicrob Agents Chemother*. 2017;61(7):1-10.

23. Canafax DM, Yuan Z, Chonmaitree T, *et al*. Amoxicillin Middle Ear Fluid Penetration and Pharmacokinetics in Children with Acute Otitis Media. *Pediatr Infect Dis J*. 1998;17(2):149-156.

24. Yazdani-Brojeni P, Garcia-Bournissen F, Fujii H, *et al*. Relative Bioequivalence of Amoxicillin Dissolved in Breast Milk. *Arch Dis Child*. 2014;99(3):258-61.

25. Horber FF, Frey FJ, Descoeudres C, *et al*. Differential Effect of Impaired Renal Function on the Kinetics of Clavulanic Acid and Amoxicillin. *Antimicrob Agents Chemother*. 1986;29(4):614-619.

26. Willmann S, Lippert J, Sevestre M, *et al*. PK-Sim®: A Physiologically Based Pharmacokinetic 'Whole-body' Model. *Biosilico*. 2003;1(4):121-124.

27. Li M, Anderson GD, Phillips BR, *et al*. Interactions of Amoxicillin and Cefaclor with Human Renal Organic Anion and Peptide Transporters. *Drug Metab Dispos*. 2006;34(4):547-555.

28. Philipson A, Sabath LD, Rosner B. Sequence Effect on Ampicillin Blood Levels Noted in an Amoxicillin, Ampicillin , and Epicillin Triple Crossover Study. *Antimicrob Agents Chemother*. 1975;8(3):311-320.

29. Chen N, Aleksa K, Woodland C, *et al*. Ontogeny of Drug Elimination by the Human Kidney. *Pediatr Nephrol*. 2006;21(2):160-8.

30. Zhang Y, Mehta N, Muhari-stark E, *et al*. Pediatric Renal Ontogeny and Applications. *J Clin Pharmacol*. 2019;59(S1):S9-S20.

31. Rhodin MM, Anderson BJ, Peters AM, *et al*. Human Renal Function Maturation: A Quantitative Description Using Weight and Postmenstrual Age. *Pediatr Nephrol*. 2009;24(1):67-76.

32. Thelen K, Coboeken K, Willmann S, *et al*. Evolution of a Detailed Physiological Model to Simulate the Gastrointestinal Transit and Absorption Process in Humans , Part 1 : Oral Solutions. *J Pharm Sci*. 2011;100(12):5324-5345.

33. Fallon RM, Kuti JL, Doern G V., *et al*. Pharmacodynamic Target Attainment of Oral β-lactams for the Empiric Treatment of Acute Otitis Media in Children. *Pediatr Drugs*. 2008;10(5):329-335.

34. Turnidge JD. The Pharmacodynamics of β-Lactams. *Clin Infect Dis*. 1998;27(1):10-22.

35. Lennernäs H. Human Intestinal Permeability. *J Pharm Sci*. 1998;87(4):403-410.

36. Lennernäs H. Intestinal Permeability and its Relevance for Absorption and Elimination.

Xenobiotica. 2007;37(10-11):1015-1051.

37. Felix IMB, Moreira LC, Chiavone-Filho O, *et al*. Solubility Measurements of Amoxicillin in Mixtures of Water and Ethanol From 283.15 to 298.15 K. *Fluid Phase Equilib*. 2016;422:78-86.

38. Rose C, Parker A, Jefferson B, Cartmell E. The Characterization of Feces and Urine : A Review of the Literature to Inform Advanced Treatment Technology. *Crit Rev Environ Sci Technol*. 2015;45:1827-1879.

39. Shanson DC, McNabb R, Hajipieris P. The Effect of Probenecid on Serum Amoxycillin Concentrations Up to 18 Hours After a Single 3 g Oral Dose of Amoxycillin: Possible Implications for Preventing Endocarditis. *J Antimicrob Chemother*. 1984;13:629-632.

40. Shitara Y, Sato H, Sugiyama Y. Evaluation of Drug-Drug Interaction in the Hepatobiliary and Renal Transport of Drugs. *Ann Rev Pharmacol Toxicol*. 2005;45:689-723.

41. De Cock PAJG, Standing JF, Barker CIS, *et al*. Augmented Renal Clearance Implies a Need for Increased Amoxicillin-clavulanic Acid Dosing in Critically Ill Children. *Antimicrob Agents Chemother*. 2015;59(11):7027-7035.

42. Batchelor H. Influence of Food on Paediatric Gastrointestinal Drug Absorption Following Oral Administration: A Review. *Children*. 2015;2(2):244-271.

43. Agostoni C, Carratù B, Boniglia C, *et al*. Free Amino Acid Content in Standard Infant Formulas: Comparison with Human Milk. *J Am Coll Nutr*. 2000;19(4):434-438.

44. Nøhr MK, Holm R, Thale ZI, *et al*. Intestinal Absorption of the Antiepileptic Drug Substance Vigabatrin is Altered by Infant Formula In Vitro and In Vivo. *Int J Pharm*. 2014;466(1-2):18-20.

45. Morimoto K, Kishimura K, Nagami T, *et al*. Effect of Milk on the Pharmacokinetics of Oseltamivir. *J Pharm Sci*. 2011;100(9):3854-3861.

46. Wise R, Gillett AP, Cadge B, *et al*. The Influence of Protein Binding upon Tissue Fluid Levels of Six β-Lactam Antibiotics. *J Infect Dis*. 1980;142(1):77-82.

47. Bergan T, Engeset A, Olszewski W. Does Serum Protein Binding Inhibit Tissue Penetration of Antibiotics? *Rev Infect Dis*. 1987;9(4):713-718.

48. de Velde F, de Winter BCM, Koch BCP, *et al*. Non-linear Absorption Pharmacokinetics

of Amoxicillin: Consequences for Dosing Regimens and Clinical Breakpoints. *J Antimicrob Chemother*. 2016;71(10):2909-2917.

CHAPTER 5 : CONCLUSIONS AND FUTURE DIRECTIONS

Historical Context for Pediatric Clinical Trials and Dose Determination

In drug development, pediatric clinical research has historically been difficult to perform due to ethical considerations as well as high costs, leading to the pediatric population being an understudied group. Children and infants are difficult to recruit and enroll into clinical trials, present ethical problems in obtaining consent, must be enrolled as patients rather than healthy volunteers, and have logistical issues such as smaller blood volume available for monitoring. Thus, by some estimates between 50-75% of drugs used in pediatric therapy are used off-label without adequate scientific data[1] or proper clinical studies, resulting in the use of inappropriate doses of pediatric drugs. Neonates are an especially understudied and vulnerable population, and up to 99.5% of infants in neonatal intensive care units receive drugs off-label[2]. This off-label use and limitations in obtaining pediatric clinical data have contributed to situations in which the pharmacokinetics (PK) and disposition of pediatric drugs are well understood in adults, but not in children or infants. Without the PK data, the relationship between drug concentration levels and safety/efficacy, and consequently, the ability to select appropriate pediatric dose is compromised.

Historically, pediatric doses for drugs were often selected by extrapolating adult doses in lieu of performing pediatric clinical trials. Body weight, surface area, or allometric scaling equations were typically used to adjust adult doses for children. These scaling methods typically assume linear relationships between dose and body weight or surface area, or utilize an

empirically determined allometric coefficient[3]. Thus, developmental changes that often do not develop linearly in children, are not taken into consideration. For example, during development, there are changes in total body composition, GI function, organ sizes, blood flow, renal function, and ontological changes in the expression and function of DMEs and drug transporters[3,4,5,6]. For infants and young children, who are most physiologically different from adults, the scaling approaches and allometric calculations for dose selection are thus most likely to be inappropriate[4], and in fact tend to overestimate drug clearance in young children[5,6].

In the United States, regulatory approaches have been used to provide incentives and requirements for pharmaceutical companies to address pediatric drug development. The BPCA provides incentives such as extension of existing patents and market exclusivity for studying indications in pediatric patients, even if the indication has previously been approved for adults[7]. In contrast, the PREA of 2003 requires that license application for all new drugs and biological products must include assessment of safety and effectiveness in relevant pediatric subpopulations, including dosage. The 2007 reauthorization of PREA requires studies of drugs and biological products in pediatric populations when other approaches are insufficient to ensure that the products are safe and effective in these populations. Sponsors must provide a Pediatric Study Plan to the U.S. Food and Drug Administration (FDA) by the time of the End of Phase II meeting during clinical development, unless an exemption is obtained[7]. The regulatory incentives and requirements, coupled with the difficulties and expense to perform extensive pediatric clinical PK and safety studies, have created a need for alternate approaches to more efficiently utilize the limited pediatric clinical data available and/or replace some studies with *in silico* modeling approaches.

Modeling Approaches in Pediatric Drug Development: PBPK Modeling

To address the risks, expenses, and logistical issues in performing pediatric clinical PK trials, one approach being utilized is to optimize sampling and study power, and analyze data using a population PK approach. Sparse blood sampling techniques or scavenged blood samples can be used in such an approach[8]. Population PK can be used to analyze the concentration data and perform PK simulations from pooled data obtained from multiple clinical studies[9]. However, this approach requires obtaining existing pediatric concentration data.

An alternative approach is the use of PBPK modeling, which can be used with top-down or bottom-up approaches, as well as a middle-out approach that combines the two. PBPK modeling and simulation take a mechanistic approach in modeling drug disposition in physiological compartments. The incorporation of physiology allows a PBPK model developed for adults to be adapted for a pediatric population if the role of relevant physiological parameters in the disposition of a drug is understood. Thus, a pediatric PBPK model can be developed from a validated adult PBPK model to simulate pediatric PK even in the absence of a clinical PK study. PBPK modeling is an increasingly accepted approach by regulators as a tool in pediatric drug development. An overview of PBPK approaches in FDA submissions (as of 2012) showed that PBPK modeling has been used to optimize clinical study designs, verify data extrapolated for pediatric age groups, recommend starting pediatric doses, and assist in covariate analysis[5].

A top-down approach to PBPK modeling uses PK parameters obtained from clinical studies; this approach requires less systems pharmacology and mechanistic information but applies clinical data from multiple studies. The advantage is that if the PK data are already available in children, a PBPK model can be quickly built and used to perform simulations for additional subpopulations, for optimizing doses, or other special case scenarios. The

disadvantage of this approach is that it can be difficult to adjust clearance values and PK parameters obtained *in vivo* without performing *in vitro* studies in cases where an age-dependent process is involved (*e.g.*, clearance by a DME that shows an age-dependent pattern of expression), and that PK data are required and difficult to obtain for multiple pediatric age groups. The bottom-up approach, in contrast, does not require pediatric clinical PK data before model building and performing simulations, but does require an understanding of the mechanisms involved in drug disposition as well as the physicochemical properties of the drug, physiological data, *in vitro* kinetics, and expression of DMEs and/or transporters. The approach that has been used in the Thakker Laboratory is to build a PBPK model for adults and refine it using the available adult clinical PK data while developing a clear understanding of the clearance mechanisms (*i.e.*, metabolic clearance mediated by specific enzymes) for the drug in adults[10]. It is safe to assume that a similar clearance mechanism is involved in pediatric populations, and thus the adult model can be adapted to a pediatric model. A bottom-up PBPK model can be used to simulate pediatric PK early in drug development, before any clinical data have been obtained, to assist in dose selection and clinical study design. Ontogeny functions can be incorporated to account for multiple disposition and clearance processes that, in children, may develop at different rates. Incorporating *in vitro* data for specific mechanisms also permits the PBPK models to be used to investigate hypothetical scenarios, *e.g.*, the impact on PK in a pediatric population with a genetic polymorphism resulting in higher expression of a DME.

PBPK Modeling of Drugs with Transporter-Mediated Disposition: Vincristine and Amoxicillin

Although PBPK modeling approaches have become more common in drug development, its use still has significant limitations for modeling drugs with transporter-mediated disposition.

Unlike DMEs, data on the ontogeny of drug transporters were limited until recently, and are still not well studied in the intestine and kidney[11,12]. Modeling of drugs with DME-transporter interplay can also be challenging. For oral drugs, there are additional challenges in accounting for the effects of drug solubility, dissolution, and precipitation in a pediatric population where the impact of age on GI physiology and intestinal drug transporters are not well understood[11,13].

In this work, a PBPK modeling approach was used to predict pediatric doses of two drugs with transporter-mediated disposition: (1) vincristine, a drug that undergoes hepatic clearance by both DMEs (CYP3A4/5) and the efflux transporter P-gp[14], and (2) amoxicillin, an orally administered drug for which the intestinal AP uptake transporter PEPT1 has been implicated in its absorption[15–17].

PBPK Models of Vincristine Revealed a Role of Intracellular Tubulin Binding in Vincristine Disposition

The anti-cancer agent vincristine was selected as a proof of concept for pediatric PBPK modeling of an intravenously administered drug that is cleared by both DMEs and a hepatic efflux transporter. Vincristine undergoes hepatic clearance *via* metabolism by CYP3A4/5[18–20] and efflux into bile by P-gp[14]. Vincristine is subject to age-related differences in its PK, as clearance of this drug in infants and children is higher than in adults[21,22,23]. CYP3A4 levels increase after birth and reach adult levels around one year of age, while CYP3A5 expression does not change with age although it is genotype-dependent[24]. The hepatic expression of P-gp is age-dependent, and is approximately ~60% and 80% of adult levels in infants and children, respectively[25].

As shown in Chapter 2, a preliminary PBPK model for vincristine in adults was developed using the previously well-established clearance mechanisms, *i.e.*, hepatic metabolism

by CYP3A4/3A5 and hepatic biliary excretion mediated by P-gp, However, incorporation of the intracellular binding of vincristine to β-tubulin was necessary for development of a model that adequately predicted vincristine PK parameters. This refinement of the model was considered appropriate because binding with intracellular β-tubulin is the mechanism of action for vincristine's anticancer effect. The PBPK model constructed with vincristine PK data in adults enabled *in silico* investigation of potential mechanisms underlying vincristine PK differences between adults and children, *e.g.*, the impact of specific binding of vincristine to intracellular β-tubulin. Initial attempts at adapting the adult PBPK model to simulate the PK behavior of vincristine in children (using age-related differences in physiologic parameters, and most importantly, its metabolic and transport clearance mechanisms) led to the observation that the pediatric model was over-predicting plasma concentrations during the distribution phase. It was recognized that any potential error in the incorporation of the ontogeny of CYP3A enzymes or P-gp in the adult PBPK model would not explain the discrepancy between the pediatric PBPK model prediction and observed plasma concentration data because these proteins contribute to the clearance of vincristine and not to its distribution. In evaluating the importance of the binding of vincristine to β-tubulin in the pediatric PBPK model, it appeared that there could be an age-related difference in the extent of vincristine intracellular binding which could explain the differences in vincristine pediatric PK compared to adults. Specifically, simulating higher expression levels of β-tubulin in children (approximately a 4.9-fold increase over adult expression) improved model predictions of vincristine concentrations in the distribution phase, as well as predictions of the volume of distribution. Interestingly, sensitivity analyses not only confirmed the importance of β-tubulin binding in vincristine PK and V_D, but also surprisingly indicated that P-gp did not appear to be a critical parameter in the model despite its importance

in the biliary excretion of vincristine. This is consistent with other reports that biliary excretion of vincristine *via* P-gp also does not appear to be the rate-limiting step in its hepatic clearance, but rather passive uptake into hepatocytes (which is not age-dependent)[26,27].

The research presented in Chapter 2 has made several important contributions: (i) This is the first demonstration of the use of PBPK modeling to uncover the importance of intracellular binding of a drug in defining its PK properties. (ii) The study has generated a novel testable hypothesis that the distribution phase of vincristine in children is more pronounced than in adults because of relatively higher intracellular binding to β-tubulin. (iii) The study provides an important new insight that P-gp, which is implicated in the clearance of vincristine, is not the rate-limiting step in vincristine clearance and does not play a major role in defining the systemic PK properties of the drug. This can be explained if we assume that while P-gp may facilitate biliary excretion of vincristine, the rate-limiting factor in the hepatobiliary disposition of vincristine is its uptake into hepatocytes across the sinusoidal membrane, either transporter-mediated or *via* passive diffusion, or both. (iv) The PBPK models developed in this study predict vincristine PK in adult and pediatric populations, which is of value in future studies to understand the relationship between vincristine PK and its efficacy as well as adverse effects; specifically, the models can stimulate future modeling studies to improve dosing strategy in pediatric patients in order to avoid undue adverse effects of this narrow therapeutic index drug.

PBPK Modeling of Oral Amoxicillin in Adult and Pediatric Populations

The β-lactam antibiotic amoxicillin was selected for the research proposed in this dissertation to assess if a pediatric PBPK model could be developed for an orally administered drug that is absorbed *via* a transporter-mediated process. Amoxicillin is a clinically important drug in pediatrics. It is one of the most frequently prescribed drugs in infants and children[28,29],

and is the first-line treatment for the common childhood disease AOM. Amoxicillin demonstrates dose-dependent oral bioavailability, decreasing from 90% for a 50 mg dose to 22% at a 10 g dose[30]. The high oral bioavailability at any dose of amoxicillin is surprising given its properties; as a hydrophilic and zwitterionic drug that is charged at physiological pH, amoxicillin would be expected to have poor membrane permeability. Thus, it is reasonable to conclude that intestinal absorption of amoxicillin is mediated by one or more transporter(s). In light of the hydrophilicity, charge, and small size of amoxicillin, it is also likely that paracellular transport may play an important role in its absorption, although the mechanisms of amoxicillin intestinal absorption are not well understood despite the long history of its use. Hence, before PBPK modeling of oral amoxicillin was undertaken, it was necessary to conduct *in vitro* studies to better understand the intestinal absorption of amoxicillin, including the contribution of PEPT1 that is implicated in amoxicillin transport and of other transporters that may be involved. These studies are described in Chapter 3.

Since multiple drug transporters are often involved in the intestinal absorption of drugs with poor membrane permeability such as amoxicillin, understanding the mechanism of intestinal absorption is required for determining the involvement of intestinal transporters and their contribution to transcellular transport, as well as the contribution of paracellular transport to the overall absorptive transport. Transcellular transport (across the intestinal epithelial layer) of a drug requires both uptake across the AP membrane of enterocytes and egress across the BL membrane; thus, both AP uptake and BL efflux transporters must be considered in amoxicillin absorptive transport. In addition, AP efflux transporters could potentially attenuate amoxicillin absorptive transport through the transcellular pathway; hence, the role of these transporters also had to be considered. Although paracellular transport is generally a slow, inefficient process

through the tight junctions between adjacent intestinal epithelial cells[31,32], it was likely to play a role in amoxicillin absorptive transport as it is a small and hydrophilic molecule. Finally, it is known that the intestinal epithelium is more permeable in neonates than in adults[33,34]; hence, for subsequent modeling studies, it was important to elucidate the contribution of the paracellular route to the absorptive transport of amoxicillin.

The *in vitro* studies described in Chapter 3 were performed in two different models of human intestinal transport (Caco-2 cell monolayers and adult intestinal epithelium isolated from fresh jejunal tissue). These studies supported a role for the AP uptake transporter PEPT1 in the intestinal absorption of amoxicillin, as well as a significant (~20%) contribution of passive paracellular transport. In addition, the results showed that an AP uptake transporter in the OATP family may play a role in amoxicillin AP uptake, a new finding that has not previously been reported for amoxicillin. The BL efflux of amoxicillin was found to be quite efficient (more efficient than AP efflux from preloaded Caco-2 cell monolayers), suggesting that AP uptake by PEPT1 and other transporters could be the rate-limiting step in amoxicillin intestinal absorption. Although the specific BL efflux transporter involved was not identified, the studies suggested that a bidirectional peptide transporter (which uses a facilitative transport mechanism[35,36]) may be responsible for amoxicillin BL efflux. This is based on preliminary results (Chapter 3) that amoxicillin is unlikely to be transported by a BL transporter from the MRP class (MRP1, MRP3, or MRP4), which are known to transport anionic and zwitterionic compounds, or by OSTα/β. Interestingly, amoxicillin exhibits a surprisingly high passive transport (*i.e.*, in ice cold conditions) when studied in *in vitro* models. In part, this could be explained by a relatively large contribution of the paracellular route to the absorptive transport of amoxicillin, as shown in the studies described in Chapter 3. Since paracellular transport cannot be directly measured, the

cellular kinetic data (AP and BL uptake, AP and BL efflux) were used to construct a three-compartment model, as has been done with other hydrophilic charged compounds (ranitidine[37] and metformin[38]). This modeling approach enabled quantitative evaluation of the contribution of the paracellular route to the absorptive transport of amoxicillin in Caco-2 cell monolayers and fresh human intestinal epithelium, and suggested that ~20% of amoxicillin absorptive transport across the intestinal epithelium occurs *via* the paracellular route.

Thus, the studies reported in Chapter 3 provided significant new insights into the intestinal absorption mechanism of amoxicillin, although questions still remain about several aspects of this mechanism. The results have provided direction for future studies, such as identifying the specific OATP transporter(s) involved in the AP uptake of amoxicillin into the intestinal epithelium, confirming that MRPs are not involved in BL efflux of amoxicillin and confirming the involvement of a BL peptide efflux transporter. It is important to note that the results presented in Chapter 3 provide the basis for understanding the saturability and dose-dependency of amoxicillin oral absorption (bioavailability). Due to the increase in antibiotic resistance worldwide, the recommended pediatric doses of amoxicillin for AOM have been increased[29,39]; however, subsequent studies suggest that the higher doses may not be improving efficacy against AOM[40,41]. Therefore, future studies to further explore these *in vitro* findings and understand the limits of amoxicillin intestinal absorption may help to explain why the higher pediatric doses of amoxicillin do not improve efficacy or penetration into MEF.

In Chapter 4, PBPK models of oral amoxicillin were developed to predict PK in adults and in young children (infants and children ≤ 5 years of age). The approach used was similar to that used previously in the Thakker Laboratory in that a PBPK model was developed in adults based on the available clinical data and known mechanisms of clearance, and then

refined/validated using additional adult clinical data. The adult model was then adapted to a pediatric model based on the physiologic differences in relevant tissues and proteins (*e.g.*, ontogeny factors for albumin and for GFR, and age-appropriate GI surface area, lengths, volumes, and transit times) between adults and the target pediatric populations. These PBPK models were able to predict PK parameters in adults and in two virtual pediatric populations representing children under 5 years of age. A pediatric PBPK model of amoxicillin has utility in simulating various dosing strategies of amoxicillin and predicting amoxicillin PK and plasma concentrations, which has become important with the increase in antibiotic resistance and the need to predict efficacy outcomes (*e.g.*, dosing interval during which concentrations are above the MIC). The amoxicillin pediatric PBPK model, as with the vincristine PBPK model in Chapter 2, also provides a basis for future hypothesis-generating investigation of mechanisms underlying amoxicillin disposition. In Chapter 3, *in vitro* studies suggested a role of PEPT1 and OATP transporters in AP uptake and a BL peptide efflux transporter in amoxicillin intestinal absorption; with additional *in vitro* information and kinetic data, the role and contribution of these transporters could be incorporated into future iterations of PBPK models.

Limitations of the Experimental Approach

PBPK Modeling and Software

As the use of PBPK modeling in drug development and regulatory submissions is still fairly recent, and the applications so broad, the best practices for model development and validation are still evolving and there are no FDA guidances yet for the use of such models in regulatory submissions. General modeling approaches and flowcharts for pediatric modeling approaches have been discussed elsewhere[6,42,43], but generally involve developing and validating an adult PBPK model prior to adaptation for a pediatric population. The goals of a pediatric

PBPK model can also vary widely, and therefore, the standard for the data incorporated into the model and for model validation may differ accordingly. For example, a pediatric PBPK model developed early in the drug development process to assist in a clinical pediatric study design would be held to different standards compared to a PBPK model intended to simulate and replace a clinical pediatric drug-drug interaction study.

For the PBPK studies described in Chapter 2 and Chapter 4, criteria of 2-fold difference between the model simulated and the observed PK data was considered to be acceptable model performance. Concentration-time profiles were also compared to observed concentration data, and when a majority of observed data fell within the 95% prediction interval, the model performance was considered satisfactory. The 2-fold criteria is a commonly applied acceptance criteria for PBPK model evaluation[44]. However, a limitation of the 2-fold criteria is that it is applied equally to clinical data, regardless of the study sample size, inter-study variability, or inter-subject variability. Thus, the 2-fold criteria may be too broad for drugs with low variability, but too narrow for others[45]. Other PBPK model evaluation criteria exist, including specifying that a ratio of certain calculated PK parameters must be within 30% (or alternately, within 2-fold) of the ratio of the observed PK parameters (for drug-drug interactions studies), or that calculated PK parameters must be within 30% of observed parameters[44]. Alternate validation approaches have also been proposed that would account for the study size and variability of the observed trials, but these do not seem to have been widely adopted yet[45].

Ideally, a different clinical data set (*i.e.*, a training dataset) would be used for the initial model development than used for model validation[43]. In practice, sufficient clinical concentration and PK data may not be available to generate two separate datasets, especially from the literature and from pediatric PK studies. In the vincristine and amoxicillin PBPK models described in

Chapter 2 and Chapter 4, most of the clinical data were extracted from publications and concentration data were limited in availability. Thus, it was not always feasible to have separate training set and model validation sets. Instead, concentration *vs.* time data (pooled from multiple published studies where available) and published PK data were used in model refinement and validation. As an informal measure of model robustness, the PBPK models were used where possible to independently simulate data from multiple publications and at multiple doses where available.

The availability of experimental data, literature data, physiological data, and expression data can also be a limitation in developing and applying PBPK models. For pediatric populations, comprehensive physiological data and DME/transporter expression data may not always be available or may be limited in scope such that the true inter-individual variability is unknown, thus decreasing the accuracy of pediatric model simulations.

Finally, PBPK modeling in the pharmaceutical industry today is primarily performed with proprietary software such as SimCYP and GastroPlus[43]. PK-Sim®, originally developed by Bayer Technology Services[46], has since been released as open source software. When using software packages for PBPK modeling, additional issues may arise that are specific to the software. For example, the calculation methods for extrapolation may not always be clear, and there may be limitations in the type of mechanistic input information. For some types of software, the number of physiological compartments cannot be altered, or intracellular binding cannot be implemented. *In vitro* to *in vivo* calculations and calibrations may also differ and may have been optimized for one type of data over another (*e.g.*, extrapolations of hepatic clearance that are optimized for microsomal data but not for hepatocytes).

Studying Vincristine Intracellular Binding to β-tubulin

During PBPK model development for vincristine, the feasibility of determining specific binding kinetics (*i.e.*, on rate and off rate) of vincristine to β-tubulin were considered. Although similar kinetic values are available for other vinca alkaloid drugs, including vinblastine, there are published reports that vincristine interferes with the stopped-flow light scattering assays that are used to study the kinetics of tubulin binding[47,48]. Vincristine binds to β-tubulin subunits *in vitro*, forming dimers that aggregate into large spirals described as "sheets" or "rods" that interfere with light-scatter measurements[47]. This phenomenon was not observed with the other vinca alkaloids tested, vinblastine or vinrelbine. For the purposes of PBPK model development, the kinetics of vinblastine binding were used instead (Chapter 2). However, the aggregation of vincristine-β-tubulin polymers *in vitro* suggests a possible avenue of exploration into whether the extent of vincristine intracellular accumulation might differ from other vinca alkaloids, if this phenomenon were to occur *in vivo* as well.

Challenges of using Caco-2 Cell Monolayers and Human Intestinal Epithelia, and studying PEPT1

One of the major challenges in studying amoxicillin intestinal absorption was evaluating data from the two *in vitro* models used, Caco-2 cell monolayers and adult human intestinal epithelia, which differ with respect to paracellular porosity. Both of the models exhibit variability with respect to PEPT1 expression.

Caco-2 cell monolayers are a common *in vitro* model for studying drug transport and permeability; however, they are derived from human colon carcinoma and thus have key differences from the human jejunum, where a majority of drug absorption occurs. For example, Caco-2 cells have a smaller average pore radius and higher TEER compared to the human jejunum[49]. Thus, Caco-2 measurements have a tendency to underpredict the permeability of

hydrophilic compounds with significant contribution of paracellular transport routes. Expression of drug transporters in Caco-2 cell monolayers, including PEPT1, are highly dependent on cell culture conditions including the passage number, seeding density, the type of membrane support used in the Transwell™ culture system, and the culture time[50,51]. Expression of PEPT1 has also been shown to be significantly different depending on the source of the Caco-2 clone[51]. PEPT1 protein expression and permeability of β-lactam antibiotics (amoxicillin was not studied) are highly correlated in Caco-2 cell monolayers[52], indicating that this would be an appropriate *in vitro* model to study amoxicillin transport.

Inter- and intra-laboratory variability and reproducibility of Caco-2 cell results is also a common problem, minimized here by obtaining Caco-2 cells from a single source (American Type Culture Collection, ATCC) and with cell culture and experiments performed in the same laboratory. The gene expression of nine drug transporters, including PEPT1, was evaluated in Caco-2 cell monolayers and compared to transporter expression in the duodenum, ileum, jejunum, and colon. Of these intestinal regions, the pattern of relative transporter expression in Caco-2 cells appeared most similar to that of the jejunum, although expression of OATP2B1, BCRP, and MRP2 differed by more than 5-fold[53]. Aside from transporter expression, the potential for DME and transporter induction also appears to differ in Caco-2 cells compared to human intestine[54].

In the studies described in Chapter 3, all adult intestinal epithelia were obtained from jejunal tissue that is normally discarded during roux-en-y bariatric surgery. Fresh adult human intestinal epithelia mounted in Ussing chambers have been used to perform drug metabolism and transport studies[55,56]. In contrast to Caco-2 cell monolayers, the jejunum is more porous with greater paracellular transport. In adults, protein expression of PEPT1 in the jejunum is not

significantly different in morbidly obese patients[57]. Diet may impact the expression of PEPT1 in the jejunum; in rats, PEPT1 gene expression and activity (determined by the uptake of the substrate glysar) is increased and appears to be mediated by the nuclear receptor peroxisome proliferator-activated receptor (PPAR) α[58]. Thus, the impact of obtaining tissue from obese bariatric patients fasted for surgery is unclear, but all tissues were obtained under similar conditions. Fresh human intestinal epithelia maintain metabolism and transport activity for up to six hours, and the villi remain intact as the tissue is mounted[59,60]. Maintaining the freshness of the tissue is important, and viability is maintained by controlling the temperature (37^{o}C) and continuous oxygenation.

PEPT1 is highly expressed in the intestine and plays a major role in the absorption of dietary peptides[61]. In addition to the probable high variability in PEPT1 expression, PEPT1 presented a challenge because of the low affinity of the transporter for its substrates, including dietary peptides and peptidomimetic drugs such as amoxicillin, and its high capacity for transport. As a result, it was difficult to inhibit PEPT1 both in Caco-2 cell monolayers and in the human intestinal epithelia by chemical means. Preliminary inhibition studies in Caco-2 cell monolayers showed no differences in amoxicillin accumulation or AP uptake in the presence of glysar, a known substrate and inhibitor of PEPT1. A more potent inhibitor, valacyclovir[62], was used instead to evaluate amoxicillin accumulation at 60 minutes (Chapter 3). Concentration-dependent AP uptake studies performed in human intestinal epithelia showed that transport increased linearly with concentration, with no saturation of absorptive transport up to the maximum concentrations of amoxicillin within the limits of its solubility. Although a saturable component of amoxicillin transport was identified in AP uptake studies in the Caco-2 cell

monolayer model, it was not possible to demonstrate the dose-dependent amoxicillin absorption that is observed *in vivo*.

Future Directions and Alternative Approaches

Vincristine

In considering the future directions for the PBPK modeling studies of vincristine in adults and children after IV administration reported in this dissertation, more comprehensive β-tubulin expression data in tumors and platelets of adult and pediatric patients should be collected. This would help to determine the validity of the proposed hypothesis arising from the current work that higher β-tubulin expression in the pediatric population accounts for a more pronounced distribution phase in this population. It is possible that the hypothetical increase in β-tubulin in the pediatric population represent a physiological compartment with high β-tubulin expression that is not present in the adult population: in this case, the solid tumor (Wilms tumor) in the pediatric population. Furthermore, various vinca alkaloids bind with varying affinity to the different β-tubulin isoforms expressed throughout the body[63]. These β-tubulin isotypes are expressed to a different degree, and some are tissue-specific[64]. If tissue expression of these isotypes could be determined, it could be theoretically possible to evaluate the extent of vincristine binding and accumulation in specific areas. For example, the β-tubulin class III isotype is neuron-specific, and the higher affinity of vincristine for this subtype compared to vinblastine and vinorelbine may partially explain the greater degree of neurotoxicity observed with vincristine[63].

Additional applications include the use of PBPK models to simulate vincristine PK in populations of high CYP3A5-expressing patients, although this would require PK data from populations of known CYP3A5-expressors in order to validate the model. Since vincristine is

selectively metabolized more efficiently by CYP3A5 than by CYP3A4[18], the difference in clearance due to differential expression of catalytically competent CYP3A5 is likely to contribute to differences that have been observed in treatment response and the risk of adverse effects[65].

Amoxicillin

The research described in Chapter 3 confirmed previous reports that PEPT1 is involved in the AP uptake of amoxicillin in the intestine, and identified a role for several possible drug transporters in the absorptive transport of amoxicillin, including an OATP transporter in its AP uptake, and a bidirectional peptide efflux transporter involved in its BL efflux. In order to be able to incorporate these transporters in a future iteration of a PBPK model for oral amoxicillin, the specific transporters should be identified in a series of *in vitro* studies with the appropriate inhibitors, and/or in a cell model overexpressing the transporter of interest. The kinetics of amoxicillin transport by each transporter should be characterized in order to estimate their contribution to the overall transport of amoxicillin. Ideally, this should include studies with the bidirectional peptide efflux transporter, although it has not been fully characterized to date and very little is known about its properties other than that it appears to have a passive facilitative transport mechanism[35]. In a PBPK model of amoxicillin intestinal absorption, this could theoretically be incorporated by assuming a high degree of passive permeability only on the BL membrane, but current software limitations preclude this.

Furthermore, obtaining PEPT1 protein expression in adult and infant tissue would help to evaluate if there might be differences in expression that are age-dependent or due to the increased ingestion of milk peptides in infants. Other studies suggest that the gene expression of

PEPT1 do not differ between infants and adults[61]; however, gene expression, protein expression, and transporter function do not always correlate.

Although the focus of Chapters 3 and 4 was primarily on the transporter-mediated intestinal absorption of amoxicillin, transporters also play a key role in the renal clearance of amoxicillin. Amoxicillin is cleared renally (accounting for up to 80% of amoxicillin elimination[66]) at a rate that exceeds the GFR, indicating active tubular secretion that must also be transporter-mediated. In Chapter 4, the renal clearance of amoxicillin was incorporated by using an estimate of the fraction of GFR. An alternate approach would be to incorporate transporter-mediated reabsorption (by PEPT1 and PEPT2) and secretion, if the renal transporters involved in secretion are identified. Although amoxicillin is not a substrate for OAT1[67], an important uptake transporter in the kidney must be involved in its secretion as its renal clearance is significantly reduced by the OAT inhibitor, probenecid[68]. Evaluating the potential of amoxicillin as a substrate of the other OAT transporters (OAT2, 3, or 4) or of the organic cation transporters (OCT2, OCTN2) may be helpful in understanding and modeling the renal secretion of amoxicillin.

PBPK Models – Development and Validation

In addition to the vincristine- and amoxicillin-specific approaches described above, there are alternative approaches common to both PBPK models that could be used in future modeling exercises. As with other pediatric drugs, a population PK approach to future clinical studies would be useful for generating additional PK parameters and maximizing the utility of sparse clinical PK sampling. Although the paucity of pediatric data is often a concern in developing PBPK models, obtaining PK parameters from population PK studies can augment the limited clinical concentration and PK data available from the literature.

Lastly, the field of PBPK modeling and its best practices continue to evolve. In recent cases, PBPK models generated in GastroPlus and in SimCYP have been used successfully in regulatory submissions to obtain waivers for performing bioequivalence studies, to inform dose selection in children for a pediatric trial, and to simulate a drug-drug interaction study in a pediatric population[43]. As additional pediatric physiological data is collected, especially for drug transporters, the use of PBPK modeling for drugs with transporter-mediated disposition will continue to improve. With adequate pharmacodynamic data, PBPK models could also be used to better understand the relationship between PK parameters, concentrations, and clinical outcomes in children.

REFERENCES

1. Roberts R, Rodriguez W, Murphy D, *et al*. Pediatric Drug Labeling: Improving the Safety and Efficacy of Pediatric Therapies. *JAMA*. 2003;290(7):905-911.

2. Balan S, Azmi M, Hassali A, *et al*. Two Decades of Off‐label Prescribing in Children: a Literature Review. *World J Pediatr*. 2018;14(6):528-540.

3. Samant TS, Mangal N, Lukacova V, *et al*. Quantitative Clinical Pharmacology for Size and Age Scaling in Pediatric Drug Development: A Systematic Review. *J Clin Pharmacol*. 2015;55(11):1207-1217.

4. Kearns GL, Abdel-Rahman SM, Alander SW, *et al*. Developmental Pharmacology--Drug Disposition, Action, and Therapy in Infants and Children. *N Engl J Med*. 2003;349(12):1157-67.

5. Leong R, Vieira MLT, Zhao P, *et al*. Regulatory Experience with Physiologically Based Pharmacokinetic Modeling for Pediatric Drug Trials. *Clin Pharmacol Ther*. 2012;91(5):926-31.

6. Maharaj A, Edginton A. Physiologically Based Pharmacokinetic Modeling and Simulation in Pediatric Drug Development. *CPT Pharmacometrics Syst Pharmacol*. 2014;3:e148.

7. Penkov D, Tomasi P, Eichler I, *et al*. Pediatric Medicine Development: An Overview and Comparison of Regulatory Processes in the European Union and United States. *Ther Innov Regul Sci*. 2017;51(3):360-371.

8. Neely M, Bayard D, Desai A, *et al*. Pharmacometric Modeling and Simulation Is Essential to Pediatric Clinical Pharmacology. *J Clin Pharmacol*. 2018;58(May):S73-S85.

9. Mehrotra N, Bhattaram A, Earp JC, *et al*. Role of Quantitative Clinical Pharmacology in Pediatric Approval and Labeling. *Drug Metab Dispos*. 2016;44(July):924-933.

10. Zane NR, Thakker DR. A Physiologically Based Pharmacokinetic Model for Voriconazole Disposition Predicts Intestinal First-pass Metabolism in Children. *Clin Pharmacokinet*. 2014;53(12):1171-1182.

11. Abdel-Rahman SM, Amidon GL, Kaul A, *et al*. Summary of the National Institute of Child Health and Human Development-best Pharmaceuticals for Children Act Pediatric Formulation Initiatives Workshop-Pediatric Biopharmaceutics Classification System Working Group. *Clin Ther*. 2012;34(11):S11-24.

12. Taskar K, Reddy VP, Burt H, *et al*. PBPK Models for Evaluating Membrane Transporter Mediated DDIs: Current Capabilities, Case Studies, Future Opportunities and Recommendations. *Clin Pharmacol Ther*. 2019:Just Accepted.

13. Batchelor HK, Kendall R, Desset-Brethes S, *et al*. Application of In Vitro Biopharmaceutical Methods in Development of Immediate Release Oral Dosage Forms Intended for Paediatric Patients. *Eur J Pharm Biopharm*. 2013;85(3 PART B):833-842.

14. Wang F, Zhou F, Kruh GD, *et al*. Influence of Blood-brain Barrier Efflux Pumps on the Distribution of Vincristine in Brain and Brain Tumors. *Neuro Oncol*. 2010;12(10):1043-1049.

15. Wang L, Wang C, Liu Q, *et al*. PEPT1- and OAT1/3-mediated Drug-Drug Interactions Between Bestatin and Cefixime In Vivo and In Vitro in Rats, and In Vitro in Human. *Eur J Pharm Sci*. 2014;63:77-86.

16. Luckner P, Brandsch M. Interaction of 31 Beta-lactam Antibiotics with the H +/peptide Symporter PEPT2: Analysis of Affinity Constants and Comparison with PEPT1. *Eur J Pharm Biopharm*. 2005;59(1):17-24.

17. De Cock PAJG, Standing JF, Barker CIS, *et al*. Augmented Renal Clearance Implies a Need for Increased Amoxicillin-clavulanic Acid Dosing in Critically Ill Children. *Antimicrob Agents Chemother*. 2015;59(11):7027-7035.

18. Dennison JB, Kulanthaivel P, Barbuch RJ, *et al*. Selective Metabolism of Vincristine In Vitro by CYP3A5. *Drug Metab Dispos*. 2006;34(8):1317-1327.

19. Dennison JB, Jones DR, Renbarger JL, *et al*. Effect of CYP3A5 Expression on Vincristine Metabolism with Human Liver Microsomes. *J Pharmacol Exp Ther*. 2007;321(2):553-63.

20. Dennison JB, Mohutsky M a, Barbuch RJ, *et al*. Apparent High CYP3A5 Expression is Required for Significant Metabolism of Vincristine by Human Cryopreserved Hepatocytes. *J Pharmacol Exp Ther*. 2008;327(1):248-257.

21. Stevens JC, Hines RN, Gu C, *et al*. Developmental Expression of the Major Human Hepatic CYP3A Enzymes. *J Pharmacol Exp Ther*. 2003;307(2):573-582.

22. Crom WR, de Graaf SS, Synold T, *et al*. Pharmacokinetics of Vincristine in Children and Adolescents with Acute Lymphocytic Leukemia. *J Pediatr*. 1994;125(4):642-9.

23. Gidding CE, Meeuwsen-de Boer GJ, Koopmans P, U *et al*. Vincristine Pharmacokinetics After Repetitive Dosing in Children. *Cancer Chemother Pharmacol*. 1999;44(3):203-9.

24. Zane NR, Chen Y, Wang MZ, *et al*. Cytochrome P450 and Flavin-containing Monooxygenase Families: Age-dependent Differences in Expression and Functional Activity. *Pediatr Res*. 2018;83(2):527-535.

25. Prasad B, Gaedigk A, Vrana M, *et al*. Ontogeny of Hepatic Drug Transporters as Quantified by LC-MS/MS Proteomics. *Clin Pharmacol Ther*. 2016;100(4):362-370.

26. Nicolaï J, Thevelin L, Bing Q, *et al*. Role of the OATP Transporter Family and a Benzbromarone-Sensitive Efflux Transporter in the Hepatocellular Disposition of Vincristine. *Pharm Res*. 2017;34(11):2336-2348.

27. Dennison JB, Mohutsky M a, Barbuch RJ, *et al*. Apparent High CYP3A5 Expression is Required for Significant Metabolism of Vincristine by Human Cryopreserved Hepatocytes. *J Pharmacol Exp Ther*. 2008;327(1):248-57.

28. Chai G, Governale L, McMahon AW, *et al*. Trends of Outpatient Prescription Drug Utilization in US Children, 2002-2010. *Pediatrics*. 2012;130(1):23-31.

29. Lieberthal AS, Carroll AE, Chonmaitree T, *et al*. The Diagnosis and Management of Acute Otitis Media. *Pediatrics*. 2013;131(3):e964-99.

30. Piotrovskij VK, Paintaud G, Alván G, *et al*. Modeling of the Saturable Time-Constrained Amoxicillin Absorption in Humans. *Pharm Res*. 1994;11(9):1346-1351.

31. Itallie CM Van, Anderson JM. Claudins and Epithelial Paracellular Transport. *Annu Rev Physiol*. 2006;68:403-429.

32. Shen L, Weber CR, Raleigh DR, *et al*. Tight Junction Pore and Leak Pathways : A Dynamic Duo. *Annu Rev Physiol*. 2011;73:283-309.

33. van Elburg RM, Fetter WPF, Bunkers CM, *et al*. Intestinal Permeability in Relation to Birth Weight and Gestational and Postnatal Age. *Arch Dis Child Fetal Neonatal Ed*. 2003;88(1):F52-F55.

34. Riezzo G, Indrio F, Raimondi F, *et al*. Maturation of Gastric Electrical Activity, Gastric Emptying and Intestinal Permeability in Preterm Newborns During the First Month of Life. *Ital J Pediatr*. 2009;35(1):6.

35. Irie M, Terada T, Okuda M, *et al*. Efflux Properties of Basolateral Peptide Transporter in Human Intestinal Cell Line Caco-2. *Pflugers Arch Eur J Physiol*. 2004;449(2):186-194.

36. Terada T, Sawada K, Saito H, *et al*. Functional Characteristics of Basolateral Peptide Transporter in the Human Intestinal Cell line Caco-2. *Am J Physiol*. 1999;276(6 Pt 1):G1435-G1441.

37. Bourdet DL, Thakker DR. Saturable Absorptive Transport of the Hydrophilic Organic Cation Ranitidine in Caco-2 cells: Role of pH-dependent Organic Cation Uptake System and P-glycoprotein. *Pharm Res*. 2006;23(6):1165-1177.

38. Proctor WR, Bourdet DL, Thakker DR. Mechanisms Underlying Saturable Instestinal Absorption of Metformin. *Drug Metab Dispos*. 2008;36(8):1650-1658.

39. Lister PD, Pong A, Chartrand SA, *et al*. Rationale Behind High-dose Amoxicillin Therapy for Acute Otitis Media Due to Penicillin-nonsusceptible Pneumococci: Support from in Vitro Pharmacodynamic studies. *Antimicrob Agents Chemother*. 1997;41(9):1926-1932.

40. Harrison CJ, Welch DF. Middle Ear Effusion Amoxicillin Concentrations in Acute Otitis Media. *Pediatr Infect Dis J*. 1988;17(7):657-658.

41. Sox CM, Finkelstein JA, Yin R, *et al*. Trends in Otitis Media Treatment Failure and Relapse. *Pediatrics*. 2008;121(4):674-679.

42. Khalil F, Läer S. Physiologically Based Pharmacokinetic Models in the Prediction of Oral Drug Exposure over the Entire Pediatric Age Range-sotalol as a Model Drug. *AAPS J*. 2014;16(2):226-39.

43. Shebley M, Sandhu P, Emami Riedmaier A, *et al*. Physiologically Based Pharmacokinetic Model Qualification and Reporting Procedures for Regulatory Submissions: A Consortium Perspective. *Clin Pharmacol Ther*. 2018;104(1):88-110.

44. Sager JE, Yu J, Ragueneau-Majlessi I, *et al*. Physiologically Based Pharmacokinetic (PBPK) Modeling and Simulation Approaches: A Systematic Review of Published Models, Applications, and Model Verification. *Drug Metab Dispos*. 2015;43(11):1823-1837.

45. Abduljalil K, Cain T, Humphries H, *et al*. Deciding on Success Criteria for Predictability of Pharmacokinetic Parameters from In Vitro Studies : An Analysis Based on In Vivo Observations s. 2014:1478-1484.

46. Willmann S, Lippert J, Sevestre M, *et al*. PK-Sim®: a Physiologically Based Pharmacokinetic 'Whole-body' Model. *Biosilico*. 2003;1(4):121-124.

47. Lobert S, Vulevic B, Correia JJ. Interaction of Vinca Alkaloids with Tubulin: A

Comparison of Vinblastine, Vincristine, and Vinorelbine. *Biochemistry*. 1996;35(21):6806-14.

48. Lobert S, Correia JJ. Methods for Studying Vinca Alkaloid Interactions with Tubulin. *Methods Mol Med*. 2007;137:261-280.

49. Linnankoski J, Ma J. Paracellular Porosity and Pore Size of the Human Intestinal Epithelium in Tissue and Cell Culture Models. *J Pharm Sci*. 2010;99(4):2166-2175.

50. Behrens I, Kissel T. Do Cell Culture Conditions Influence the Carrier-mediated Transport of Peptides in Caco-2 Cell Monolayers? *Eur J Pharm Sci*. 2003;19(5):433-442.

51. Behrens I, Kamm W, Dantzig AH, *et al*. Variation of Peptide Transporter (PepT1 and HPT1) Expression in Caco-2 cells as a Function of Cell Origin. *J Pharm Sci*. 2004;93(7):1743-1754.

52. Chu XY, Sánchez-Castaño GP, Higaki K, *et al*. Correlation Between Epithelial Cell Permeability of Cephalexin and Expression of Intestinal Oligopeptide Transporter. *J Pharmacol Exp Ther*. 2001;299(2):575-582.

53. Englund G, Rorsman F, Rönnblom A, *et al*. Regional Levels of Drug Transporters Along the Human Intestinal Tract: Co-Expression of ABC and SLC Transporters and Comparison with Caco-2 cells. *Eur J Pharm Sci*. 2006;29(3-4 SPEC. ISS.):269-277.

54. Brück S, Strohmeier J, Busch D, *et al*. Caco-2 cells – Expression, Regulation and Function of Drug Transporters Compared with Human Jejunal tissue. *Biopharm Drug Dispos*. 2017;38:115-126.

55. Gotoh Y, Kamada N, Momose D. The Advantages of the Ussing Chamber in Drug Absorption Studies. *J Biomol Screen*. 2005;10(5):517-23.

56. Van De Kerkhof EG, Ungell ALB, Sjöberg ÅK, *et al*. Innovative Methods to Study Human Intestinal Drug Metabolism In Vitro: Precision-cut Slices Compared with Ussing Chamber Preparations. *Drug Metab Dispos*. 2006;34(11):1893-1902.

57. Miyauchi E, Tachikawa M, Declèves X, *et al*. Quantitative Atlas of Cytochrome P450, UDP-Glucuronosyltransferase, and Transporter Proteins in Jejunum of Morbidly Obese Subjects. *Mol Pharm*. 2016;13(8):2631-2640.

58. Shimakura J, Terada T, Saito H, *et al*. Induction of Intestinal Peptide Transporter 1 Expression During Fasting is Mediated via Peroxisome Proliferator-activated Receptor Alpha. *Am J Physiol Gastrointest Liver Physiol*. 2006;291(5):G851-6.

59. Gotoh Y, Kamada N, Momose D. The Advantages of the Ussing Chamber in Drug Absorption Studies. *J Biomol Screen*. 2005;10(5):517-523.

60. Van De Kerkhof EG, Ungell a. LB, Sjöberg Å K, *et al*. Innovative Methods to Study Human Intestinal Drug Metabolism In Vitro: Precision-cut Slices Compared with Ussing Chamber Preparations. *Drug Metab Dispos*. 2006;34(11):1893-1902.

61. Mooij MG, de Koning BAE, Lindenbergh-Kortleve DJ, *et al*. Human Intestinal PEPT1 Transporter Expression and Localization in Preterm and Term Infants. *Drug Metab Dispos*. 2016;(July):1014-1019.

62. Pak YA, Long AJ, Annes WF, *et al*. In Vitro and Clinical Evaluations of the Drug-Drug Interaction Potential of a Metabotropic Glutamate 2/3 Receptor Agonist ProDrug with Intestinal Peptide Transporter 1. *Drug Metab Dispos*. 2017;45(2).

63. Lobert S, Frankfurter A, Correia JJ. Energetics of Vinca Alkaloid Interactions with Tubulin Isotypes: Implications for Drug Efficacy and Toxicity. *Cell Motil Cytoskeleton*. 1998;39(2):107-121.

64. Leandro-García LJ, Leskelä S, Landa I, *et al*. Tumoral and Tissue-specific Expression of the Major Human Beta-tubulin Isotypes. *Cytoskeleton*. 2010;67(4):214-223.

65. Egbelakin A, Ferguson MJ, MacGill EA, *et al*. Increased Risk of Vincristine Neurotoxicity Associated with Low CYP3A5 Expression Genotype in Children with Acute Lymphoblastic Leukemia. *Pediatr Blood Cancer*. 2012;56(3):361-367.

66. Thambavita D, Galappatthy P, Mannapperuma U, *et al*. Biowaiver Monograph for Immediate-Release Solid Oral Dosage Forms : Amoxicillin Trihydrate. *J Pharm Sci*. 2017;106(10):2930-2945.

67. Li M, Anderson GD, Phillips BR, *et al*. Interactions of Amoxicillin and Cefaclor with Human Renal Organic Anion and Peptide Transporters. *Drug Metab Dispos*. 2006;34(4):547-555.

68. Shanson DC, McNabb R, Hajipieris P. The Effect of Probenecid on Serum Amoxycillin Concentrations Up to 18 Hours After a Single 3 g Oral Dose of Amoxycillin: Possible Implications for Preventing Endocarditis. *J Antimicrob Chemother*. 1984;13:629-632.